EGFR Phosphorylation Determines Its Progression From Early To Late Endosomes

An Analysis of Receptor-Mediated Endocytosis by Advanced Confocal Imaging

Merete Storflor

Thesis for the Master of Science degree in Molecular Biology

UNIVERSITY OF OSLO

2015

© Merete Storflor

2015

EGFR phosphorylation determines its progression from early to late endosomes - An analysis of receptor-mediated endocytosis by advanced confocal imaging

Merete Storflor

http://www.duo.uio.no/

Press: Reprosentralen, University of Oslo

Table of Contents

Abstract

Upon ligand stimulation the epidermal growth factor receptor (EGFR) is autophosphorylated at specific C-terminal tyrosines. The phosphotyrosines form docking sites for signaling proteins important for signal transduction and attenuation. Previous work has indicated that the phosphotyrosine docking sites have an impact on receptor trafficking, but have not yet determined the specific temporal regulatory role the phosphotyrosine docking sites have in receptor trafficking. In this project we introduce a novel method for trafficking analysis based on live cell imaging and colocalization analysis. We describe a series of colocalization studies performed with three mutant EGF receptors containing mutations at specific phosphotyrosines (Y1045, Y1068, and Y1086). These mutations abrogate the receptor phosphorylation sites where Cbl and Grb2 are known to bind to the receptor. Our results show that an altered phosphorylation pattern has major implications for EGFR trafficking by regulating endosomal maturation.

Acknowledgements

The study presented in this thesis was carried out in the laboratory of Professor Bakke at the Department of Biosciences, Faculty of Mathematics and Natural Sciences, University of Oslo, January 2014 - June 2015.

First and foremost, I would like to thank Oddmund Bakke for giving me the opportunity to perform the work presented in this study and for allowing me access to the exciting field of live cell imaging. I valued the independence given and the chance to prepare my Master's degree in such an enthusiastic environment.

I wish to express my sincerest appreciation to my fabulously awesome supervisors Frode M. Skjeldal, and Catherine A. Heyward. Thank you for sharing your overwhelming expertise and passion. I have learned so much from you both. Thank you for all the support, hilarious conversations, and most importantly thank you for taking time out of your extremely busy schedules to give me feed-back and guidance.

Thank you to all my new friends at "Bakkelab", for imparting your expertise. We've shared some unforgettable times, and undeniably consumed lethal amounts of coffee. I have looked forward to coming into the lab, because of each and every one of you.

Special thanks to my wonderful parents Aud and Harry, for the encouragement and never-ending support, and my brother Magnar who always makes me laughs. Last but not least, I wish to thank me sexy hunk of a man, Stefan, for all the love, patience, and care. You are amazing.

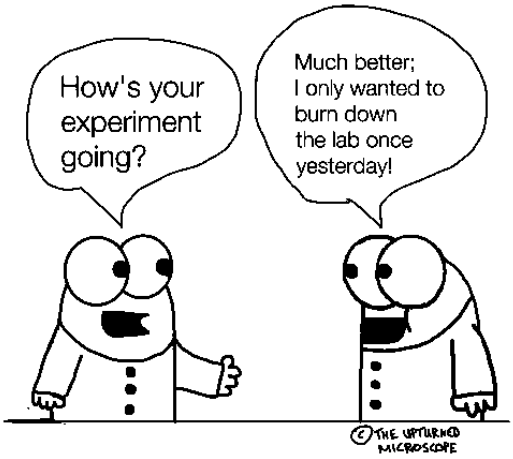

"The inverted microscope" by Nik Papageorgiou

Abbreviations

AP-2	Adaptor Protein
ATPase	Adenylpyrophosphatase
BAR	Bin-Amphiphysin-Rvs
Bb	Backbone
Cbl	Casitas B-lineage Lymphoma
CCP	Clathrin Coated Pit
CCV	Clathrin Coated Vesicle
CHC	Clathrin Heavy Chains
CHX	Cyclohexamide
CIE	Clathrin- Independent Endocytosis
CLC	Clathrin Light Chain
CME	Clathrin- Mediated Endocytosis
COP-I/ II	Coat Protein -I/ II
CORVET	class C core vacuole/endosome tethering
CREB	cyclic AMP-responsive element-binding protein
DMEM	Dulbecco's Modified Eagle Medium
DMSO	Dimethyl Sulfoxide
DTT	Dithiothreitol
DUBs	Deubiquitination Enzymes
E1	Ubiquitin-activating enzyme
E2	Ubiquitin-conjugating enzyme
E3	Ubiquitin ligase
EDTA	Ethylenediaminetetraacetic acid
EEA1	Early Endosome Antigen 1
EGF	Epidermal Growth Factor
EGFR	Epidermal Growth Factor Receptor
Eps15	Epidermal Growth Factor Receptor Substrate 15
ER	Endoplasmic Reticulum
ERAD	Endoplasmic-Reticulum-Associated Protein Degradation

ErbB	Erythroblastic Leukemia Viral Oncogene Homolog 1-4
ERK	Extracellular Signal-Regulated Kinases
ESCRT	Endosomal Sorting Complex Required for Transport
EtBr	Ethidium Bromide
FCHO 1/ 2	Fer/Cip4 Homology Domain-Only Proteins 1 and 2
FCS	Fetal Calf Serum
G418	Geneticin
GAP	Guanosinetriphosphatase Activating Protein
GDF	Guanine Dissociation Inhibitor Displacement Factor
GDI	Guanine Dissociation Inhibitor
GDP	Guanosine Diphosphate
GEF	Guanine Exchange Factor
Grb2	Growth Factor Receptor-Bound Protein 2
GTP	Guanosine Triphosphate
GTPase	Guanosinetriphosphatase
Her2	Human Epidermal Growth Factor Receptor
HOPS	Homotypic Fusion and Vacuole Protein Sorting
HSC70	Heat Shock Protein
ILV	Intraluminal Vesicles
kDa	Kilodaltons
LAMP-1	Lysosomal-Associated Membrane Protein 1
LB	Lysogeny Broth
LIMP	Lysosome Integral Membrane Protein
MAPK	Mitogen-Activated Protein Kinases
MVB	Multivesicular Bodies
MHC class II	Major Histocompatibility Complex
MTOC	Microtubule-Organizing Center
NSF	N-Ethylmaleimide Sensitive Fusion Protein
PAE	Porcine Aortic Endothelial (PAE) cell
PBS	Phosphate Buffered Saline
PFA	Paraformaldehyde Fixation

PI(3)-kinase	Phosphoinositide 3-Kinase
PI(3)P	Phosphatidylinositol 3-Phosphate
PI(3,5)P2	Phosphatidylinositol 3, 5-Bisphosphate
PI(4,5)P_2	Phosphatidylinositol 4, 5-Bisphosphate
PTK	Protein Tyrosine Kinase
pY	Phosphotyrosine
Rab	Ras-Related Proteins in Brain
Raf-1	Proto-Oncogene c-Rapidly Accelerated Fibrosarcoma
Ras	Rat sarcoma
REP	Ras-Related Proteins in Brain escort protein
RILP	Rab-interacting lysosomal protein
RING	Really Interesting New Gene
RME	Receptor- Mediated Endocytosis
RT	Room Temperature
RTK	Receptor Tyrosine Kinases
SAND-1 / MON-1	Monensin Sensitivity 1
SH2/ 3	Src Homology 2/ 3
Shc	Src homology 2 domain containing
SNAP	Soluble N-etylmaleimide-sensitive factor attachment protein
SNARE	Soluble N-ethylmaleimide-sensitive factor attachment protein receptor
SNX	Sorting nexins
SOS	Son of Sevenless
Src	Proto-oncogene tyrosine-protein kinase Sarcoma
TAE	Tris-acetate-EDTA
TBST	Tris-Buffered Saline and Tween 20
TGF	Transforming Growth Factor
Ub	Ubiquitin
VAMP	Vesicle Associated Membrane Proteins
V-ATPase	Vacuolar-type H+- Adenylpyrophosphatase
Wt	Wildtype

1 Introduction

Intracellular transport consists of a finely tuned and highly regulated network of complex machinery, compartments and pathways that ensure the integrity, sorting and correct contents of the endomembrane system. The sorting is initiated by recognition of structural information present on proteins, which are then ushered into the appropriate pathway. The specific transport mechanism then targets the protein to its final destination. Trafficking is a multi-step process, and basic functions and mechanisms are under constant control. Disruption at any part of this process could have severe consequences for the organism as a whole. Faulty trafficking has been found to be the underlying reason in many human diseases. Increased understanding of the mechanisms and proteins involved gives the potential for improved treatments of human diseases such as leukemia [1], Menkes' disease [2], and Prion disease [3].

The epidermal growth factor receptor (EGFR) is a transmembrane tyrosine kinase receptor, essential to normal cell functions. EGFR activity is important for growth, motility, and proliferation. The signaling strength and duration is therefore tightly regulated by feedback mechanisms. The signal is most commonly attenuated by endocytosis [4]. The overexpression and abnormal activities of EGFR has been associated with cancer progression and metastasis, which is why it has been under scrutiny for the past few decades. Historically EGFR was the first receptor found to contain a tyrosine kinase [5], in addition to being the first receptor linked to human cancer [6]. Since then it has been widely used as a model system for various studies.

1.1 Endocytosis

Endocytosis provides the opportunity for transportation of large quantities of material across phospholipid barriers. The process is highly regulated [7] and essential for cell maintenance, and fine-tuning of signaling pathways [8]. Macromolecules are internalized by a controlled invagination and budding of the membrane. The newly formed vesicles are sorted into intracellular organelles called early endosomes. Ingested cargo, such as signaling receptors and membrane proteins, can be recycled back via recycling endosomes [9]. Other cargo is passed onto late endosomes, and will eventually be degraded in lysosomes [10].

There are multiple types of endocytic processes, generally distinguished by the kind of endosome formed, type of cargo, and machinery involved. A few of the many strategies cells have for internalizing particles and solutes are phagocytosis, pinocytosis, receptor-mediated endocytosis, and a variety of less-defined internalization pathways. Pinocytosis is generally involved in fluid and solute uptake, while phagocytosis engulfs larger particles [11]. The best-characterized internalization pathway is receptor-mediated endocytosis. Although a proportion occurs via caveolae, the majority is clathrin-dependent [12]. The cargo is selected by various adaptor proteins, which in turn recruit coat proteins, e.g. clathrin [13]. The coat proteins along with other adaptor proteins mediate membrane deformation.

Receptor-mediated endocytosis allows the cell to regulate the response to external stimuli, by internalizing the activated receptor. In general terms ligand-induced internalized vesicles are either recycled or directed to lysosomes for degradation. The internalization was originally thought to be important for negative feedback and signal attenuation [14-16]. In some cases the decrease of available receptor results in a dose response to subsequent stimuli, where a higher ligand concentration is required, otherwise known as cell desensitization [17]. Recently, it has become clear that endocytosis is more complex; signaling is not simply restricted to the plasma membrane. Instead receptor tyrosine kinase (RTK) signaling can continue from endosomes [18, 19]. After ligand binding and receptor internalization, the phosphorylated cytosolic tail is still exposed to the cytosol, allowing the receptor to continue signaling until either the ligand dissociates or the receptor is incorporated into multivesicular bodies (MVB). The term signaling endosomes has become well established in the later years, and defines endosomes, including MVBs, as microenvironments ideal for signal propagation with added specificity, functioning as signaling platforms [20-22].

1.1.1 Receptor-Mediated Endocytosis

One of the most specific pathways of internalization is receptor-mediated endocytosis (RME) and allows for the cell to regulate the response to external stimuli. Signaling molecules or ligands bind to their appropriate transmembrane receptors present on the plasma membrane, setting into action a chain of events. The receptor-ligand complexes dimerize, clustering together on the membrane. This forms concentrated domains that can more easily interact with adaptor and accessory proteins important for internalization. There is an inward budding of the plasma membrane, giving rise to endocytic vesicles that pinch off from the cell surface. The newly formed endocytic vesicles undergo a series of fusion cycles, and the cargo is trafficked to its final destination. Recently the mechanism has been implicated to have signal-propagating functions as well, evidence being based on the initial discovery that a decrease in endocytosis also hindered certain signaling pathways [8, 23].

The main groups of ligands known to internalize by such a process are cytokines, growth factors, and hormones, e.g. interleukin-1, epidermal growth factor, and insulin [24]. The afore-mentioned molecules are all signaling peptides, however transferrin, a molecule involved in cell metabolism, is also internalized by RME [25]. Alternatively the process can also be misused or “hi-jacked” by pathogens, for instance influenza virus takes advantage of RME by binding to sialic acid on cell surface receptors [26].

The main endocytic pathways are most commonly divided into clathrin- mediated, and clathrin- independent endocytosis. Clathrin-mediated endocytosis (CME) is the best understood coated pathway, mainly because this pathway utilizes a coat that can easily be distinguished by electron microscopy [27]. Clathrin- independent endocytic mechanisms like macropinocytosis and phagocytosis happen more frequently, and internalize larger volumes [28, 29]. Macropinocytosis is mainly used for replenishing nutrients, while phagocytosis is used as a defense against pathogens [11].

1.1.2 Coat Proteins

Transport between endomembrane compartments is mediated by coat proteins. Coat proteins are important for cargo selection, membrane curvature, and stabilizing the vesicle formation. Receptor-mediated endocytosis is generally facilitated by such proteins. There are three main coat proteins:

- Clathrin
- COP-I
- COP-II

The directionality of COP-I is still controversial, yet the coated transport is involved in mediating intra-Golgi transport, and retrograde transport to the endoplasmic reticulum (ER) [30]. COP-II mediates anterograde transport from the ER to the Golgi [31] and clathrin mediates trafficking from the plasma membrane and Golgi [32].

1.1.3 Clathrin

The best-characterized coat protein is clathrin. Clathrin consists of a three-legged structure formed by three clathrin heavy chains (CHC) each with a clathrin light chain (CLC) bound at the vertex, or intersection (Figure 1). The clathrin structure is referred to as a triskelion, which forms a polyhedral lattice when polymerizing on the plasma membrane [33]. The CLCs mediate clathrin assembly, and contain protein domains that bind the uncoating protein HSC70 [34]. Triskelions self-assemble into a basketlike convex structure, using the trimerization domain located at the vertex of the heavy chains [35].

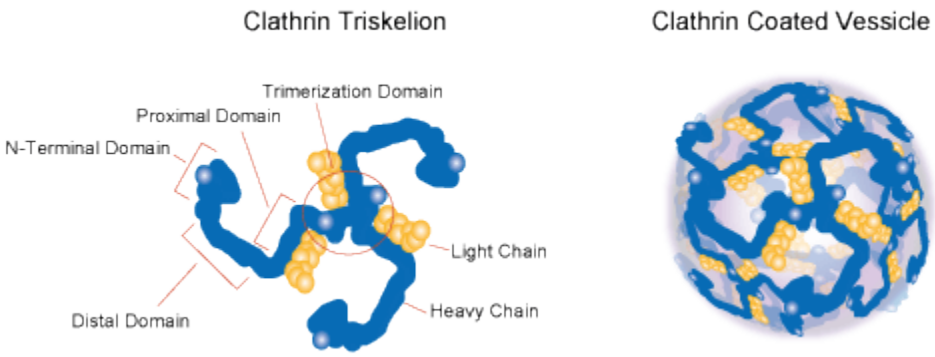

Figure 1 Schematic diagram of the Clathrin triskelion. Copyright © 2015 Sigma-Aldrich Co. LLC. All Rights Reserved [36].

The coat structure is a closed convex shell constructed of pentagons and hexagons [37]. Clathrin coated vesicle (CCV) formation is a multistep process and requires numerous different proteins, for instance adaptor proteins for cargo selection, fission factors like the GTPase dynamin and uncoating proteins like auxillin and HSC70.

1.1.4 Clathrin-Mediated Endocytosis

CME is one of the major surface receptor internalization pathways. EGFR is one of the many receptors that utilize this pathway. The initiation of CME is in part still unclear. The adaptor protein 2, AP-2, is essential for CME, acting as a stabilizing scaffold and recruiter for the clathrin triskelion [38], and crosslinking clathrin to the membrane and cargo. Upon binding the phosphatidylinositol 4, 5-bisphosphate ($PI(4,5)P_2$) containing membrane, AP-2 assumes an open conformation. The conformational change allows for binding to endocytic motifs present on the cytosolic tail of the cargo [39]. Clathrin binds weakly to AP-2 resulting in an increased incorporation rate forming the clathrin coated pit (CCP). The clathrin-AP-2 interaction is stabilized further by interactions with FCHO1/2 [40], although this mechanism is still unclear. The FCHO proteins can sense low curvature and/ or induce curvature via their N-terminal F-BAR domain [41]. This domain is similar to the BAR (Bin-Amphiphysin-Rvs) domain present in dynamin [42]. The FCHO1/2 complex may bind to the membrane at low curvature, and has been implicated in defining the site of assembly. It is important for stabilizing the forming clathrin lattice [40, 43].

Clathrin assembly must pass temporal and spatial checkpoints for progression, if not the CCP undergoes abortive turnover. A successful coat formation takes approximately 1 minute [44]. AP-2 not only recruits clathrin but also other components such as Eps15, Epsin, amphiphysin, and dynamin. These factors are necessary to drive and regulate the vesicle formation. As the membrane curvature is stabilized due to clathrin polymerization, Eps15 is recruited at the edges of the invagination [45]. In addition Eps15 is involved in assisting clathrin coat rearrangement during invagination and fission events [46], whereas Epsin drives membrane curvature [47].

Prior to membrane scission amphiphysin binds to the plasma membrane, acting as a linker-protein for both dynamin, and clathrin. Ultimately, amphiphysin assists in the dynamin localization [48]. Endophilin facilitates the membrane curvature [49], and recruits both synaptojanin and dynamin [50]. Synaptojanin is involved in vesicle uncoating and has been

indicated to regulate the activity of dynamin [51]. Dynamin is a GTPase that contains a BAR domain. The BAR domain binds and polymerizes around the neck of the vesicle and mediates vesicle scission [52]. Although this mechanism is still partially unclear, there is evidence that the subsequent pinching is due to GTP hydrolysis induced elongation of the "neck" [52]. Uncoating of the vesicle is regulated by the ATPase HSC70 and its cofactor auxillin [53].

It has been proposed that the clathrin-mediated internalization of EGFR is limited, and can become saturated at high ligand concentrations [54]. Under these conditions the receptor-ligand complex can be internalized by clathrin-independent endocytosis, although this is a much slower pathway [55].

1.1.5 Clathrin-Independent Endocytosis

Clathrin-independent endocytosis (CIE), also known as non-clathrin-mediated endocytosis refers to a range of pathways that do not involve clathrin. CIE internalizes a large variety of cargo and can be hijacked by pathogens to gain access to the cell. A vast diversity has been observed, making classification of CIE difficult. In general terms these mechanisms use various adaptor proteins to internalize cargo. These pathways can further be divided into small scale or large scale endocytosis [56].

<u>Small scale endocytosis:</u>

- Dynamin- dependent:
  - Caveolae
  - RhoA
- Dynamin- independent:*
  - CLIC/GEEC
  - Flotillin
  - Arf6

* The dynamin- independent processes may use actin polymerization and connections to mediate scission.

<u>Large scale endocytosis:</u>

- Phagocytosis
- Micropinocytosis

For further information on CIE, please see Mayor *et al.* [56].

1.2 Epidermal Growth Factor Receptor

EGFR is crucial for multicellular organisms and coordinate cell processes such as growth, differentiation, migration, apoptosis, and wound healing [57, 58]. The receptor has a complex signaling network that is normally under stringent control [59]. Overexpression or increased receptor availability often results in the uncontrolled signaling in tumors. Abnormal receptor signaling has been linked to several epithelial cancers, for example glioblastoma, prostate, breast, and colorectal carcinomas are often associated with such dysregulation [60]. EGFR's transforming ability underlines the necessity to understand the mechanisms controlling the receptor's activity, downstream signaling events, and intracellular trafficking. Signal intensity and duration is regulated by internalization. Ligand binding initiates receptor dimerization and receptor activation, followed by subsequent internalization [61]. Once internalized, the receptor-ligand complex is either recycled back to the plasma membrane or sequestered into lysosomes for degradation.

1.2.1 Epidermal Growth Factor, EGF

For humans there are more than 30 different ligands that may activate EGFR, all of which generate signals differing in strength and cellular response. The most common ligands are: EGF-like molecules, transforming growth factor (TGF)-α, and neuregulins. Other ligands include: amphiregulin, betacellulin, epigen, epiregulin, and heparin-binding-EGF [60, 62]. The ligands are synthesized as transmembrane proteins, with an EGF module. The pro-EGF is enzymatically cleaved by a metalloprotease, releasing the soluble active ligand [63, 64]. There is evidence that the different ligands initiate different trafficking. The TGF-α ligand promotes receptor recycling, since the ligand dissociates from the receptor in acidic interior of the gradually acidifying endosomes. EGF binding to EGFR is more pH stable and remains associated with EGFR in the maturing endosomes, leading to receptor degradation [65, 66]. This study has focused on EGF.

1.2.2 ErbB Family

The ErbB super family is made up of four interacting mammalian receptor types: EGFR (ErbB1/HER1), ErbB2/HER2, ErbB3/HER3, and ErbB4/HER4. The four receptor types share a common basic structure (Figure 2):

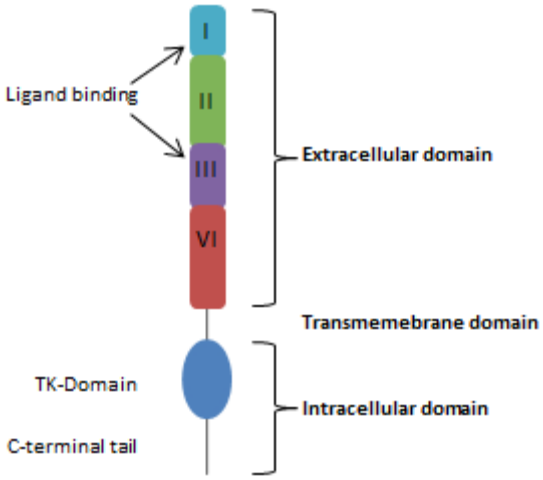

- Extracellular ligand-binding domain
  - Domain: I, II, III, VI
- Transmembrane domain, hydrophobic
- Intracellular domain
  - Conserved tyrosine kinase domain
  - C-terminal tail, the regulatory region

Figure 2 Schematic diagram of the structure of EGFR

Among the four different family members the extracellular domain is less conserved, suggesting ligand specificity[67]. The differences in the C-terminal domain of the receptor homologues generate a greater diversity of possible signaling pathways. The ErbB receptors may form homo- or hetero- dimers with other family members. ErbB2 does not seem to have a high affinity ligand, and has been proposed to act simply as a co-receptor [68]. ErbB3 has an inactive kinase domain, however it can still dimerize and activate the other monomers [69].

Main characteristics for the ErbB family are the “receptor-mediated” dimerization mechanism and the intrinsic protein tyrosine kinase (PTK) activity. Once the ligand has bound and induced a conformational change, the dimerization arm is exposed [70]. The kinase domain is activated by the conformational change induced by receptor dimerization. Furthermore the cytosolic tail contains several autophosphorylation sites implicated as a regulatory element, inhibiting the kinase domain [71, 72].

1.2.3 EGFR Structure

EGFR has a molecular weight of 175 kDa, and consists of a single polypeptide chain of 1210 amino acids [73]. It is also heavily N-glycosylated which is important for protein-protein interactions [74]. The receptor can be divided into three parts:

- The extracellular domain
- The transmembrane domain
- The intracellular domain

The extracellular domain is heavily glycosylated and has a ligand-binding domain. There are four subdomains: I, II, III and IV. Domains II and IV are homologous cysteine-rich regions, while I and III bind the ligand.

The transmembrane domain has 23 hydrophobic amino acids that form a single pass α-helix. This portion is important to propagate the allosteric conformational change initiated by ligand binding, necessary to generate a biological response [75].

The intracellular domain includes a juxtamembrane region, a kinase domain, and a C-terminal tail. The main function of this domain is to amplify and transduce the extracellular signal initiated by ligand binding. The juxtamembrane segment is between the transmembrane and the tyrosine kinase domain, and is divided into an N-terminal half, and a C-terminal half [76]. The kinase domain is an intracellular tyrosine kinase, and the catalytic part of the receptor, essential for signal transduction. The kinase domain transfers phosphate to tyrosine residues on the C-terminal tail, and is necessary for cross-phosphorylation of the receptor dimer. Endocytosis, degradation and effector molecule interaction are dependent on the autophosphoylation status of the receptor [77]. Appropriate effector and adaptor molecules are recruited to the phosphotyrosine residues, resulting in receptor clustering on the plasma membrane. The EGFR clusters are sequestered into clathrin-coated pits and internalized. Recent studies have shown that the internalization is ligand dependent, and non-clathrin endocytic pathways can supplement the clathrin-dependent pathway [78].

1.2.4 Conformational Change & Dimerization

Binding of the bivalent monomeric ligand to the receptor extracellular subdomains, I and III, imposes a constraint on the structure of the receptor, leading to a conformational change (Figure 3). As a consequence the dimerization arm, present on subdomain II, is exposed. In the receptor's inactive state the arm is tethered, forming intramolecular interactions with subdomain VI. After a ligand has bound the exposed arm reaches out, forming homo- or hetero- dimers with the other ErbB family members [79]. Dimerization is important for signal transduction, since it initiates activation of the kinase domain. The autophosphorylation in turn forms docking sites for signaling complexes.

Receptors may dimerize partially without ligand, but will detach again due to a low dimerization affinity. Ligand binding increases the affinity [80]. In certain cancer types, this delicate balance is disrupted and receptor monomers may bind even without the presence of ligand. The mutation L834R is the most common single residue mutation. In the study presented by Shan *et al.* 2012, they found L834R mutants to have a higher affinity for dimerization, lowering the threshold for activation [81]. Such mutants disrupt the receptor's intrinsic ability to regulate dimerization, elevating the receptor's basal activity.

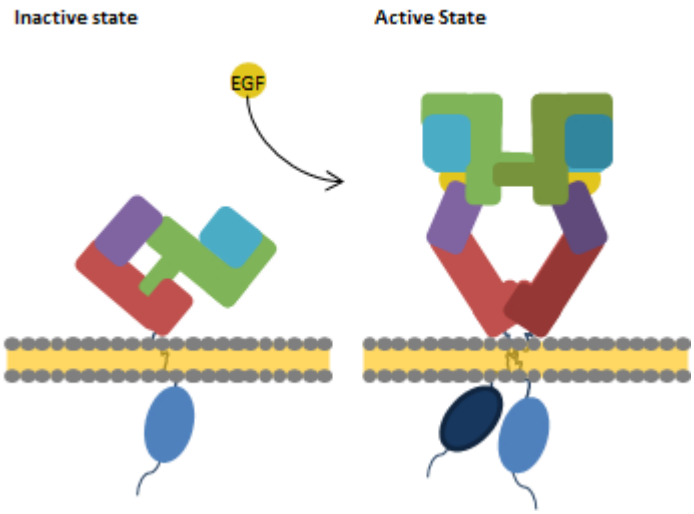

Figure 3 Schematic diagram of the extracellular conformational change upon ligand binding resulting in receptor activation

1.2.5 Activation

Once the growth factor binds and the monomeric receptor dimerizes, the receptor activates by autophosphorylation. The phosphotyrosine residues form docking sites for adaptor proteins containing Src Homology 2 (SH2) domains [82]. Numerous signaling proteins are then recruited, including the adaptor protein growth factor receptor-bound protein 2 (Grb2). Grb2 is a small protein (25kDa), consisting of one SH2 domain flanked by two SH3 domains [83]. The adaptor is involved in coupling the activated receptor with intracellular signaling [84]. Subsequently, signal down-regulation is initiated through internalization and ubiquitin-targeted degradation. Grb2 may bind to the activated EGFR, either directly at phosphotyrosine (pY) 1068 and pY1086 [85], or indirectly through Shc [86]. Shc has been found to bind Y1148 and Y1173 on the receptor [87]. Grb2 can also recruit the E3 ubiquitin ligase, Casitas B-lineage Lymphoma (Cbl), via interaction between the SH3 domain of Grb2 and the proline rich- region of Cbl [88]. Alternatively, Cbl can directly dock to the receptor at pY1045, binding via its N-terminal tyrosine-kinase-binding (TKB) domain. The binding of Cbl to EGFR results in its ubiquitination [89-91], at various lysine residues in the EGFR kinase domain [92]. Multiple docking sites ensure that the dimeric receptor is ubiquitinated, and internalized in an endocytic vesicle. It has been shown that a certain ubiquitin density is necessary for lysosomal targeting and degradation [92].This indicates that internalization and degradation is uncoupled.

Cbl is an E3 ubiquitin ligase, and is required for targeting the receptor for degradation. The ligase allows for involvement of the Endosomal Sorting Complex Required for Transport (ESCRT) machinery. The Cbl family consists of conserved negative regulators that attenuate RTK signaling. There are three known homologues, c-Cbl, Cbl-b and Cbl-3. The N-terminal domains are essential for the E3 ligase activity [93], and contains the tyrosine-kinase-binding, linker and RING finger domains. Cbl binding is important for EGFR ubiquitination, by interacting with SH2 and SH3 domain-containing proteins. Sigisimund *et al.* presented the possibility for a threshold-controlled mechanistic model, where the EGF concentration could control the cell's response. Under conditions of a linear increase in ligand, the ubiquitination level has a sigmoidal increase, generating a threshold EGF concentration above which the EGFR was internalized by CIE [78].

1.2.6 EGFR Signaling

Activation of EGFR stimulates several signaling pathways, often with similar physiological outcome. By activating the Shc, Grb2, and Ras/MAPK signaling pathway, the signal transduction initiates processes like cell division, differentiation, survival, apoptosis, and migration [94, 95]. The main adaptor protein for activation of the Ras pathway is Grb2. When EGFR is inactive, Grb2 is usually localized in the cytosol bound to either Cbl or son of sevenless (SOS), a Ras exchange factor. SOS binds to one of the two SH3 domain on Grb2, forming a complex. Upon activation of EGFR, the Grb2 SH2 domain may bind to the phosphotyrosines 1068, and 1086 [85]. Ras proteins associate with the plasma membrane, and interact with the Grb2/SOS complex. The interaction results in Ras activation by exchanging GDP to GTP. Ras then activates Raf-1 which initiates activation of ERK [96]. ERK then enters the nucleus and activates transcription factors [97] such as cyclic AMP-responsive element-binding protein (CREB) [98].

Upon EGF stimulation Shc, itself, becomes phosphorylated creating a binding site for the SH2-domain of Grb2, acting as a link between the RTK and Ras activation via Grb2 [82]. Grb2 binding initiates both signal propagation and attenuation, by activation of several signaling cascades, internalization of the receptor and ubiquitination-targeted degradation via the recruitment of Cbl. The main regulator of the signal transduction is internalization of the receptor-ligand complex which can result in either degradation in the late endosome/ lysosome, or recycling back to the cell surface [99].

1.3 The Endocytic Pathway

After EGFR the signal transduction is controlled by the endocytic pathway. Newly formed vesicles containing the receptor move along the cytoskeleton and undergo highly regulated fusion events with the endosomal compartment. There is a continuous cycle of fusion and fission that remodels the endomembrane system. This is essential for intracellular trafficking.

1.3.1 Cytoskeleton

The cytoskeleton is a highly dynamic and well distributed network used by endosomes to navigate through the cell interior. Compared to diffusion rates the presence of a network greatly facilitates the trafficking from donor to target compartment [100]. The network consists of actin filaments, microtubules, and intermediary filaments. The microtubule and actin networks act as a highway for intracellular transport, with motor proteins moving along the cytoskeleton driving the transport. Myosin, dynein, and kinesin are the main classes of motor proteins that mediate transportation. These proteins are energy dependent, and the driving force of cellular trafficking. The molecular motors function by attaching to either a vesicle or organelle, and pulling their cargo to its destination.

Myosin is actin- dependent, while dynein and kinesin move along microtubules. The microtubule network mediates most of the intracellular traffic [101]. The plasma membrane is connected to the actin-based cytoskeleton, and is required for vesicle transport. Actin, along with the motor protein, myosin, mediates the vesicle budding and fission. At a later point the vesicle switches from actin filaments to microtubules, and continues the trafficking [102]. The coordinated motors walk along the tracks in a hand-over-hand- manner, before eventually the vesicle is released at its destination [103-105].

An intact cytoskeleton is necessary for most types of endocytosis. Several accessory proteins are involved in endocytosis by directly or indirectly regulating actin dynamics and assembly. This is especially true for CME, where actin is implicated in the invagination of the plasma membrane.

1.3.2 Endosomal Sorting

Trafficking of the newly internalized material involves both homotypic and sequential fusion of endosomal compartments, using appropriate machinery, such as SNAREs, and Rab proteins. The newly formed endosomes undergo a maturation process, generally described as an "early" to "late" transition, during which some cargo molecules are sorted for recycling and others for lysosomal degradation. Rab proteins, for example Rab5 and Rab7, regulate the maturation and guide the endosome to its correct location. They are compartment specific and can be used to distinguish between endosomal compartments; Rab5 marks early endosomes and Rab7 marks late endosomes. Rab proteins form distinct domains on the endosomal membranes and are important for regulation and recruitment of compartment specific effectors [106]. While the conversion of early endosomes to late endosomes is a maturation process [107], trafficking to lysosomes is a combination of "kiss and run" events and sequential fusion [108].

At all stages, protein interactions between donor and acceptor membranes are required to overcome the energy barrier for membrane fusion. Tethering proteins, such as EEA1, CORVET and HOPS, bring the opposite membranes closer [109]. SNARE proteins such as VAMP-synaptobrevin and SNAP-25 are considered to be essential for fusion events [110]. The donor and acceptor membranes are brought into close proximity, so that SNARES can drive the fusion of lipid bilayers. v-SNAREs pair up to their specific t-SNAREs, giving an extra degree of specificity. After the fusion event N-ethylmaleimide sensitive fusion protein (NSF) is required for untangling the SNAREs [109].The newly formed vesicles fuse with early endosomes which are Rab5 positive. Here the cargo undergoes selective sorting; it may be recycled back to the PM or trafficked through the endocytic compartment to the lysosome for proteolytic degradation.

1.3.3 Rab Proteins

Rab proteins are master regulators in the endocytic pathway [111]. The small monomeric GTPases mediate endosome targeting, by regulating docking and tethering. Newly synthesized Rab proteins are selectively distributed by the Rab escort protein (REP) complex, and are inserted into the correct membrane by GDI-displacement factor (GDF). The guanine dissociation inhibitor (GDI) enables recycling of the Rabs between the membranes, binding the GDP-bound form of Rab [112]. Due to their intrinsic GTPase activity Rab proteins function

as molecular switches. In the GDP-bound state they are turned off, however if the GDP is replaced with a GTP the Rab protein is active [113]. In its active state the Rab may associate with several Rab effectors, which in turn mediate endosome trafficking. The conversion from inactive to active is performed by a guanine exchange factor (GEF). GTPase-activating proteins (GAPs) catalyze the intrinsic GTPase activity of the Rab, leading to its inactivation.

There are approximately 70 known human Rab proteins, almost all of which are involved in endocytic trafficking. The Rab proteins are not only involved in selectively marking endosomes but are also important for the motor-driven transport of endosomes [114, 115]. For example the Rab7 interacting lysosomal protein (RILP) is a Rab7 effector protein, required for recruitment of dynein/dynactin motors to late endosomal compartments such as lysosomes. Eventually these compartments accumulate at the microtubule-organizing center (MTOC) [116].

Rab5 is a ubiquitous GTPase and functions in the early part of the endocytic pathway, while Rab7 facilitates the late endocytic pathway. Rab5 is primarily located on early endosomes, although it can be detected on the plasma membrane, where it facilitates CCV formation and fusion with early endosomes, as well as homotypic fusion between early endosomes. Rab7 functions downstream of Rab5 and is involved in transport between late endosomes and lysosomes [117].

1.3.4 Early Endosomes

Cargo vesicles go through homotypic fusion, growing in size and eventually develop into early endosomes [24, 118]. A major regulator of early endosome transport is Rab5. The small GTPase forms distinct domains, where there is a local synthesis of phosphatidylinositol 3-phosphate (PI3P) by PI(3)-kinase class II and III [106, 119]. The domains remain intact by protein oligomerization [120], and possibly actin interactions so to avoid lateral diffusion [106]. Rab5 recruits such effectors as the Rabaptin-5/Rabex-5 complex, Rabenosyn-5, and EEA1 (Figure 4). Rabaptin-5 forms a complex with Rabex-5, which is important for nucleotide exchange of Rab5. Active Rab5 then recruits other Rab5 effectors [121]. Rabenosyn-5 is necessary for clathrin coated vesicle fusion with early endosomes, and early and late endosome fusion [122]. A critical regulator for early endosomes fusion is the tether protein EEA1, which forms a complex with Syntaxin and NSF [119].

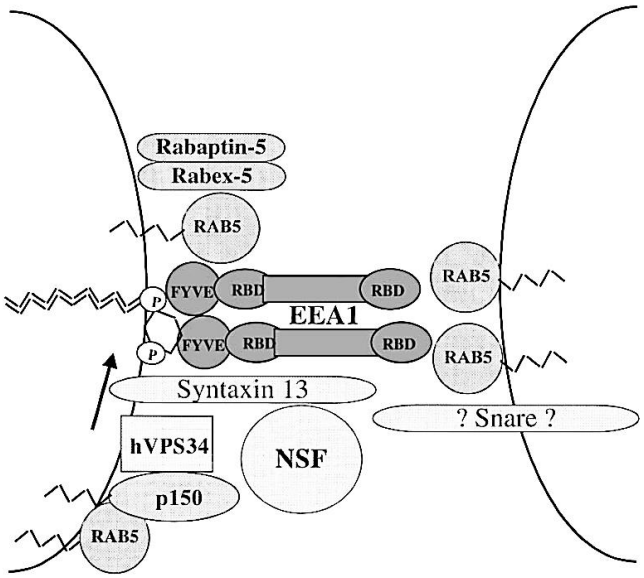

Figure 4 A model of homotypic fusion, showing the oligomeric complexes and EEA1 mediated tethering with active Rab5. Figure was adapated from Backer 2000

Early endosomes are thought to be the main sorting compartment in the endocytic pathway, receiving endocytosed material from several different pathways, not just receptor-mediated endocytosis [123]. The early endosomal compartment has a complex morphology, including a tubulovacular structure which is essential for protein sorting [124] (Figure 5). Receptors destined for recycling back to the plasma membrane are sequestered into tubular parts of the early endosome. The tubules are severed by fission events mediated by SNX proteins, and transported to the plasma membrane [125].

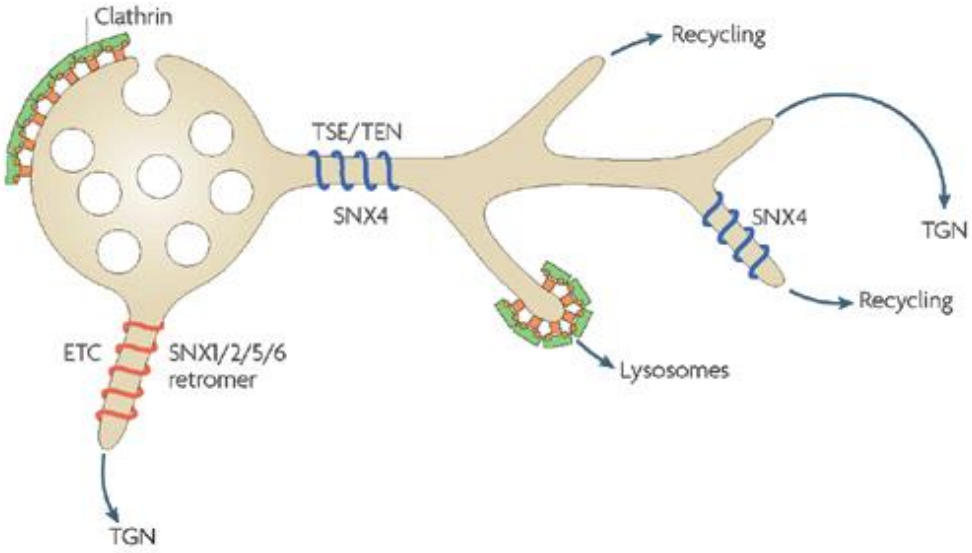

Figure 5 Schematic diagram of the early endosomal compartment. The clathrin bilayer involved in the formation of ILVs and the tubular endosomal network important for sorting, adapted from Cullen 2008.

1.3.5 Recycling

There are two main recycling pathways: a rapid, Rab4-dependent pathway, and a slow Rab11-dependent pathway. After endocytosis most membrane proteins are recycled back to the PM, along with liquid and lipids. The Rab4-dependent rapid recycling aids in restoring the membrane removed from the plasma membrane during endocytosis. Recycling allows the cell to return molecules back to their appropriate compartment, for instance resident ER and Golgi proteins. It is also energy efficient if the cell can reuse certain proteins. Endocytosis has been shown to have a dual function: signal attenuation and signal transduction, providing the cell with both spatial and temporal dimensions to signaling events. Consequently, recycling of the receptor has a profound impact on signal longevity.

Recycling back to the plasma membrane can occur directly from the early endosome. There is also an endosomal compartment closer to the MTOC, known as the endocytic recycling compartment. The slow recycling route involves trafficking cargo from early endosomes to the endocytic recycling compartment, back to the plasma membrane. The route is highly regulated, more so than the recycling tubules involved in rapid recycling from the early endosome and is Rab11-dependent.

Receptors and other proteins that are to be degraded are concentrated into the vesicular part of the early endosome. These will eventually be internalized into small intraluminal vesicles, ILVs. Formation of ILVs takes place on the early endosome at characteristic bilayered clathrin microdomains, ushering ubiquitinated protein into the degradative pathway [126]. This process is facilitated by ESCRT and other factors [127]. Eventually these endosomes mature into multivesicular late endosomes. The ubiquitin attachments on EGFR are removed upon ILV formation, by deubiquitination enzymes (DUBs), to avoid unnecessary loss of ubiquitin [128]. The receptor is dephosphorylated by protein tyrosine phosphates, further promoting ILV internalization [129].

1.3.6 Multivesicular Bodies, MVBs

Endocytic cargo is transported from late endosomes to lysosomes via what has been suggested as a “kiss-and-run” event. The term “kiss-and-run” was coined to describe the transient fusion events between endosomes and lysosomes. In order to explain the discrepancies between the maturation model and observations, complete fusion between the compartments has also been proposed.

There are two major pathways for protein degradation, either by the proteasomes or in lysosomes. The proteasome may be involved in degradation of membrane proteins through the Endoplasmic-Reticulum-Associated Protein Degradation (ERAD) process, after they have become poly-ubiquitinated. However this process is mostly used for misfolded proteins, retrotranslocated from the ER. Lysosomal degradation is the main pathway for integral membrane proteins. Multivesicular bodies (MVBs) form along the pathway to late endosome, by invagination of the limiting membrane creating ILVs. Upon fusion with lysosomes the content is exposed to lysosomal hydrolase and degraded. The lysosomal pathway is important for degradation of membrane proteins, which are then broken down to building blocks ready for reuse [125, 130] .

The endosomal sorting complex required for transport, ESCRT complex, aids in MVB biogenesis, and consists of:

- ESCRT-0
- ESCRT-I
- ESCRT-II
- ESCRT-III

The ESCRT complex is ubiquitin-dependent, and is thought to recruit cargo to MVBs and mediate the internalization process. ESCRT-0 is involved in membrane recruitment and specificity. ESCRT-I is important for cargo selection. ESCRT-II and –III guide the cargo into the ILVs under MVB formation. Ubiquitin is removed as the cargo is sorted into the MVB lumen. The ESCRT complex is released from the MVB and recycles for the next round of MVB sorting [131].

1.3.7 Ubiquitination

Ubiquitin is involved in internalization of several membrane proteins, by mediating the interactions between the membrane protein and the sorting machinery. ESCRTs recognize the ubiquitin, covalently attached to cargo, and direct the ubiquitinated protein into MVB. Further the post-translational modification is important for other protein functions as well, for example, targeted protein degradation, protein-protein interactions and subcellular localization [132].

Ubiquitin is a small regulatory protein (8kDa) and may be attached to a protein either as a single attachment (mono) or in chains. Protein ubiquitination involves three main enzymes:

- E1, ubiquitin-activating enzyme
- E2, ubiquitin-conjugating enzyme
- E3, ubiquitin ligase

First ubiquitin is activated; the C-terminal tail forms a thioester bond with a cysteine residue on E1. This mechanism is ATP-dependent. Next ubiquitin is transferred to a catalytic cysteine residue on E2. E3 then binds both the ubiquitin-E2, and substrate, so to catalyze the transfer of ubiquitin to a lysine residue on the substrate, resulting in a monoubiquitination. Once this has happened, certain E2/E3 complexes can further utilize other lysines on the substrate-conjugated ubiquitin, generating polyubiquitination. A key feature of ubiquitin is that its C-terminus contains seven lysine residues, which may be used during polyubiquitin chain formation, providing the potential for both linear and branched polyubiquitin chains [133, 134].

Cbl, the E3-ligase, transfers ubiquitin from E2 ubiquitin-conjugating enzymes to EGFR, promoting lysosomal degradation. It has been shown that c-Cbl does not associate with EGFR1044, a mutant where the receptor is truncated after residue 1044. The receptor is internalized similar to the wild type (Wt) receptor, although not initially ubiquitinated. c-Cbl does not seem to be required continuously for degradation of EGFR, as suggested by dissociation at the same time as Y1045 is dephosphorylated [135]. Previous work by Eden et al found ubiquitin to be a key regulator of EGFR degradation, as well as showing that non-ubiquitinated receptors fail to interact with ESCRT and will not promote ILV formation.

1.3.8 Late Endosomes

Endosomal maturation from early to late is a multi-step process consisting of ILV formation mediated by ESCRT, acidification by V-ATPase [136], and a change in lipid composition PI(3)P → PI(3,5)P_2 [137]. As the endosome matures the tubular network disappears, and relocates towards the perinuclear region [117]. The Rab protein subdomains that coordinate transport and fusion through recruitment of tethering and docking factors change from Rab5 positive to Rab7 positive. In addition tethering proteins are switched (Figure 6). The endosomal tethering proteins CORVET and HOPS have gained increasing importance for endosomal maturation, their main functions being; bringing endosomal membranes together, interacting with Rab proteins, and regulating SNARE pairing [109]. Together Rab5, CORVET, and PI(3)P recruits SAND-1/ Mon1-Ccz1 [138]. SAND-1 drives the Rab conversion, by displacing Rab5 and recruiting Rab7[139] (Figure 7) . Subsequently HOPS replaces CORVET. This alters the endosome fusion specificity, resulting in a different coordination and control of endosomal traffic to the lysosome [140]. Late endosomes are generally rounder than early endosomes. They have a lower density, the membrane surface is negatively charged.

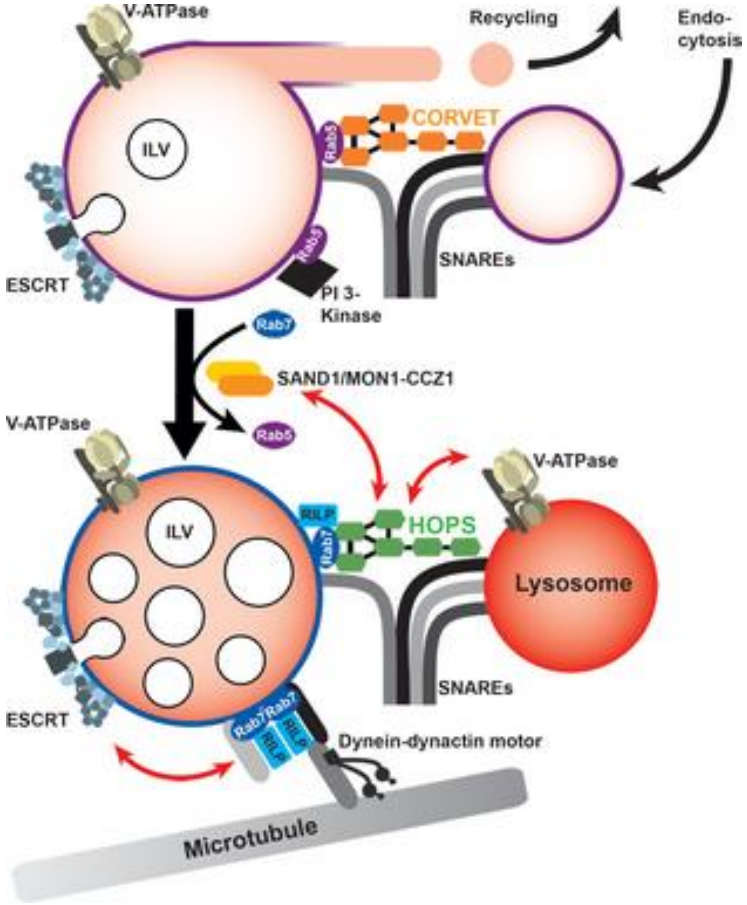

Figure 6 Endosome maturation: As the early endosome acidifies by V-ATPase, there is ILV formation. The PI(3)P-rich membrane is converted to PI(3,5)P2 by phosphatidylinositol 3-kinase and phosphatases, and a Rab conversion is mediated by Sand-1/ Mon1-Ccz1. The CORVET/HOPS complex mediates membrane fusion, and stabilizes SNARE attachments. Figure was adapted from Solinger 2013.

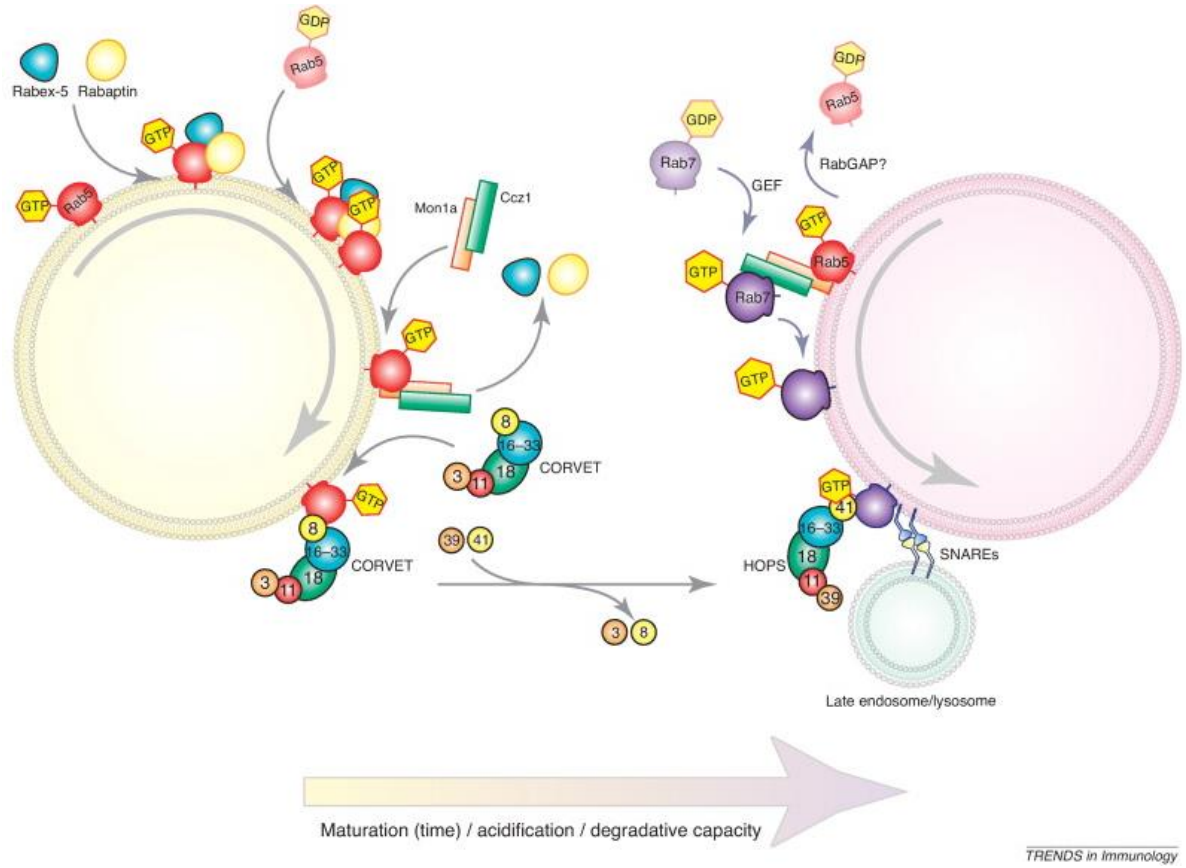

Figure 7 Rab5 to Rab7 conversion: Inactive Rab5 and Rab7 are located in the cytosol bound to GDI. ATP bound Rab5 present on early endosomes is activated by Rabex-5. Rabaptin5 mediates the Rabex-5 activity. Sand-1/ Mon1-Ccz1 drives the Rab conversion by displacing Rabex-5 from the membrane. This promotes the recruitment and activation of Rab7 on late endosomes. The endosomal tethering complex CORVET is replaced by HOPS. Figure was adapted from Fairn 2012.

1.3.9 Lysosomes

Lysosomes are similar to late endosomes in their biochemical makeup, however their functions are different. The limiting membrane contains lysosome associated membrane protein, LAMP, and lysosome integral membrane protein, LIMP, V-ATPase, and several transporters. LAMP and LIMP are also found on late endosomes. LAMP has been suggested to maintain the integrity of lysosomes by preventing the escape of hydrolase and cathepsins, in addition to being implicated in fusion between lysosome and autophagosomes [141]. LIMP has been implicated in transportation of lysosomal hydrolase [142], and fusion with phagosomes [143]. V-ATPase transports protons into the lumen, generating a highly acidic environment, necessary for the function of lysosomal hydrolase [144].

Recycling events from the late endosome has been discovered, for instance by fusing with the plasma membrane and releasing the ILVs as exosomes [145]. Cargo that is to be degraded cannot escape the degradative route, once present in lysosomes. Molecules required for the

functionality of the lysosomes are also retained within lysosomes. Furthermore lysosomes have a higher density, and may be separated from other endosomes by subcellular fractionation, a property discovery by Christian de Duve [146].

1.4 EGFR and Cancer

Proper EGFR signaling is key to a plethora of biological responses such as, apoptosis, cell division, motility, and differentiation [147]. Malignant mutations may effect downstream effectors and in turn alter transcription, inducing an uncontrolled cell growth, survival and migration[148]. Expression of certain mutations, for example a truncated receptor or an altered kinase domain, can result in the receptor being constitutively active [149]. In addition activated RTKs may interact with Src kinases, and regulate proliferation through the MAPK pathway. EGFR and Src have synergistic effects when the two kinases are trafficked together, as they often are [150]. Generally cancerous mutations impair interactions with Cbl, resulting in prolonged signaling. This is not the case for the most common EGFR variant of cancer, glioblastoma, where the receptor has a deletion of amino acid 267. The mutant receptor does not bind the ligand, yet it is active. In this case the receptor is not truncated, maintaining the regulatory C-terminal tail. The signal may be downregulated by Cbl-mediated ubiquitination.

1.4.1 Therapies

Chemoradiotherapy is the standard treatment for cancers. The treatment is a combination of two DNA-damaging agents; radiation and an alkylating agent. The main type of compounds used for targeting EGFR malignancies are, monoclonal antibodies such as, cetuximab, and a tyrosine kinase inhibitor such as, gefitinib. Cetuximab targets the receptor extracellularly, while, gefitinib targets intracellular domains. The two compounds both suppress EGFR stimulation. However they do not work for all cancer types, and there are secondary effects to the treatments. In addition the radiation itself may activate EGFR in a ligand-independent manner [151, 152].

The details of endocytic EGFR trafficking are still uncertain, including how chemoradiation therapy alters this process and how EGFR signaling responds to such a treatment. For this reason, elucidating the EGFR trafficking events is essential to developing future treatment.

2 Aim of the Study

EGFR has several important cellular functions including differentiation, apoptosis, and migration [147]. Upon ligand activation, the receptor dimerizes and undergoes a conformational change that activates the cytosplasmic kinase domain. The kinase domain then autophosphorylates the C-terminal tail containing several tyrosine residues. These phosphotyrosine residues form docking sites for adaptor proteins such as Grb2 and Cbl, which mediate EGFR signal propagation and degradation, respectively. Due to the position of the phosphotyrosines, the receptor can continue signaling after its internalization. Signalling is terminated by subsequent internalization of the endosomal EGFR into intraluminal vesicles. Overexpression in EGFR signaling has been observed as the cause in many cases of tumor progression and metastasis [153]. It is therefore necessary to examine the intricate details of signal attenuation. A greater understanding of the EGFR trafficking mechanisms will provide insights into how to approach the defects often associated with diseases.

The overall aim of the study is to elucidate the impact the phosphorylation pattern has on receptor trafficking. The properties will be explored by use of live cell imaging, visualizing the endocytic pathway by fluorescent markers, and examining the temporal and spatial distribution of EGFR. This includes the following sub aims:

- Developing a method valid for examining receptor trafficking through the endocytic pathway.
- Determining how receptors' phosphorylation regulates the receptors' trafficking.
- Elucidate the temporal regulation of receptor trafficking/sorting.

3 Materials and Methods

For product information see List of Materials, appendix 8.1.

3.1 Cell Culture: Maintenance

Cell Cultures

The experiments were carried out with HeLa cells, a human cervical cancer cell line (University of Oslo, Norway). All cells were routinely maintained in OK medium, consisting of: Dulbecco's Modified Eagle Medium (DMEM), supplemented with 25U/ml penicillin/streptomycin, 2 mM L-glutamine, and 10% fetal calf serum (FCS). Cell cultures, were incubated in at 37^{o}C in 95% humidified 5% CO_2 air incubator. The passage number did not exceed 20-25. Stably transfected Porcine Aortic Endothelial (PAE) cells were kindly provided by I.H Madshus and E. Stang. Four stable PAE cell lines each expressing either: Wt-, Y1-, Y2-, or Y3-EGFR were maintained under selection as appropriate. Y2 required Puromycine (1μg/ml) and Y1 and Y3 used G418 (400μg/ml).

3.2 Cell Treatment

Constructs

The constructs used are listed in the table below.

Table 1 Constructs used in this study

Gene/ Insert name	Named	Backbone	Produced by
EGFR	Wild type (wt)	pEGFP-N1	Madhus, IH
EGFR Y1045F	Y1	pEGFP-N1	Mutagenex Inc.
EGFR Y1068F Y1086F	Y2	pEGFP-N1	Mutagenex Inc.
EGFR Y1045F Y1068F Y1086F	Y3	pEGFP-N1	Mutagenex Inc.
Rab5-mCherry		pcDNA3	Skjeldal, FM [154]
Rab7-mCherry		pcDNA3	Skjeldal, FM [154]
Rab7		pmApple	Davidson, M. (Addgene plasmid # 54945)

DNA Transfection

HeLa cells were transiently transfected with one or two of the constructs described above, using Lipofectamine 2000. Transfection solutions were made as described below, cells were maintained in DMEM without antibiotics (-ps). Transfections followed the manufacturer's protocol with slight modification to reduce the amount of Lipofectamine2000.

Table 2 Transfection reactions

Plate type	Experiment	DNA (μg)	Lipofectamine (μl)	opti-MEM (μl)
35mm dish	Imaging	0.5-1	1.5	100
6 well plate (1well)	Stable cell line	0.5-1	1.5	100
12 well plate (1well)*	Immunofluorescence	0.25-0.5	7.5	50

Cells were plated on uncoated 35mm glass-based dishes so that at the time of transfection, they were 70-90% confluent. Lipofectamine 2000 and DNA were diluted in separate eppendorf tubes, 100μl/sample Opti-MEM, was added, and incubated at room temperature (RT) for 5min. The diluted DNA was then added to diluted Lipofectamine 2000 in a 1:1 ratio, total volume: 200μl/dish.

3.3 Microbiological Techniques

Transformation by Heatshock, Non-Viral Introduction of DNA into Bacteria

200μl competent cells (Top10F) cells were thawed and transferred to a chilled Eppendorf tube. 1μg DNA was added to each tube and incubated on ice for 10min. The competent cells were heatshocked at 42^{o}C for 1min, and placed on ice, 2min. 1ml LB medium was added and cells were incubated at 37^{o}C for 60min. Cells were pelleted by centrifugation 3220 x g for 5 min. Pellet was resuspended in 50μl LB medium and chosen amounts, generally 5 μl, were plated on agar plates containing the appropriate selection marker, in a sterile environment. Plates were incubated overnight at 37^{o}C. EGFP and mApple constructs required selection with Kanamycin, 50μg/ml. The mCherry constructs required Ampicillin, 100μg/ml.

The following day, a single colony was picked and used in inoculate 5ml LB medium with the appropriate antibiotic in a 15ml tube. Cultures were incubated at 37^{o}C, with shaking, until the

end of the day, ~8 hours. After the incubation period, 1ml of bacteria stock was used to inoculate a fresh 50ml LB culture in a 250ml Erlenmeyer flask with appropriate antibiotic. This culture was incubated at 37^{o}C overnight with shaking. The day after a Wizard Midiprep was performed to extract the DNA, according to the manufacturer's protocol (see appendix section 8.3). The yielded DNA concentration was measured with a NanoDrop ND-1000 Spectrophotometer (Saveen & Werner, AB, Malmö, Sweden).

3.4 Imaging Techniques

Fluorescent imaging is a valuable method for analyzing cellular functions, such as subcellular localization of proteins and organelles. By examining colocalization of two florescent labels, it is possible to determine distribution and infer interactions among molecules on larger structures such as membranous compartments [155]. This tool can be used to track protein interactions on either fixed or live samples.

Confocal Microscopy

Confocal microscopy is a specialized fluorescence imaging technique that improves image quality and resolution. The confocal microscope reduces background fluorescence by having a conjugate pinhole to the focal plane of the lens. In this project we used a point scanning laser confocal microscope, in which the excitation laser is scanned across the sample by two scanning mirrors. A pinhole is used to block the out-of-focus light that is emitted by the illuminated sample.

Confocal live cell imaging was carried out using an Olympus Fluoview 1000, inverted microscope mounted with a PlanApo 60x/1.42 oil immersion objective (Olympus, Hamburg, Germany) and photomultiplier tube detectors. Cells were maintained in an incubator chamber while imaging that kept stable 37^{o}C, and 5% CO_2 levels. Fluorochromes were excited with diode lasers.

Colocalization analysis: HeLa Paris cells were prepared for imaging as described above. EGF [100ng/ml] was added onstage during image acquisition. Cells transfected with Rab5-mCherry were imaged every 30seconds, for 1hour.

Rab7a -mCherry/ -mApple were imaged every 30seconds, for 2hour. The transfection rate of Rab7-mApple appeared to decrease the efficiency of EGFR transfection. It was therefore decided to transfect a lower concentration of the Rab7-mApple construct [0.25µg/µl]. For the Rab7 colocalization experiments HeLa-Kyoto cells were used. HeLa-Kyoto cells migrate less than HeLa Paris cells, and were therefore used for the 2hour and overnight experiments.

Spinning Disc

Cells were plated and treated as described for confocal microscopy. The Andor Revolution spinning disc microscope comprises an Olympus IX 71 inverted microscope fitted with spinning disc unit CSU22 and an iXon EMCCD camera for image capture, used with a PlanApo N 60x/1.42 NA oil immersion objective. The spinning disc uses a multiple pinhole disc to exclude out of focus light. The dichroic mirror, between the collector and pinhole disc, separates the emission light from the excited light. The imaging process is faster than single point scanning confocal microscopy and has a relatively low phototoxicity, which is good for live cell imaging.

Total Internal Reflection Fluorescence, TIRF

Cells were plated as described for confocal microscopy. The specimen must be mounted on a glass coverslip in an aqueous medium in order to ensure a sufficiently large change in the refractive index as excitation light passes through the glass into the sample. The principle is based on exciting the fluorophores closest to the glass coverslip, having a max depth of approximately 250nm. By exciting the specimen at a critical angle an evanescent wave or electromagnetic field is created in the medium, due to the refractive index difference between the glass and aqueous solution. The wave excites the fluorophores; due to the exponential decay of the evanescent wave only fluorophores closest to the interface are excited. TIRF microscopy generates images with a greater signal-to-background ratio for fluorophores close to the interface such as at the plasma membrane.

Unfortunately images acquired were deleted during a failed transfer. The samples had been transfected with the various receptors and Grb2, hoping to look at recruitment and internalization with EGF-Alexa 647.

Chase Experiment with LysotrackerRed

Cells were plated and transfected as previously described, and induced with 100ng/µl EGF for 15min at RT. Cells were then washed twice with 1x PBS. 2ml –ps DMEM was added and the cells were placed in the cell incubator for 1.5h.

All samples were plated on uncoated 35mm glass-based dishes. Cell samples were either designated for live cell imaging or for PFA fixation. For live cell imaging, cells were stained with 1µl LysoTracker® Red DND-99 for 30 minutes. A stronger concentration of LysoTrackerRed was required for fixed cells. For PFA fixation cells were stained with 5ul LysoTrackerRed for 30 minutes, washed twice with 1xPBS, and 300µl PFA 3% in PBS was added. After 20 minutes, PFA was removed, 1ml 1xPBS was added and the cells were refrigerated in aluminum foil. Cells were imaged using the confocal microscope.

Inhibitors

Pitstop2 was dissolved in DMSO, and used at a final concentration of 25µM in 2ml imaging medium with HEPES, ensuring that the final concentration of DMSO would not exceed 0.1%. Cells were plated as described for confocal microscopy. The day after, Pitstop2 was added 10min before imaging, the entire experiment taking no more than 30min. As specified by the company, longer incubation times could lead to non-specific binding of Pitstop2.

Microscopy Troubleshooting

Cells presenting characteristics of stress such as blebbing, or fluorescent protein aggregates, were avoided when imaging. To avoid phototoxicity and bleaching repeated illumination was kept at a minimum. In addition, the laser power during imaging was kept as low as possible, ranging between 0.2-1.5%. Even though the chosen fluorophores had narrow emission spectra, spectral overlap was avoided by choice of fluorophore combinations and sequential scanning.

Quantitative Analysis

A quantitative approach examining the colocalization between the receptor and Rab proteins was used to analyze the temporal colocalization of the two fluorescent markers. Image J was used to analyze the image stacks. The images were first converted to 8bit, and processed with

a rolling ball background subtraction, rolling ball= 5 pixels. The ImageJ Colocalization plugin was used [156]. This plugin combines two 8-bit (0-255) images or stacks and measures the overlapping intensities, considered to be colocalization. The mean average of the colocalization areas were normalized and plotted into a graph using Prism6. The data was presented in a scatter plot, where area percentage was plotted against time. We decided to refrain from fitting the graphs since this removes data points, and one can easily see differences that occur between the plots presented. To better analyze the different colocalization pattern through time, we selected specific time points and measured the total percentage of vesicles that colocalized with EGFR. The results were presented in a bar graph that summarizes the variety among the different receptors' progression through the endocytic pathway.

As a complementary colocalization analysis on fixed time points with LysotrackerRed and the respective receptors we introduced an object-based colocalization. Background was removed by rolling ball=5, and manual thresholding was performed on the receptor channel (488nm), finally using a median filter of 1. The image stack was converted to binary and the endosomes were compared with the original channel. This was done to make sure that we had not over-thresholded. We created masks based on the fluorescent signal from receptor positive endosomes. These specific masks were superimposed onto the second, Rab5 channel; the pixel overlap was then measured. By this approach we can measure the number of receptor positive endosomes with a positive signal from the second fluorescent signal, Rab5-mCherry or Rab7-mApple. The measured values were then plotted as the total number of receptor positive endosomes with a detected signal from the fluorescent Rab proteins.

3.5 DNA Techniques

Restriction Digest

The EGFR-mCherry construct (kindly provided by Kalina Hristova) was sent for sequencing at GATC Biotech (Konstanz, Germany). The sequencing results showed a mutation in the last 10 amino acids: a glutamine had been changed to a glutamate. Glutamine has a polar uncharged side group, while glutamate is negatively charged. It is unknown if this mutation affects the receptors trafficking and/or interactions. It was decided to change the mutation back to the original sequence published in Genbank, the same sequence in the pEGFR-EGFP construct used in this study (Figure 8). Restriction sites were chosen using the program Snapgene. We decided to use digest sites flanking the three phosphotyrosine mutations as well as the C-terminal glutamine/glutamate mutation, in order to create Wt, Y1, Y2, and Y3 mCherry constructs.

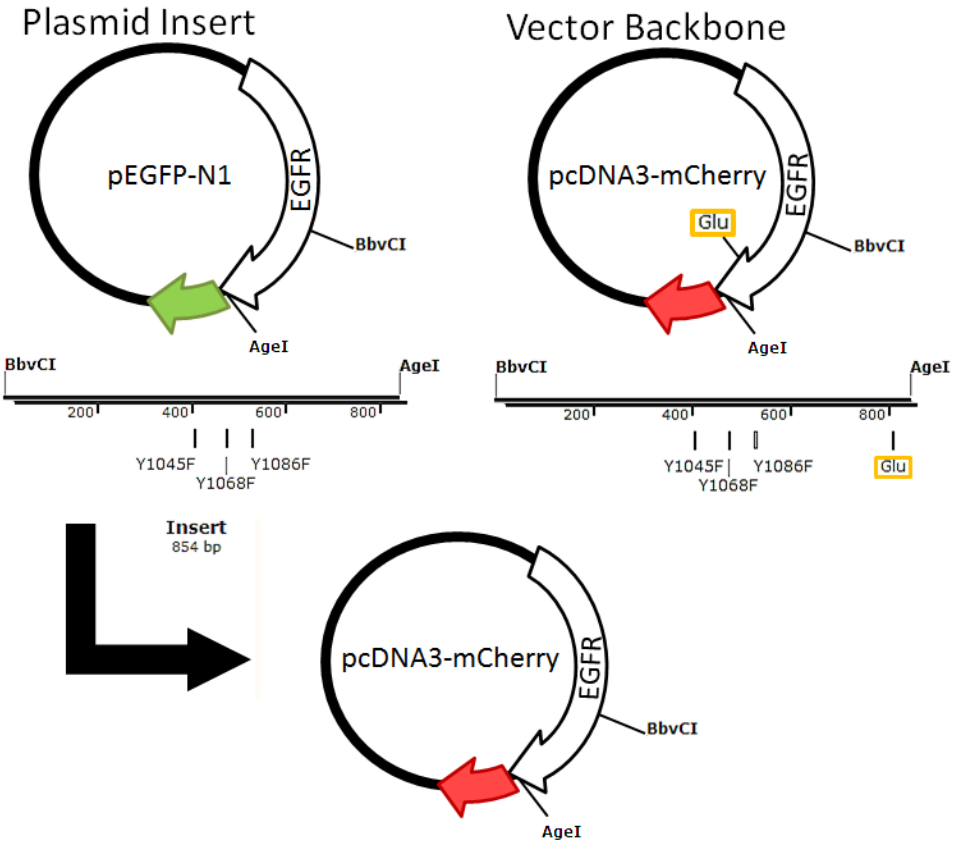

Figure 8 Schematic diagram of the restriction digest. The plasmid insert was extracted from pEGFP-N1 (EGFR-EGFP). pcDNA3-mCherry was used as the vector backbone. Both EGFR-EGFP and pcDNA3-mCherry were digested with AgeI and BbvCI, producing fragments of ~8kb and ~0.8kb. The ~800bp fragment from EGFR-EGFP was inserted into the pcDNA3-mCherry Backbone (~8kb).

Restriction enzymes BbvCI, and AgeI were used in Cutsmart buffer. BbvCI has 100% digestion in this buffer, while AgeI has a 75%digestion. Both restriction enzymes had single restriction sites in these plasmids. Expected fragments were ~800bp and ~8kb. The original EGFR-mCherry construct was used as the destination backbone (Bb). Digestion reactions were set up according to the table below, also including uncut EGFP-EGFR as control. The digests were incubated at 37^{o}C for 2hours. Digested DNA was then purified by gel electrophoresis.

Construct	**EGFR-mCherry**	**Wt**	**Y1**	**Y2**	**Y3**
[DNA] (μg/μl)	1.4	2.4	2.0	2.1	1.8
DNA (μg)	1	1	1	1	1
BbvCI (μl)	1	1	1	1	1
AgeI* (μl)	1.5	1.5	1.5	1.5	1.5
10x Cutsmart buffer (μl)	5	5	5	5	5
dH_2O (μl)	~42	~42	~42	~42	~42
Total Volume (μl)	50	50	50	50	50

*The glycerol final concentrations did not exceed 5% of the solution to avoid Star activity.

Gel Electrophoresis

A 0.7% agarose gel was prepared by dissolving 0.35g agarose in 50ml 1xTAE. 4 µl EtBr was added after the solution had cooled and the gel was poured into a suitable tray. Once the gel had set the 8-well comb was removed and ~200ml, 1xTAE, buffer with 4µl EtBr was poured in the chamber. 6µl GeneRuler 1 kb was used as DNA Ladder. Samples were applied as indicated below. Gel was run at 75V for ~1.5h, gel was checked every 30min. The results are shown in Figure 9, and Figure 10.

Wells	1	2	3	4	5	6	7	8
Samples	Empty	mCherry	Ladder	Empty	Wt	Y1	Y2	Y3

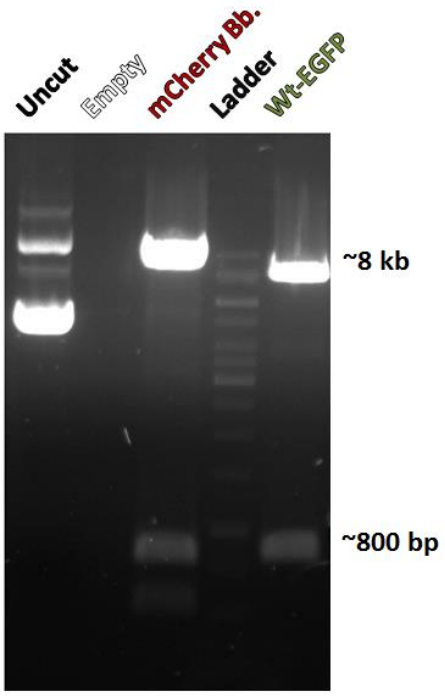

Figure 9 Restriction digests of EGFR-mCherry, the Wt-EGFR-EGFP with uncut EGFRmCherry as control. Digestion was performed with the restriction enzymes Age1 and BbvCI, and yielded the expected fragments insert (~800bp), and Bb (~8kb)

Ladder: GeneRuler 1 kb

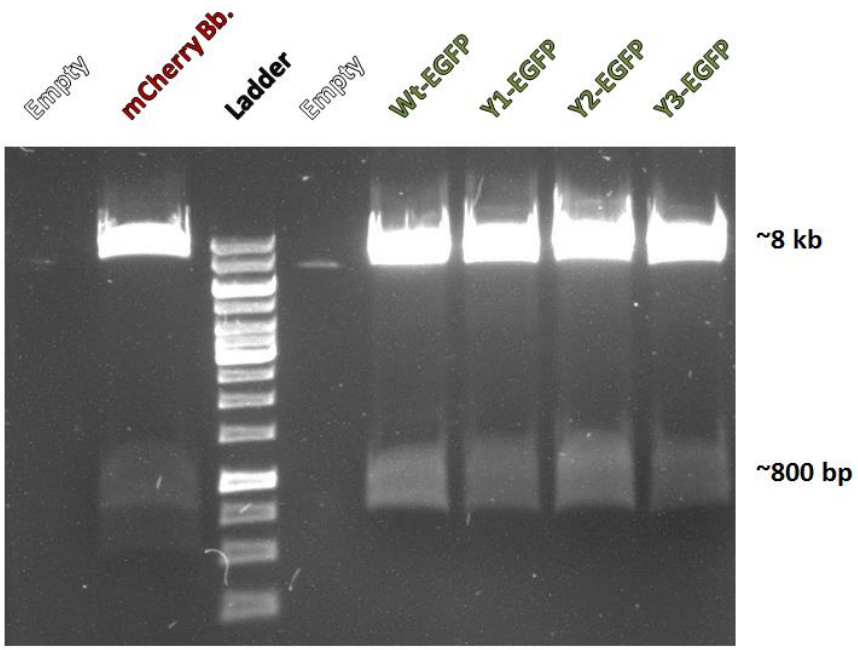

Figure 10 Restriction digests of EGFR-mCherry, the Wt-EGFR-EGFP, and mutant EGFR-EGFP. Digestion performed with restriction enzymes Age1 and BbvCI, and yielded the expected fragments insert (~800bp), and Bb (~8kb)

Ladder: GeneRuler 1 kb

DNA Extraction from Gel

The appropriate bands were cut out and placed in Eppendorf tubes, over UV-light, UV transilluminator TL-33 (UVP, CA, USA). DNA was extracted using QIAquick Gel extraction kit (QIAGEN, Limburg, Netherlands). Company protocol was followed (see appendix section: 8.3).

Cohesive End Ligation

5µl each extracted DNA was run on a 0.7% agarose gel to determine the correct amounts for the desired backbone: insert DNA ratio. The Nebiocalculator (Biolabs) was used to calculate to mass of insert required for a molar ratio of 3:1. As the Y1 receptor did not properly digest after two attempts we continued only with the other constructs.

	Control	**Wt**	**Y2**	**Y3**
Backbone, 25ng (µl)	1.25	1.25	1.25	1.25
Insert, 7.5ng (µl)	0	1.5	1.5	1.5
Buffer10x (µl)	2	2	2	2
dH_2O (µl)	15.75	14.25	14.25	14.25
Ligase (µl)	1	1	1	1
Total Volume	20	20	20	20

Ligation reactions were set up on ice, T4 DNA ligase was added last. The inserts and backbone had cohesive ends so the ligation reactions were incubated 20min at RT, then heat deactivated at 65^{o}C for 10min. Samples were chilled on ice and Top10F competent cells were transformed as previously described. Resulting colonies were picked and used to inoculate mini-prep DNA cultures, and the purified plasmids sent for sequencing by GATC.

Blunt End Ligation

The ligation of insert in the mCherry backbone had created a frameshift at the BbvCI cut site. The glutamine/glutamate mutation was corrected. However, the fluorescent protein tag was rendered non-functional. The design was therefore modified to include blunt-end ligation in order to keep the mCherry open reading frame. The vectors were first cut with AgeI. The 3' overhang was filled in with Klenow, a DNA polymerase I. Subsequent digestion with BbvC1 required first incubation with EDTA at 75^{o}C to inactivate the Klenow polymerase, then

removal of the EDTA by gel purification as otherwise this would inhibit BbvC1. In the end it proved to be too difficult to obtain sufficient yields of the inserts after all these steps, so it was decided to send the sample to Mutagenex, and have the constructs made.

3.6 Protein Techniques

EGFR Degradation Assay

In order to quantify the degradation of Wt-EGFR and mutant receptors, a degradation assay was set up. Stably-transfected PAE cells, kindly provided by I.H. Madshus and E. Stang, were used for the degradation assay. Four PAE cells lines each with stable expression of one of the four EGFR constructs used in this study. Cells were plated on 60mm dishes to be 90% confluent on the day of the experiment. The stably-transfected PAE cells were treated with cyclohexamide (5ug/ml), and stimulated EGF [100ng/ml] for 2, 4, and 6 hours. Unstimulated cells were used a control. Cells were then lysed as described below

Cell Lysis

Eppendorf tubes and 1xPBS were chilled on ice, and lysis buffer was prepared (see appendix 8.2). After stimulation, cells were washed twice with 1xPBS on ice. 150µl lysis buffer was added to cell plates. Cells were scraped and transferred to the pre-chilled tubes, incubated on a rotor at 4^{o}C for 20min then centrifuged at 16100 x g, at 4^{o}C for 20min. Supernatants were transferred to fresh chilled tubes. Lysates could then be frozen at 20^{o}C for storage. The lysate protein concentration was measured by Bradford protein assay. Bradford protein reagent was diluted, 200µl reagent, 800µl dH_2O per sample, in a 1ml disposable cuvette. 1µl sample was added, and blank was prepared. Samples were incubated for 5min at RT. Absorbance was measured, and protein concentration was calculated by using the equation: $A595 \times 18.4 = \frac{\mu g}{\mu l}$

Western Blotting & Transfer

Each well would contained equal quantities of protein mass. Samples were combined with 2x Laemmli, and incubated 5min at 95^{o}C. A 10-well gel was used for the protein separation, and run at 100V for ~1hour in running buffer (see appendix, section: 8.2).

Transfer buffer was prepared before protein separation was complete. PVDF membrane was activated in methanol 15 seconds, washed in dH_2O for 2 minutes, and rested 5 minutes in

transfer buffer, while the transfer chamber was set up. Transfer was run at 4°C at 150mA for 3 hours, with stirring. After transfer, the PVDF membrane was blocked by incubation of 5% milk/TBST, 3x 5 minutes.

Primary and secondary antibodies were diluted in 2% skimmed milk/TBST. Primary antibodies were incubated overnight, ~16 hours at 4°C. The membrane was then washed three times with 1xTBST for 5minutes, and incubated 1hour with secondary antibody at RT. The membrane was then washed in a similar manner. The HRP-conjugated antibodies were detected using the Amersham™ ECL Prime Western Blotting Detection Reagent kit, where the membrane was incubated with a 1:1 ration of solution A and B for 5minutes. The chemiluminescence was detected with Amersham Hyperfilm™ ECLHigh performance chemiluminescence film (GE Healthcare limited, Buckinghamshire, UK) through exposure to the membrane, and the film developed using an OPTIMAX X-ray Film Processor (PROTEC, Dorfwiessen,Germany).

Primary Antibodies	**Concentration**	**Class**	**Acquired from**
Anti-GFP	1:2000	Sheep lgG	Abcam, Cambridge, UK
Anti-tubulin	1:1000	Mouse lgG	Sigma- Aldrich, MO, USA
Anti-EGFR	1:2000	Goat lgG	Fitzgerald Inc., MA, USA

Secondary Antibodies	**Concentration**	**Acquired from**
ECL Anti-Rabbit Horseradish Peroxidase (HRP) linked whole antibody from donkey	1:5000	GE Healthcare, Buckinghamshire, UK
ECL Anti-Mouse Horseradish Peroxidase linked whole antibody from sheep	1:5000	GE Healthcare, Buckinghamshire, UK

4 Results

4.1 EGFR Sorting and Trafficking Analysis

The EGFR has been extensively studied, and has important roles in cell processes like migration, and mitosis [157]. The receptor has also been found to have oncogenic properties, meaning mutated and/ or overexpressed structures have been linked to several epithelial cancer types. The most common cause is continuous signaling [158]. Receptor-mediated endocytosis is initiated upon ligand activation [159]. This mechanism is important for signal attenuation, even though it has been shown that the signal continues for some time after its internalization [160].

The trafficking events of EGFR have been visualized by using fluorescent tags, and live cell microscopy. Previous work from Sorkin's group showed that the fluorescent-tagged EGFR-EGFP chimeric protein functions similarly to endogenous EGFR [161]. The receptor is internalized upon ligand binding, then trafficked towards the early endosomal compartment, and sorted to its final destination. Activation with EGF tends to promote degradation due to the pH stability of EGF binding in endosomes. Wt-EGFR-EGFP trafficking was used as a control having similar sorting to the endogenous receptor as the literature describes. From this we could compare the mutants' trafficking pattern to the Wt-EGFR-EGFP to examine whether the altered receptor phosphorylation affects receptor trafficking.

Our study used live cell imaging to look at colocalization between EGFR-EGFP and specific Rab proteins. We began with Rab5-mCherry positive endosomes, since the early endosomal compartment is specifically Rab5 positive. We then examined the later endosomal trafficking events by looking at colocalization with Rab7-mCherry/-mApple positive endosomes. We stimulated cells on the microscope stage with EGF looking at the real time trafficking from internalization to colocalization with Rab protein positive endosomes. This novel method observed temporal differences in trafficking that arose due to an altered EGFR phosphorylation pattern, in turn affecting the subsequent recruitment and binding of accessory molecules important for internalization. The study presented here is a continuation of the group's previous work on the phosphorylation mutants and interactions with the various accessory proteins Cbl, Grb2, and Hrs. (see manuscript in progress [162]).

Receptor phosphorylation is essential for trafficking and degradation. Mutations had previously been introduced at specific phosphotyrosines, thought to be important for internalization and trafficking. The EGFR-EGFP mutant constructs were produced by Mutagenex Inc. These mutations removed the receptor phosphorylation sites where Cbl and Grb2 are known to bind to the receptor [163]. Cbl can interact directly at pY1045, and indirectly in complex with Grb2 at pY1068/1086 [84, 164, 165]. As explained earlier Cbl and Grb2 are important for ubiquitinylation of the receptor, and subsequently signal attenuation by degradation [90, 164, 166] . To date there are no studies on live cell imaging of the triple mutant (Y1045/1068/1086F). The substitutions are depicted in Figure 11.

For simplicity the constructs used will be denoted:

- pEGFR-EGFP — Wt-EGFR
- Y1045F pEGFR-EGFP — Y1-EGFR
- Y1068/1086F pEGFR-EGFP — Y2-EGFR
- Y1045/ Y1068/1086F pEGFR-EGFP — Y3-EGFR

The Rab protein positive endosomes will be denoted:

- Rab5-mCherry-positive — Rab5+
- Rab7a-mCherry-positive — Rab7-mCherry
- Rab7a-mApple-positive — Rab7+

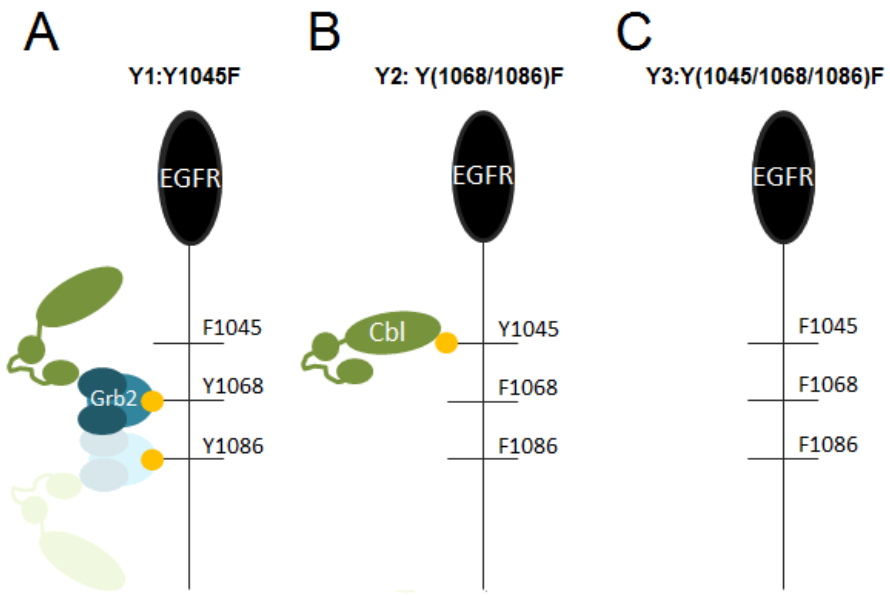

Figure 11 Schematic diagram of the EGFR mutants, each of which also carries EGFP on the C-terminus.
A: Y1 shows the pY1045F substitution. pY1068 and pY1086 are still intact
B: The Y2 shows substitutions in pY1068/1086F.
C: The Y3 mutant does not have any of the three pY-sites intact.

4.2 Rab5 Colocalization: Receptor Phosphorylation Determines Rab5-mCherry Recruitment

In order to investigate receptor progression through endocytosis, colocalization patterns of Wt-EGFR and mutants along with specific endosomal identifiers were examined. We started by studying colocalization with Rab5-mCherry (Rab5+). Rab5 is important for endosome maturation, by recruiting effector proteins that are important for endosome fusion and progression. The GTPase is specific for early endosomes, and is also vital in the biogenesis of early endosomes [167]. We have investigated whether there are any temporal differences in the colocalization between the early endosomal marker Rab5+, Wt-EGFR and the respective phosphotyrosine EGFR mutants.

We developed a method to better understand the EGFR trafficking based on live cell imaging and colocalization analysis. The system used a combination of percentage pixel overlap, and object-based colocalization. The percentage pixel overlap each frame of the timeseries was measured by the Colocalization plugin for ImageJ.

4.2.1 Establishing the Wt- EGFR Progression through Early Stage Endocytic Trafficking

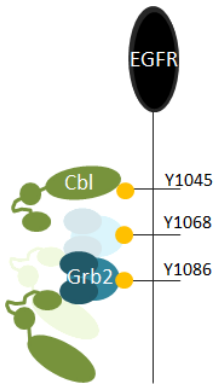

Figure 12
Schematic diagram of Wt-EGFR

To investigate the trafficking of Wt-EGFR (Figure 12) to early endosomes, HeLa cells were transiently transfected with EGFR-EGFP and Rab5-mCherry, then imaged by live cell confocal microscopy.

Before stimulation Wt-EGFR was visible at the plasma membrane. A few cells already contained internal Wt-EGFR positive endosomes (Figure 13). Rab5-mCherry positive endosomes were distributed throughout the cell, with an increased peripheral concentration.

Shortly after EGF stimulation Wt-EGFR-positive endosomes could be seen as punctate structures close to the plasma membrane (Figure 13). Initial colocalization took place within minutes as Rab5-mCherry was recruited to the newly formed vesicles. At 20 minutes there was a notable presence of yellow endosomes indicating colocalization, followed by Rab5-mCherry detaching from the EGFR positive endosomes. This indicated endosomal progression as the receptor positive endosomes migrated closer to the perinuclear region.

As indicated in the individual cell example in Figure 13, the cells' average colocalization (Figure 14) showed a steady increase as the receptor positive endosomes colocalized with Rab5-mCherry positive endosomes. At 10 minutes EGFR and Rab5-mCherry colocalization was midway to reaching its maximum colocalization, which occurred at ~23 minutes. At that time there was measured a 73% colocalization between Rab5+ endosomes and Wt-EGFR positive endosomes. Subsequently the receptor positive endosomes began to mature and Rab5-mCherry detached, so the average colocalization decreased to 30% by the end of the timecourse.

This preliminary colocalization study provided us with the specific receptor trafficking characteristics of the Wt-EGFR (Figure 14). We further used this analysis as a template for recognizing any signs of altered receptor trafficking or sorting of the respective EGFR mutants.

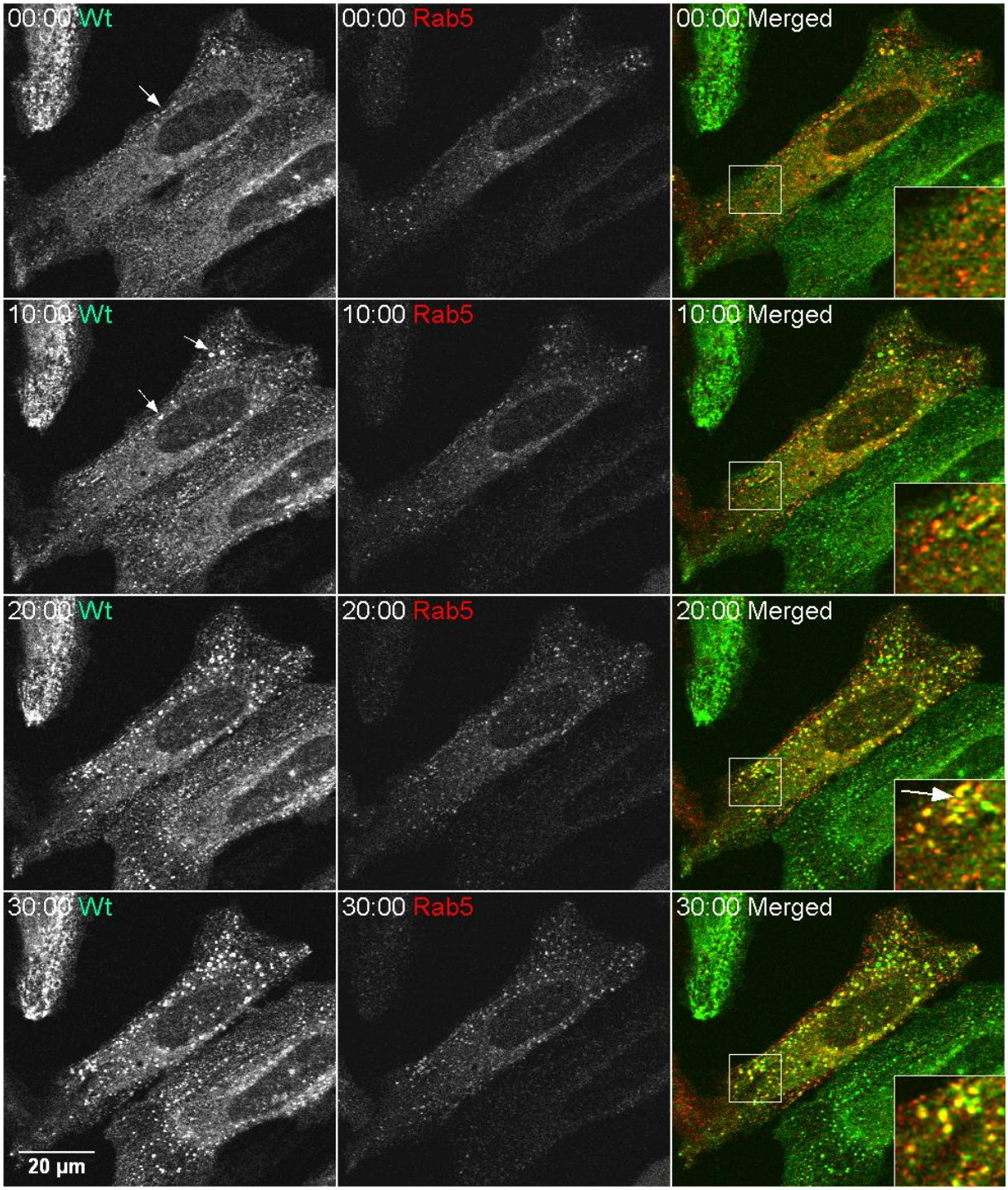

Figure 13 Montage of HeLa cells transfected with Wt-EGFP-EGFR and Rab5-mCherry at 0.5ng/µl using Lipofectamine 2000. Cells were continuously stimulated with EGF [100ng/ml]. Cells were imaged every 30 seconds for 60minutes

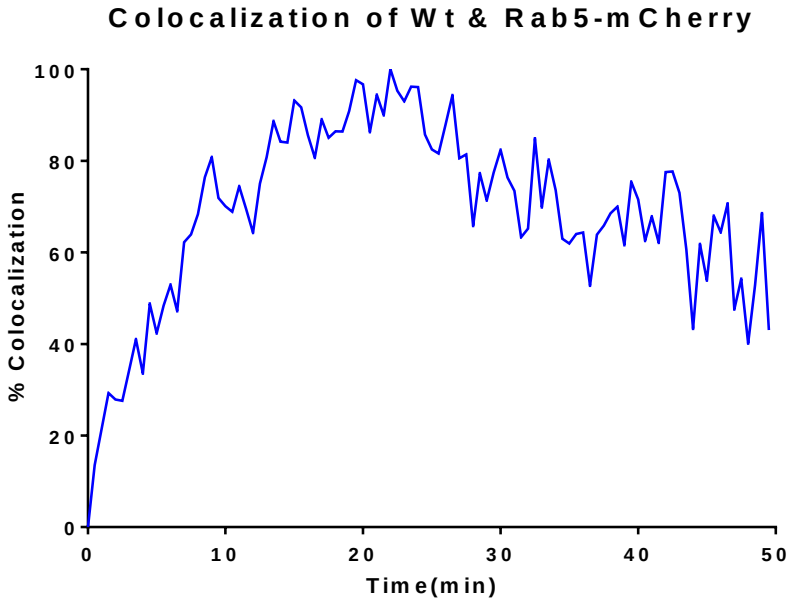

Figure 14 Colocalization of Wt - EGFR and Rab5mCherry. HeLa cells were induced with 100ng/ml EGF. Cells were imaged every 30 seconds for 60minutes. Data shown represent the mean of 9 individual cells.

4.2.2 Y1-Mutant (Y1045F) Shows Delayed Progression Towards Early Endosomes

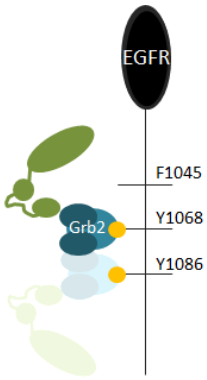

Figure 15 Schematic diagram of Y1-EGFR

The previous results showed the normal progression of EGFR trafficking, and indicated endosomal maturation as the receptor continued towards degradation.

The first mutant to be examined contained a point mutation that changed the corresponding codon, Y1045F (Figure 15). This phosphotyrosine has been shown to be the main binding site for Cbl [164].

HeLa cells were transiently transfected with Y(1045)F EGFR-EGPF, and Rab5-mCherry. The next day, cells were imaged. 100ng/ml EGF Alexa 647 was added on stage during the acquisition. Prior to EGF treatment a small proportion of internal vesicles positive for Y1-EGFR were observed. Morphologically the mutant transfected cells were similar to the Wt-EGFR and we detected a prominent band of Y1-EGFR along the plasma membrane (Figure 16). Shortly after receptor activation we could observe receptor aggregation along the cells' periphery, visible as a punctate pattern. 10 minutes after stimulation internalized endosomes positive for the mutant receptor and Rab5-mCherry were observed. Compared to the EGFR-WT, the mutant receptor positive endosomes resided close to the plasma membrane for a longer period of time. In addition

aggregated receptors were still present on the plasma membrane, indicative of a slower internalization (Figure 16, arrow).

Further analysis of the colocalization with Rab5-mCherry showed a measurable difference in receptor progression towards maximum colocalization as compared to Wt-EGFR (Figure 17). The main differences were the small amount of colocalization, and a lower initial rate. A slow increase in colocalization was measured up until 35 minutes. At ~40minutes the colocalization reached maximum saturation, and plateaued throughout the remainder of the timecourse.

These results showed that the Y1 mutant demonstrated slower progression to endosomal maturation compared to the Wt-EGFR, with both slower recruitment to Rab5-mCherry endosomes, and reduced detachment of Rab5-mCherry later in the timecourse.

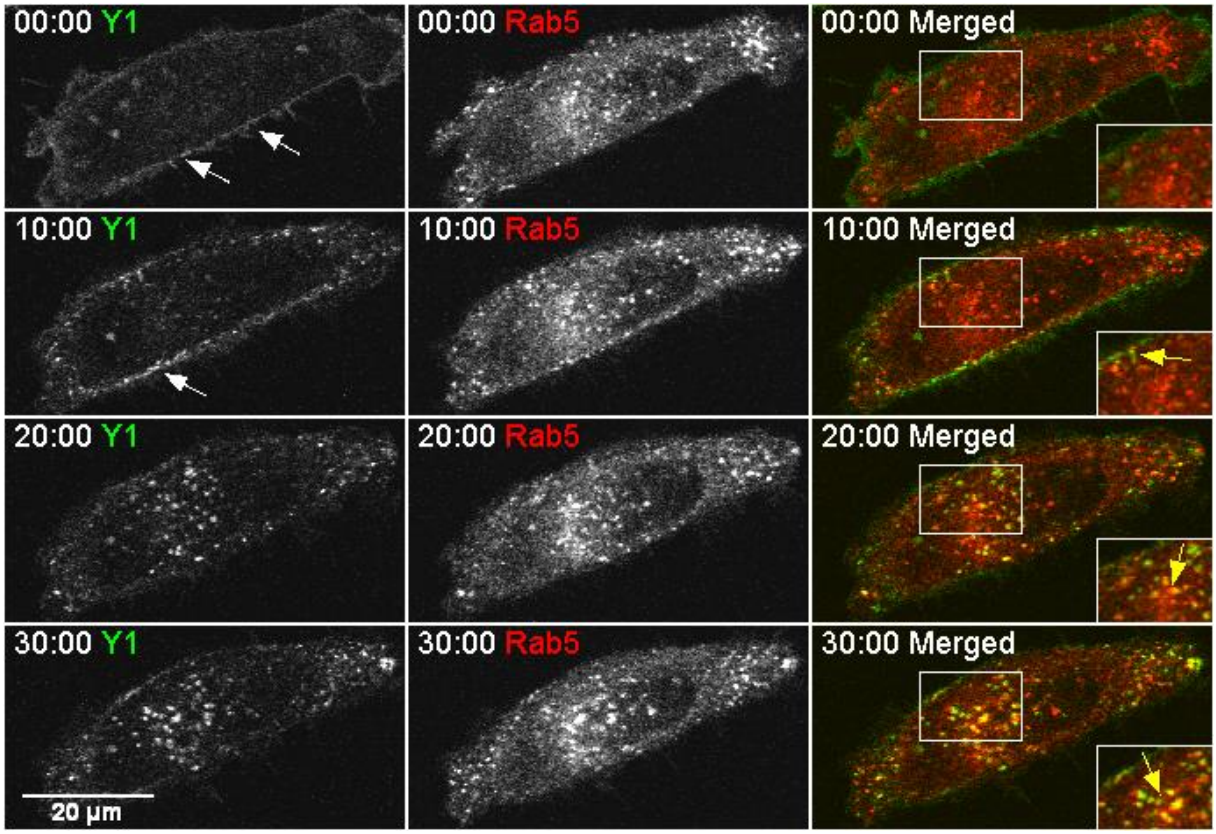

Figure 16 Montage of HeLa cells transfected with Y(1045)F EGFP-EGFR and Rab5-mCherry at 0.5ng/µl using Lipofectamine 2000 continuously induced with rhEGF [100µg/ml]. Cells were imaged every 30 seconds for 60minutes

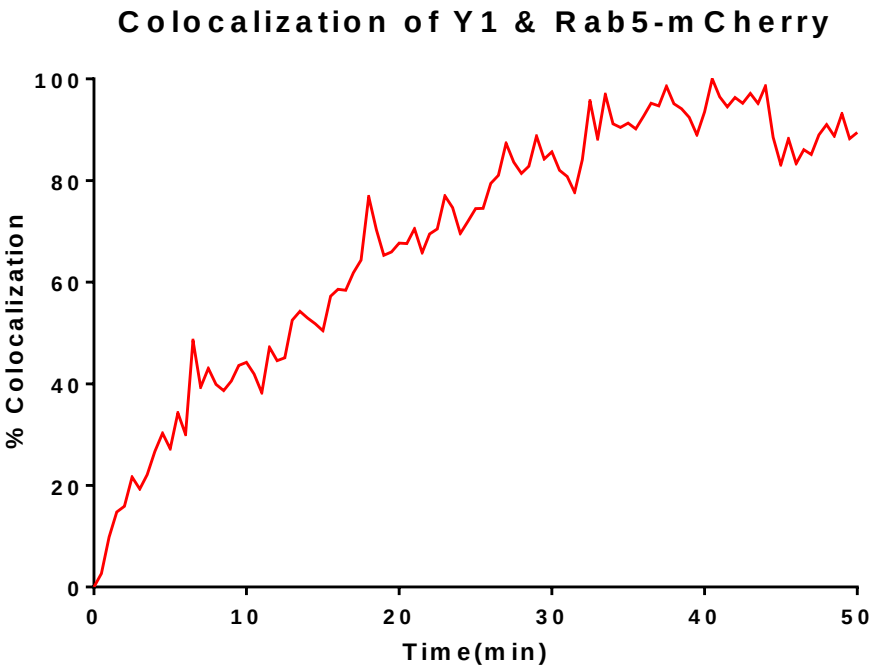

Figure 17 Colocalization of Y1 and Rab5-mCherry. HeLa cells were induced with 100ng/ml EGF alexa 647. Cells were imaged every 30 seconds for 60minutes. Data shown represent the mean of 7 individual cells.

4.2.1 Y2-Mutant (Y1068/1086F) Shows Similar Trafficking to Wt-EGFR

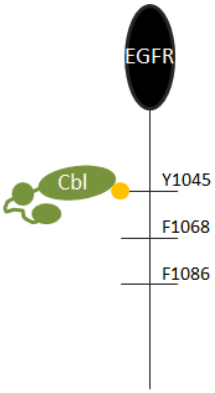

Figure 18
Schematic diagram of Y2-EGFR

The colocalization data for Y1-EGFR and Rab5+ demonstrated a continuous increase throughout the studied timecourse, indicating a slower progression towards early endosomes, and retention of receptor in early endosomes. We then examined the trafficking of the double mutant (Y2). The double substitution, Y1068/1086F, on Y2-EGFR removed the direct docking sites for Grb2 [165] (Figure 18).

Similarly to previous experiments, HeLa cells were co-transfected with Y(1068/1086)F EGFR-EGFP and Rab5-mCherry over-night for imaging the following day. Prior to ligand activation the double transfected cells were observed to have receptor localized on the plasma membrane. After ligand stimulation we could observe punctate structures positive for Y2-EGFR along the plasma membrane (Figure 19), similar to of the Wt receptor. A minor portion of the internalized receptor was detected to have colocalized with Rab5-mCherry at 10 minutes. However, receptor positive endosomes were still present on the plasma membrane.

The colocalization appeared similar to the Wt-EGFR colocalization pattern. There was an increasing amount of colocalization between Y2-EGFR and Rab5+ endosomes up to 20 minutes (Figure 20), reaching a peak in colocalization at ~23 mintues. After which the colocalization pattern plateaus, indicating that Rab5-mCherry does not detach from the receptor positive endosomes. Loss of Rab5 is a sign of endosomal maturation; both the Y1 and Y2 receptor mutants showed no measurable sign of Rab5-mCherry detachment, indicating a lack of maturation. This indicates the importance of the receptor's phosphorylation pattern regulating the endosomal progression.

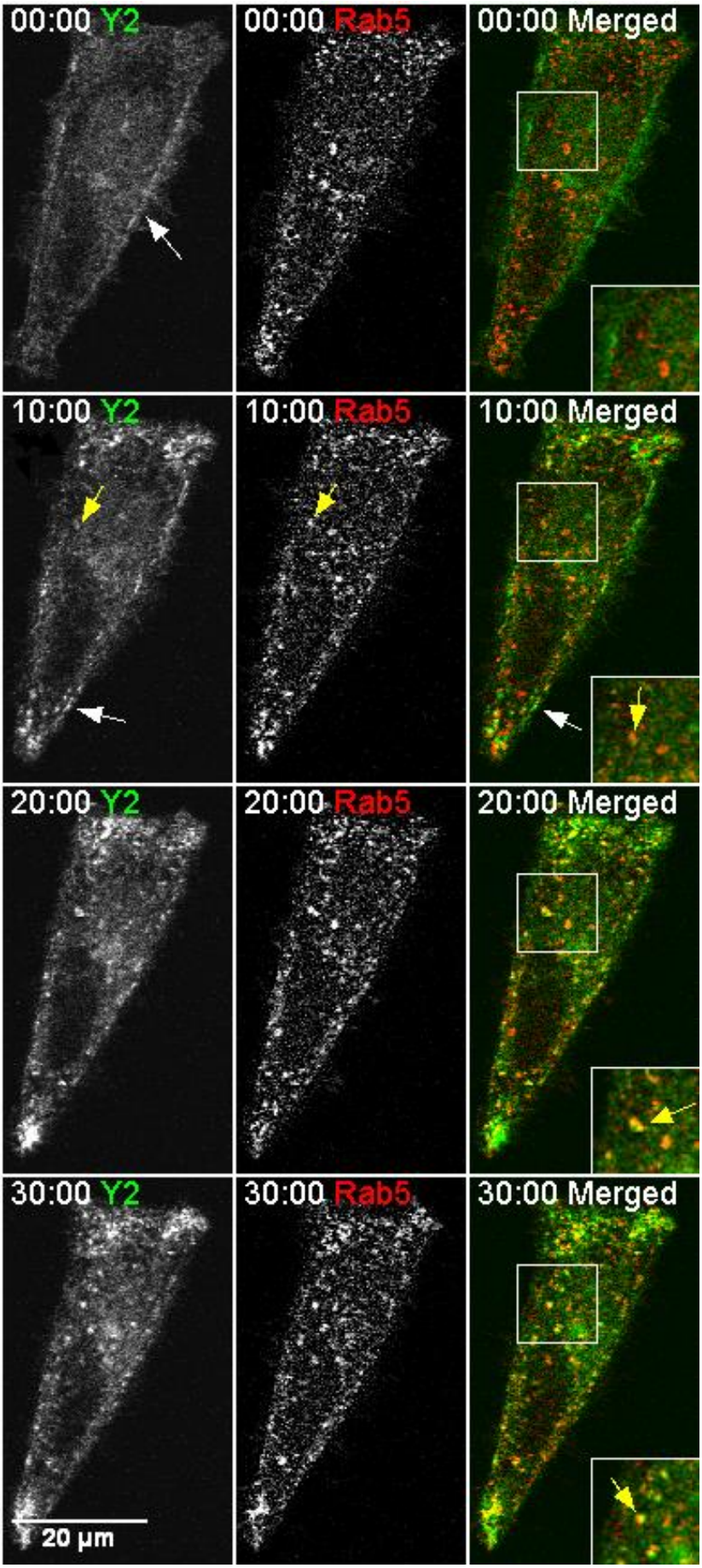

Figure 19 Montage of HeLa cells transfected with Y(1068/1086)F EGFP-EGFR and Rab5-mCherry, [0.5ng/µl] using Lipofectamine 2000. Cells were continuously induced with rhEGF [100µg/ml]. Cells were imaged every 30 seconds for 60minutes.

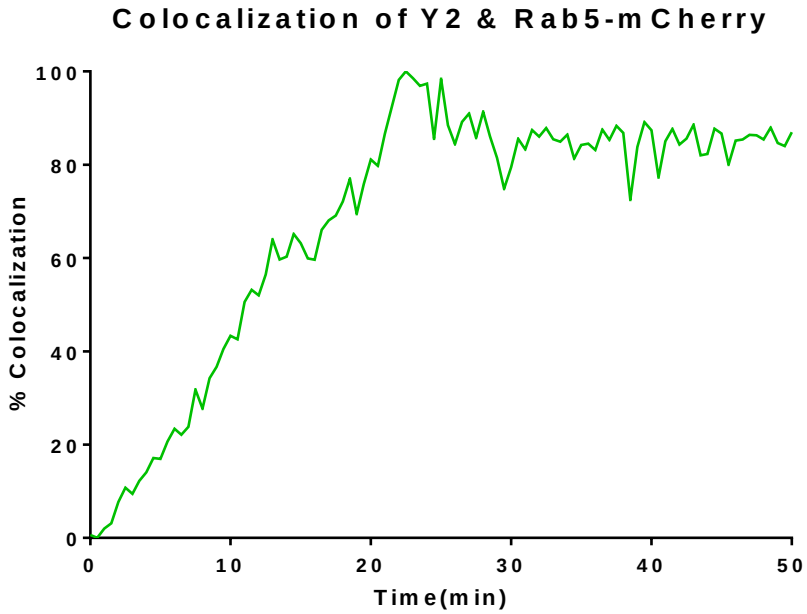

Figure 20 Colocalization of Y2-EGFR and Rab5-mCherry. HeLa cells were induced with 100ng/ml EGF alexa 647. Cells were imaged every 30 seconds for 60minutes. Data shown represent the mean of 8 individual cells.

4.2.2 Y3-Mutant (Y1045/1068/1086F) Induces a Significantly Altered Receptor Trafficking

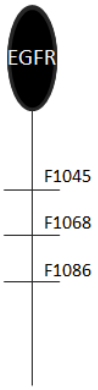

Figure 21 Schematic diagram of Y3-EGFR

In the previous section we found the Y2-EGFR mutant to have a similar colocalization pattern to the Wt-EGFR, during the first half of the timelapse. However both Y1 and Y2- EGFR demonstrated a plateau of colocalization with Rab5-mCherry which indicated that the receptors were not properly sorted. The triple mutant has site-specific point mutations at pY1045, pY1068, and pY1086 (Figure 21).

HeLa cells were transiently transfected overnight with the Y(1045/1068/1086)F EGFR-EGFP construct, and Rab5-mCherry. Similar timelapse experiments as previously described were carried out the next day. Prior to ligand stimulation cells that expressed the triple mutant displayed a different morphology, distinguishable from the Wt-EGFR, with increased protrusions along the plasma membrane (Figure 22).

Upon stimulation with EGF, the receptor lingered noticeably on the plasma membrane forming punctate aggregates before internalization (Figure 22). The newly internalized vesicles remained adjacent to the plasma membrane, increasing in size as Y3-EGFR positive endosomes underwent homotypic fusion. There were small amounts of colocalization observed early on in the timecourse. After 20 minutes the receptor-positive endosomes had

formed prominent enlarged endosomes, and the EGFR-positive endosomes localized closer to the perinuclear region. From there on there was a steady increase in colocalization with Rab5-mCherry, indicating receptor retention at the early endosome stage, possibly an avoidance of degradation. A degradation assay was performed, in order to examine this closer, discussed later (section 4.5).

The difference in morphology of the unstimulated cells indicated a large scale cellular response; further substantiated by the broad spectrum of colocalization patterns observed upon EGF-stimulation, during analysis of the co-transfected cells. The diversity suggests a physiological effect generating instability in the endocytic pathway. The colocalization pattern is presented in Figure 23. The plot shows a significantly slower occurrence of colocalization, as compared to the previous data from the Wt, Y1, and Y2 receptors. At the 10minutes time point several Y3-EGFR positive endosomes were present. However, the colocalization of Y3-EGFR and Rab5+ was below 5% at that time. The lack of colocalization further validated that there was a delay for the receptor in the endocytic pathway. The colocalization appeared to increase continuously towards the end of the timelapse.

Y3-EGFR had a prominently different trafficking compared to the Wt-EGFR, as well as the single and double mutants. The triple mutant demonstrated an obvious delay in colocalization as shown in Figure 23, formed enlarged endosomes and induced a greater morphologic diversity. From this we can conclude that the mutated phosphorylation pattern results in a continuous altered trafficking of the receptor.

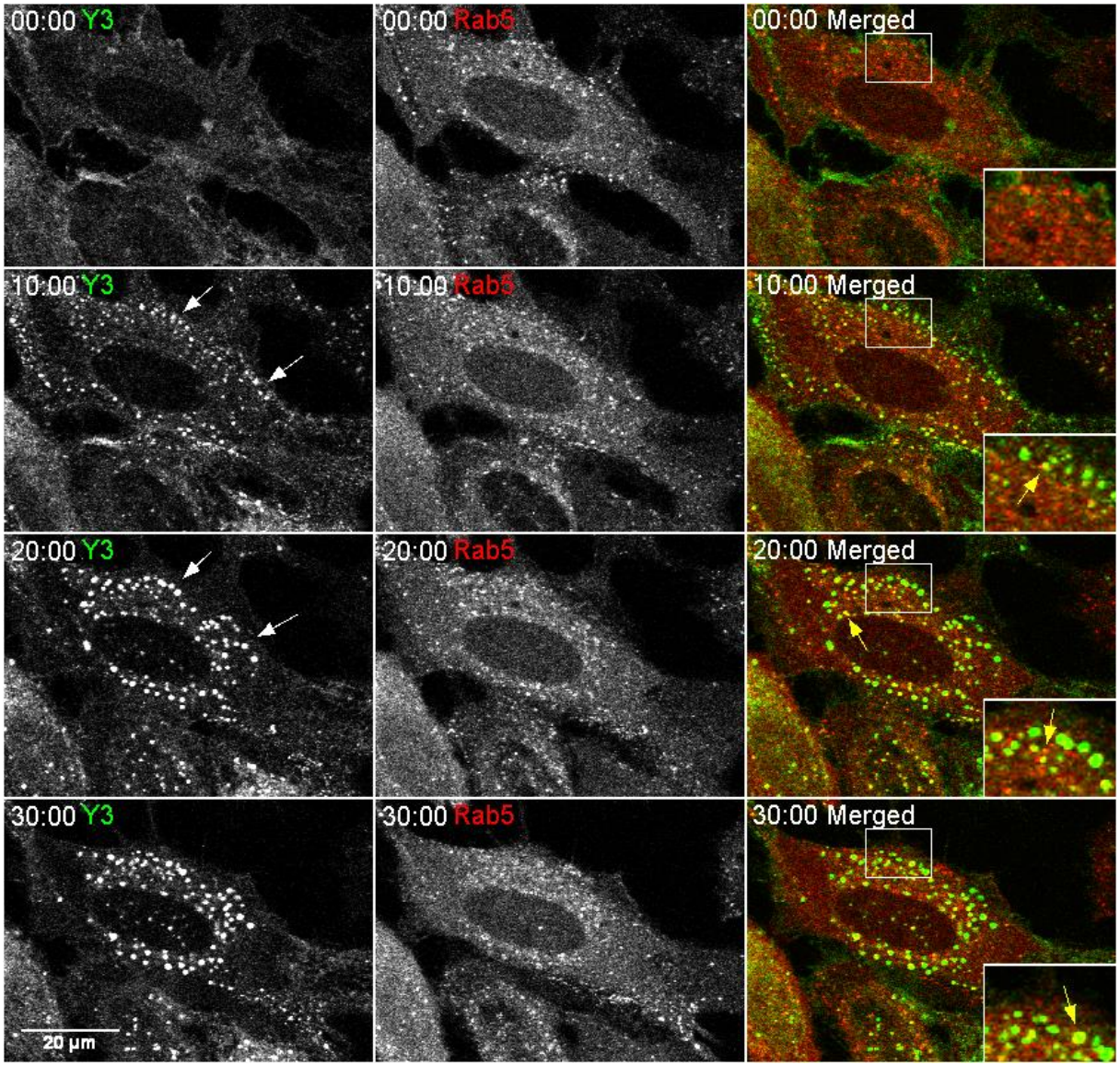

Figure 22 Montage of HeLa cells transfected with Y(1045/1068/1086)F EGFP-EGFR and Rab5mCherry, [0.5ng/µl] using Lipofectamine 2000. Cells were continuously induced with rhEGF [100µg/ml]. Cells were imaged every 30 seconds for 60minutes.

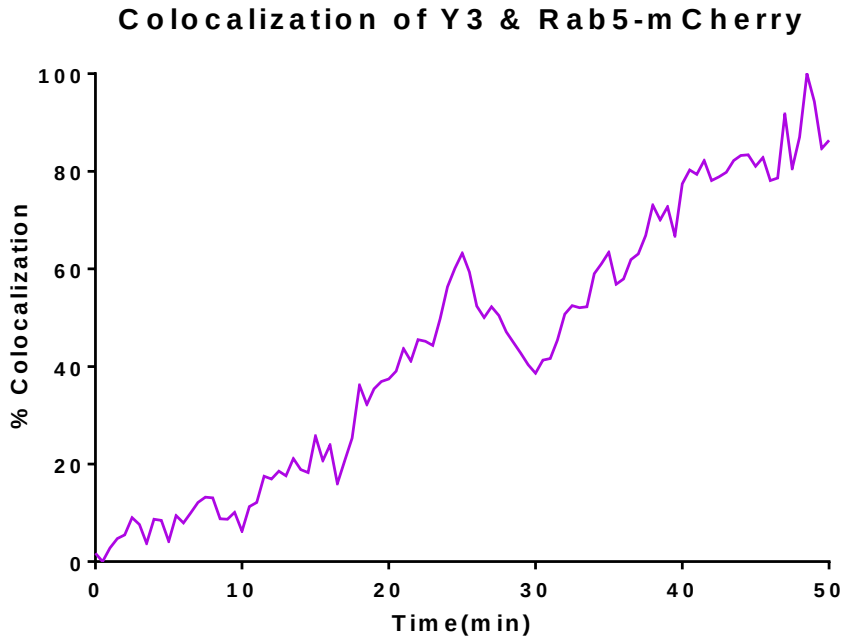

Figure 23 Y3 –EGFR colocalization with Rab5mCherry. HeLa cells were induced with 100ng/ml EGF alexa 647. Cells were imaged every 30 seconds for 60minutes. Data shown represent the mean of 6 individual cells.

By tracking individual endosomes an interesting observation was made. Rab5-mCherry was found to "fluctuate" on the enlarged Y3-EGFR positive endosomes. Rab5-mCherry attached to the receptor positive endosomes, and detached, only to repeat the action a few minutes later (Figure 24). There appeared to be a disruption of the natural maturation from the early to late endosomal compartment.

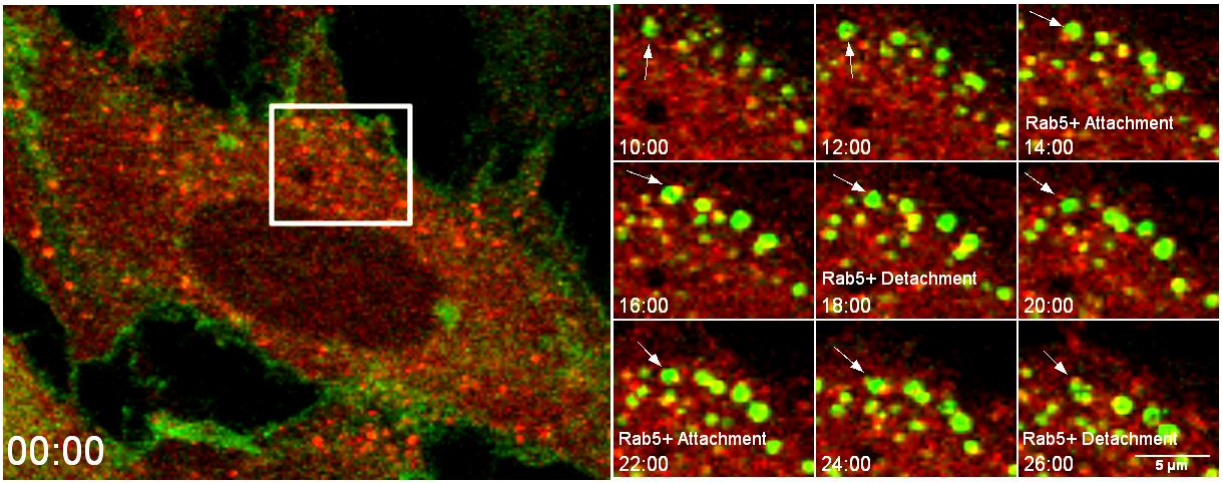

Figure 24 HeLa cells transfected with Y(1045/1068/1086)F EGFP-EGFR and Rab5-mCherry, [0.5ng/µl], continuously induced with rhEGF [100µg/ml]. Rab5-mCherry attaches and detaches from the Y3-EGFR positive endosome

4.2.3 EGFR Trafficking is Determined by Receptor Phosphorylation

In the previous sections we have analyzed the receptors individually to better understand the trafficking from the plasma membrane to early endosomes for sorting. To better comprehend the differences in trafficking of the mutated versus Wt-EGFR, we then compared the four individual experiments in one graphical plot. The presented data characterize the temporal differences in receptor trafficking depending on the phosphorylation pattern.

Endosomal progression is visible for Wt-EGFR. There is a steady increase in colocalization with Rab5-mCherry. As the endosomes mature Rab5-mCherry detaches [168], represented by a decrease in colocalization. The analysis demonstrates the altered progression of the mutant receptors visualized by the receptor/Rab5-mCherry colocalization either reaching a plateau (Y1 and Y2), or a continuous increase, as seen for Y3 (Figure 25). This indicates that there is a delay in recruitment to the Rab5+ compartment, as well as the receptors being retained within early endosomes.

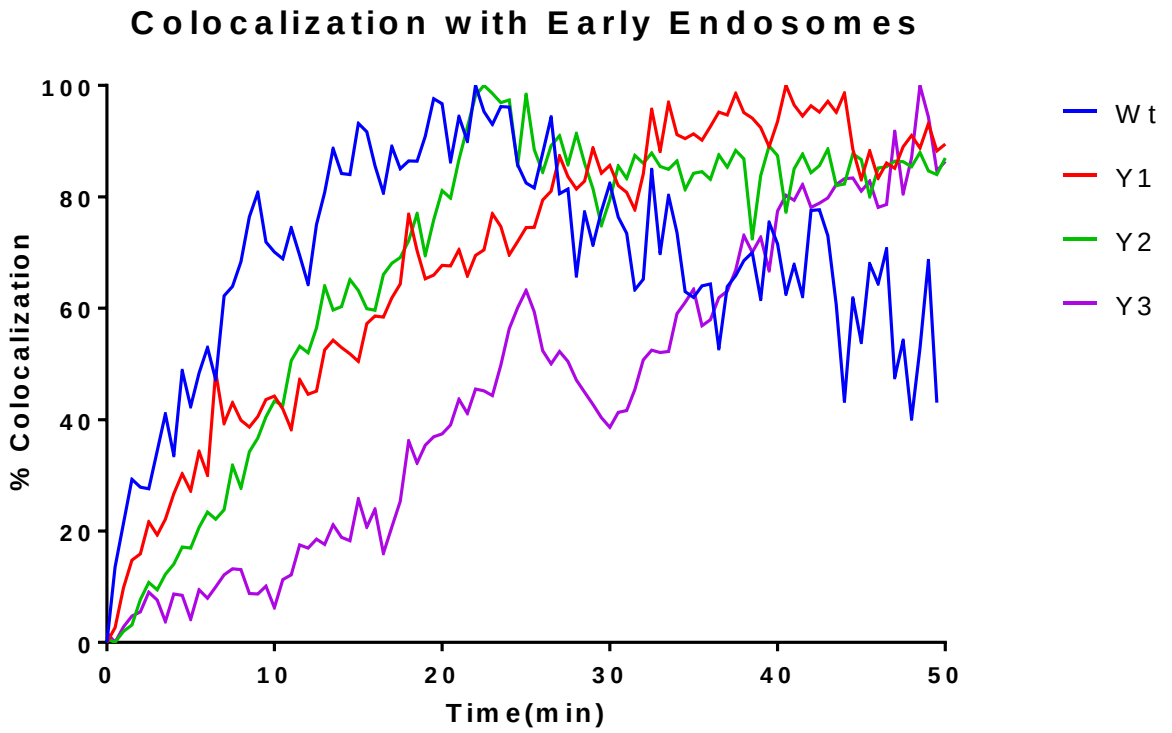

Figure 25 EGFRcolocalization with early endosomes shown as a function of time. The graph presents the colocalization of EGFR and Rab5-mCherry positive endosomes.

There is a clear difference in the trafficking pattern for the mutant receptors, especially for the triple mutant. In order to establish a better understanding of how this is propagated through the trafficking, it was decided to examine specific time points based on the Wt-EGFR sorting. The individual values were extracted from the percent pixel-based colocalization data, each of the individual values were averaged and compared by Student's t-test using Prism6 software. This method of analysis demonstrates the individual receptors colocalization with Rab5-mCherry towards maturation and sorting (Figure 26). Examining specific time points in the colocalization enhances the individual differences between the receptors.

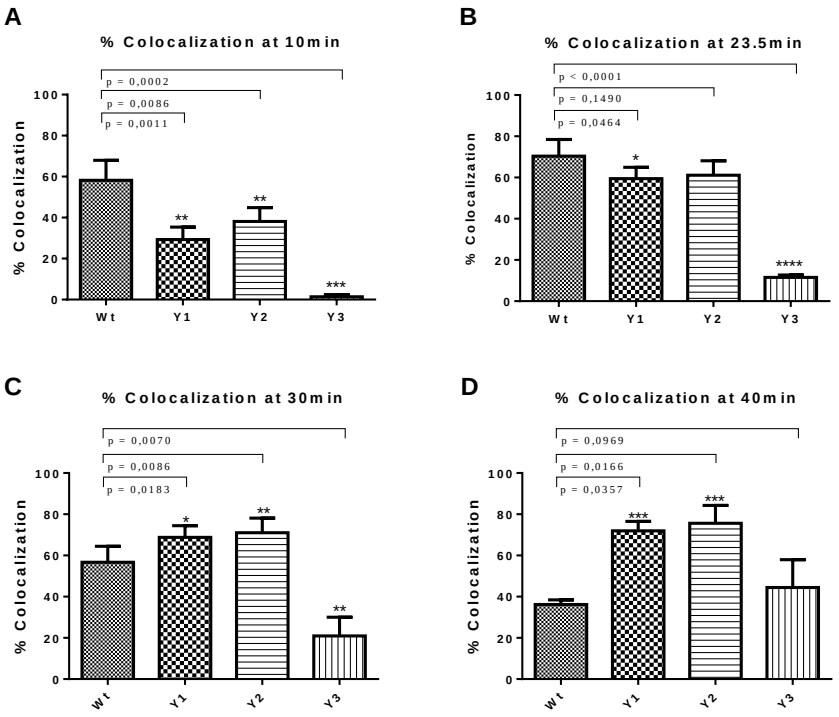

Figure 26 Colocalization with Rab5-mcherry at selected time points, analyzed with Prism6. Two tailed t-test yielded statistical significance, comparing Wt-EGFR to each receptor. Values were plotted by mean with SD. p-values are presented in the graph. Percent amount of vesicles that colocalized at A: 10min, B: 23.5min, C: 30min, D: 40min.

As previously described the Wt-EGFR rapidly increased in colocalization. Saturation was reached at 23.5 minutes, followed by a decrease in colocalization, indicating endosome maturation. The Y2-EGFR was the only mutant to reach maximum colocalization at approximately the same time as the Wt. The single mutant receptors did not reach this level of saturation until 40 minutes. At this time the triple mutant was still increasing in colocalization. At 40 minutes the Wt and Y3 have a similar percent colocalization. However, as the Wt was decreasing in colocalization, Y3-EGFR was increasing. In addition the analysis clearly demonstrates that there is a delay present at the beginning of colocalization for the mutant receptors. There was a visible temporal delay in the colocalization of the mutant

receptors with Rab5-mCherry. After 10 minutes Wt-EGFR colocalization with Rab5-mCherry had already surpassed 50% of its maximum colocalization, whereas the triple still had not begun colocalization. This is indicative of a hindered endocytosis, progression to Rab5+ endosomes, or possibly a combination of the two.

4.2.4 Colocalization Rates

To better understand the differences that occur during the trafficking pattern, we analyzed the gradient of the curves by linear regression for each individual cell. A linear model was assumed based on the time taken to reach maximum colocalization (Figure 27). Table 3 presents for each dataset when saturation occurs, the total amount of saturation, relative differences between each mutant compared to Wt, and the gradients found.

Table 3 A linear model was assumed from origin to saturation. The table indicates the rate of colocalization, presented as the gradient.

Receptor	Time(min)	Gradient
Wt-EGFR	23.5	5.3 ± 0.3
Y1-EGFR	35	2.9 ± 0.1
Y2-EGFR	24	4.1 ± 0.2
Y3-EGFR	50	1.2 ± 0.01

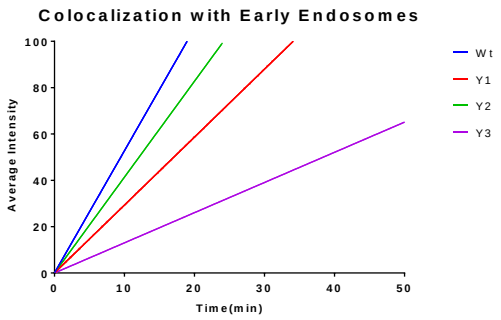

Figure 27 Linear regression showing the receptor gradients from first pixel overlap to maximum colocalization

The gradient is of interest because it describes the colocalization rate towards maximum colocalization. The Wt-EGFR had the earliest maximum value of colocalization, along with the steepest increase, as shown by the largest gradient, equal to 5. At ~23 minutes Wt receptor reached maximum colocalization between Rab5+ endosomes. The single mutant had a slower recruitment to Rab5+ endosomes, not reaching saturation until 35 minutes. Within the early part of the timecourse Y2-EGFR seemed to be the most similar to WT-EGFR, reaching capacity after 24 minutes. The triple mutant showed no signs of saturation however the gradient showed even slower recruitment of the receptor to the Rab5+ compartment, as shown by the ~25% reduction in the Y3-EGFR gradient compared to the Wt.

4.2.5 Internalization and Initial Colocalization

The gradients representing trafficking of the receptors' to the maximum colocalization with the early endosome compartment were found to be considerably different, indicating a delay possibly generated at the internalization stage. Previous work using radiolabeled EGF, ^{125}I-EGF, showed a difference in the internalization rate between the Wt-EGFR and individual mutant receptors (manuscript in progress [162]). We have chosen to include the figure in this thesis to better elucidate the differences at various stages of the endocytic pathway (Figure 28). The internalization assay shows the amount of EGF taken up by the cell, at given time points. By analyzing the signal intensities of radiolabeled EGF, the assay showed a major decrease in the internalization of the Y2 and Y3 mutant receptors.

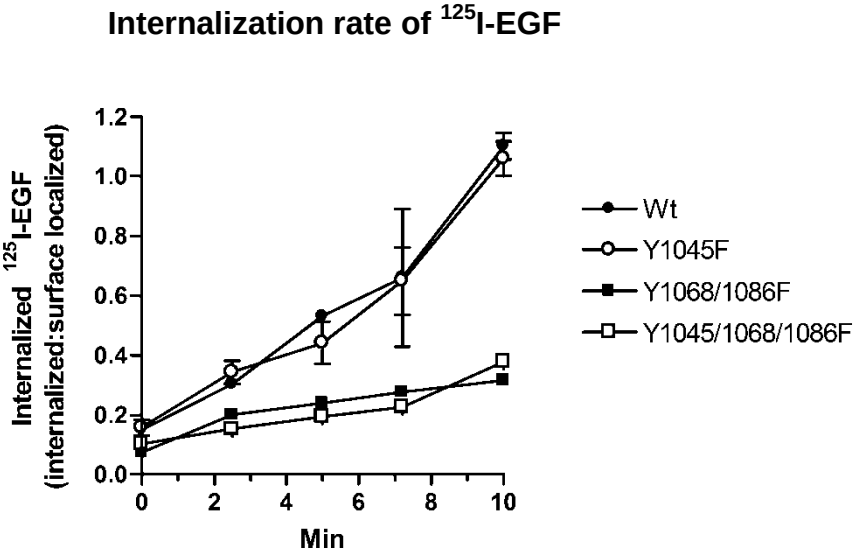

Figure 28 Internalization rate of ^{125}I-EGF for Wt and mutant receptors. Cells were stimulated with 1ng/ml EGF. Figure was adapted from manuscript in progress.

The delay in colocalization with Rab5+ endosomes present for the mutant EGFRs can be a function of both a reduced internalization rate and an altered trafficking of each receptor once internalized. The internalization assay only shows the total amount of internalized EGF present in a cell, the endosomal location of which is unknown. In order to compare the internalization and colocalization assays, we decided to examine the initial colocalization between the receptors and Rab5-mCherry at 6minutes (Figure 29).

By assessing the percentage pixel overlap of colocalization between internalized receptor with early endosomes (Figure 29), the results revealed a significant difference in the early stages of trafficking. From the analysis we could measure ~50% colocalization of Wt-EGFR and Rab5mCherry after 6minutes. Y1-EGFR was internalized similar to the Wt, however we

could measure a slower initial colocalization. Y2 had a delay present both at internalization and colocalization. Y3-EGFR was internalized similar to Y2, yet had barely begun to colocalize with Rab5-mCherry at 6minutes (Figure 29).

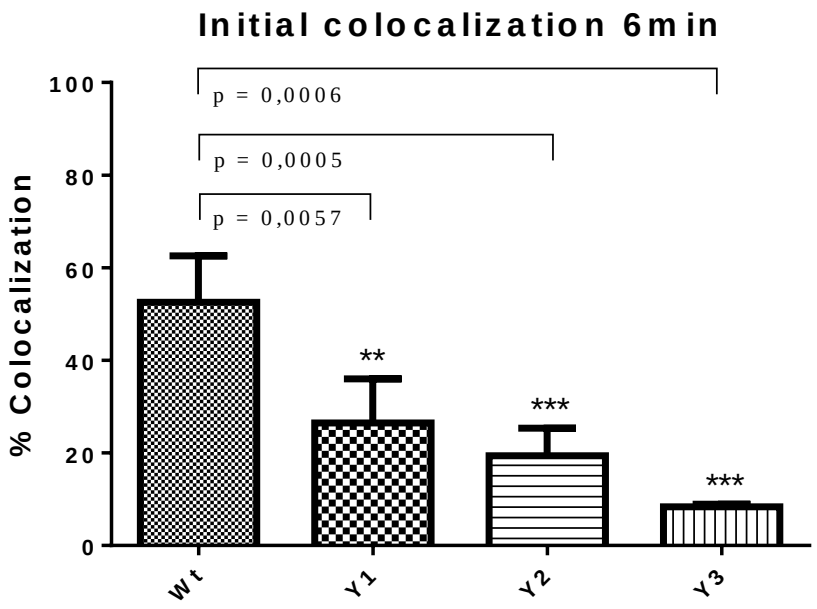

Figure 29 Colocalization with Rab5-mcherry at 6min to indicate internalization rates. Sselected time points were analyzed with Prism6. Two tailed t-test yielded statistical significance, comparing Wt to each receptor. Values were plotted by mean with SD.

The results from the internalization rate assay and the initial colocalization analysis are reminiscent of each other. There are clear similarities between the internalization and beginning of colocalization, suggesting that the delay is a result of both the internalization and the early stages of receptor trafficking, and likely due to the lack of an interaction with the mutant receptor at the plasma membrane.

4.3 Rab7 Colocalization: Y3-Mutant Evades Degradation

Our previous results show that the mutant receptors had a slower internalization rate, and the progression from the plasma membrane to early endosomes was delayed. In addition the mutants seemed to be retained in Rab5+ compartments. The Rab5-mCherry colocalization study further demonstrated that the triple mutant had a noticeably different endosomal progression. Based on these observations, it was decided to focus mainly on trafficking of Wt- and Y3-EGFR. It is well established that EGFR is transported from the early endosomes to late endosomes for lysosomal degradation [128]. We therefore continued our study by examining whether the receptor phosphorylation pattern would affect the later stages of receptor progression and/or endosomal sorting. To further elucidate the late endosomal trafficking characteristics we co-transfected HeLa cells with receptor and Rab7-mCherry, a late endosomal identifier [116], and examined the colocalization pattern.

The Rab7-mCherry construct was found to be poorly expressed. Instead of well-defined endosomes, Rab7-mCherry showed an overall cytosolic distribution. This made it impossible to distinguish Rab7-mCherry positive endosomes from background, as shown in Figure 30.

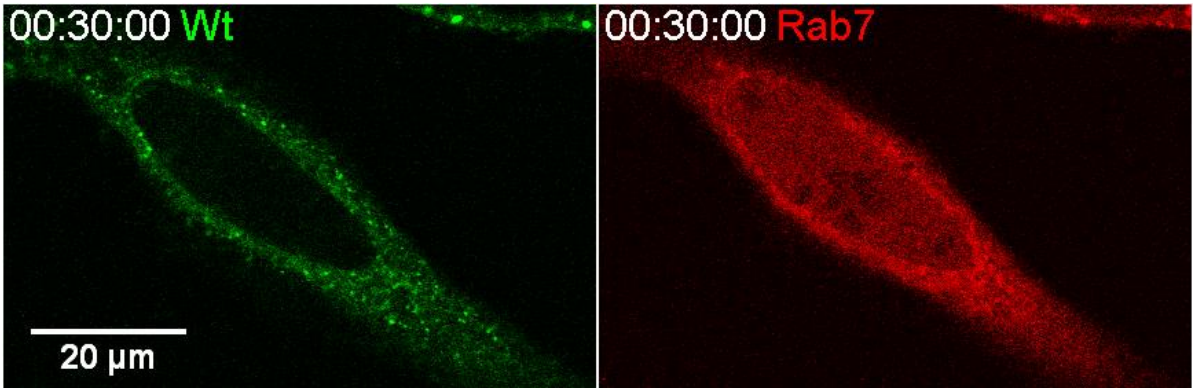

Figure 30 HeLa-cells co-transfected with Wt-EGFR Rab5-mCherry, demonstrating the cytosolic diffuse distribution of the Rab7-mCherry-construct

Previous publications have shown that the mCherry construct could be challenging to express in cell lines [169]. We therefore chose to change to a mApple-construct that has been found to form fewer aggregates and define its endosomal compartments well [170, 171]. The Rab7a-mApple was obtained from Davidson via Addgene (https://www.addgene.org/54945).

4.3.1 Wt-EGFR was Intraluminally Sorted in Late Endosomes

HeLa cells were transiently transfected with Wt-EGFR along with Rab7-mApple. On the day of imaging, cells were stimulated with EGF on-stage; image acquisition was every 30s for 2hours. Cells transfected with Rab7-mApple displayed defined Rab7-mApple positive (Rab7+) endosomes (Figure 31). Expression of the construct often resulted in enlarged endosomes, and endosomal clustering in the perinuclear region.

Before ligand stimulation Wt-EGFR was detected along the plasma membrane, similar to previous experiments (Figure 13). The majority of the Rab7-mApple positive endosomes were localized to the perinuclear region including a proportion of enlarged endosomes. We could further detect a minor proportion of Rab7-mApple positive endosomes spread throughout the cell (Figure 31). Upon EGF stimulation the receptor clustered on the membrane and was internalized. Wt-EGFR positive endosomes were observed within minutes after stimulation, followed by an increase in size and number. Soon after, Rab7-mApple was detected as small domains on the Wt-EGFR positive endosomes. As the endosomes matured, Rab7-mApple increased in concentration on the endosomal membrane (Figure 31). Pixel overlap was visible as the receptor /Rab7+ endosomes were transported to the perinuclear region. This may coincide with the switch from Rab5 to Rab7-positive coats as the endosomes mature, indicative of MVB progression to late endosome formation. Intraluminal detection of the receptor with a Rab7-mApple positive endosomal membrane was observed for the enlarged endosomes (Figure 32).

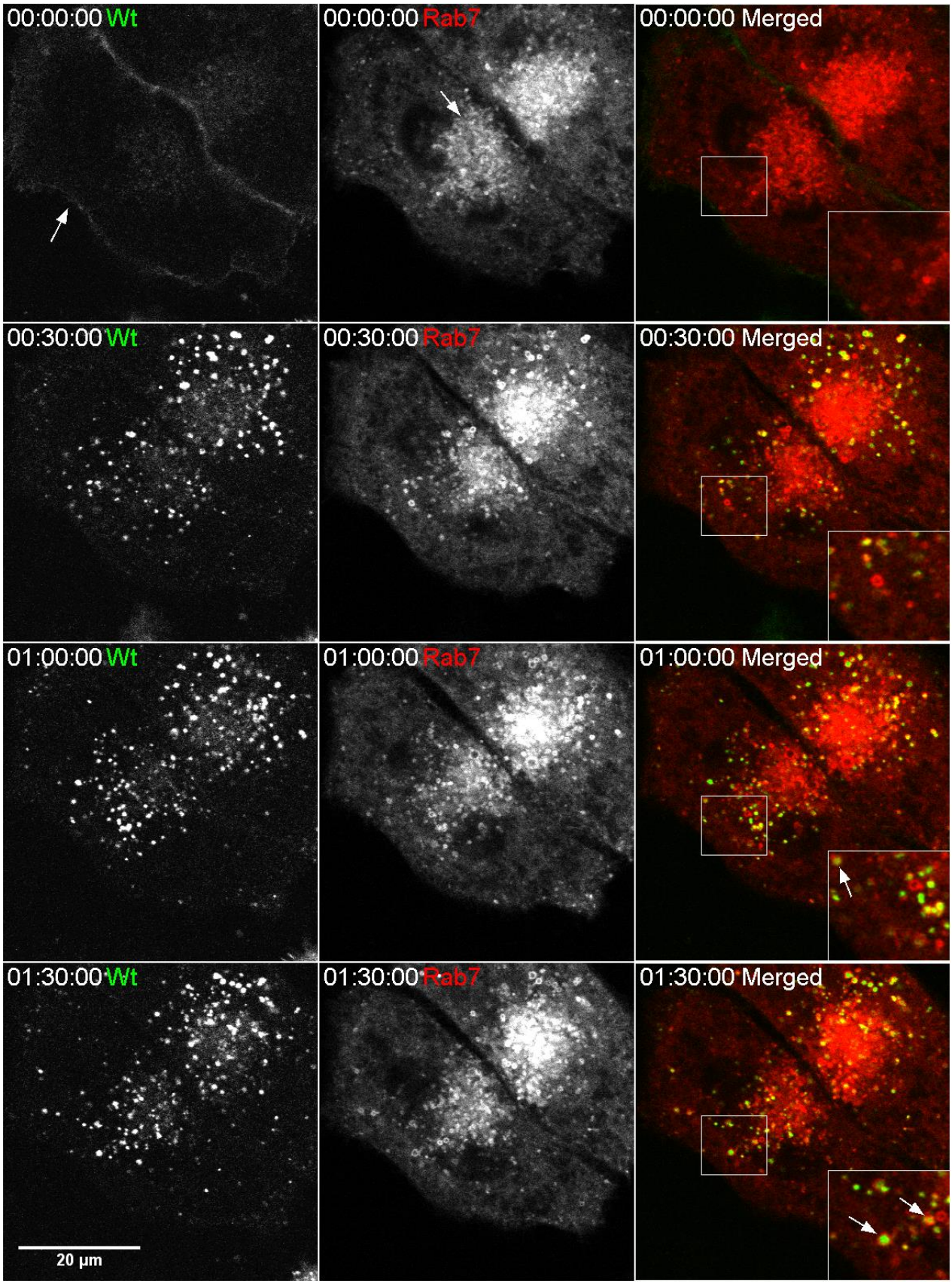

Figure 31 Montage of HeLa cells transfected with Wt- EGFP-EGFR [0.5ng/µl], and Rab7a-mApple [0.25ng/µl] using Lipofectamine 2000. Cells were continuously induced with EGF [100µg/ml]. Cells were imaged every 30 seconds for 120 minutes.

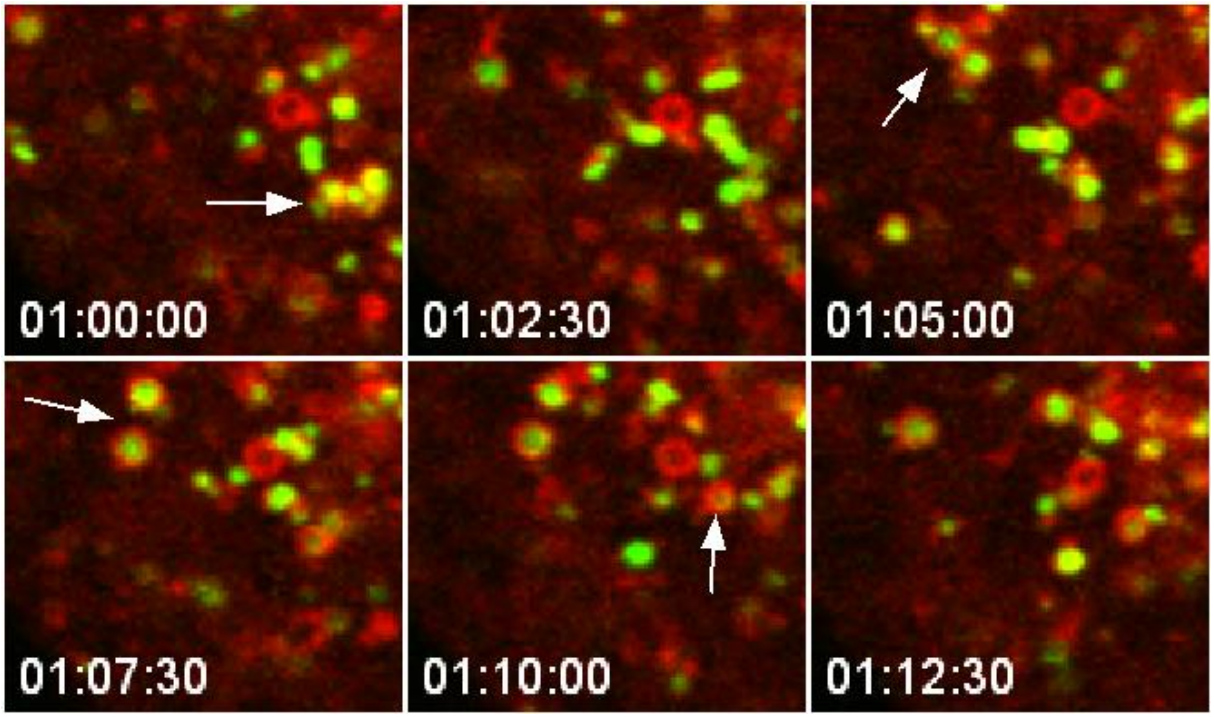

Figure 32 Colocalization of Wt-EGFR and Rab7-mApple showing EGFR fully internalized into the lumen of the late endosomes.

4.3.2 Y3-EGFR did not internalize in Rab7-mApple Positive Endosomes.

In HeLa cells co-transfected with Y3-EGFR and Rab7-mApple the receptor was detected along the plasma membrane prior to EGF stimulation. The Rab7-mApple positive endosomes were present throughout the cell, maintaining a high concentration in the perinuclear region, similar to Wt-EGFR. After EGF stimulation, punctuate Y3-EGFR positive structures formed along the plasma membrane (Figure 33), consistent with previous observations (Figure 22). Rab7-mApple attached to the receptor positive endosomes similarly to the Wt colocalization, forming small domains. Minor pixel overlap between Y3-EGFR and Rab7-mApple was observed at 30 minutes during the timelapse. Interestingly, the Y3-EGFR positive endosomes seemed to have an increased colocalization with Rab7-mApple throughout the timecourse, compared to the Wt-EGFR. This can be seen when comparing Figure 31 and Figure 33. However, closer examination showed that although there was a transient colocalization at the endosomal membrane, in Y3-EGFR-expressing cells Rab7-mApple either quickly detached from the endosome or failed to cover the receptor positive endosomes. Compared to the Wt-EGFR cells, where EGFR was visibly internalized into ILVs/ MVBs with a Rab7-mApple positive membrane surrounding endosomes (Figure 32), only a minor portion of the Y3-EGFR endosomes seemed to have intraluminal localization of receptor with Rab7+ membrane. The endosomes were observed to undergo repetitive cycles of unstable colocalization (Figure 34 & Figure 35), similar to the observations of Rab5-mCherry recruitment to Y3-EGFR positive endosomes (Figure 24). These results indicated that endosomes positive for 3Y-EGFR had an altered endosomal binding dynamic for Rab proteins.

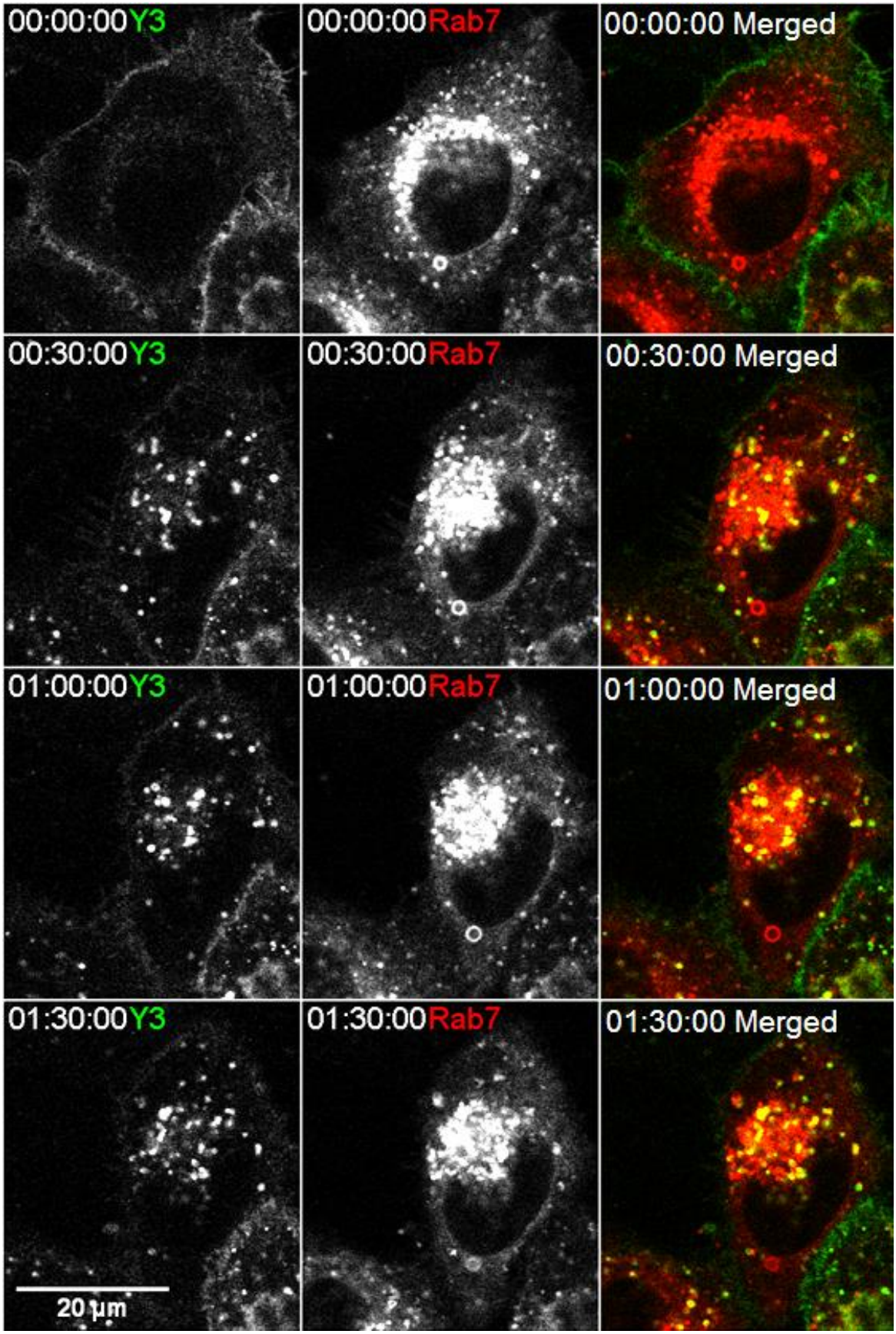

Figure 33 Montage of HeLa cells transfected with Y3- EGFP-EGFR [0.5ng/µl], and Rab7a-mApple [0.25ng/µl] using Lipofectamine 2000. Cells were continuously induced with EGF [100µg/ml]. Cells were imaged every 30 seconds for 120 minutes.

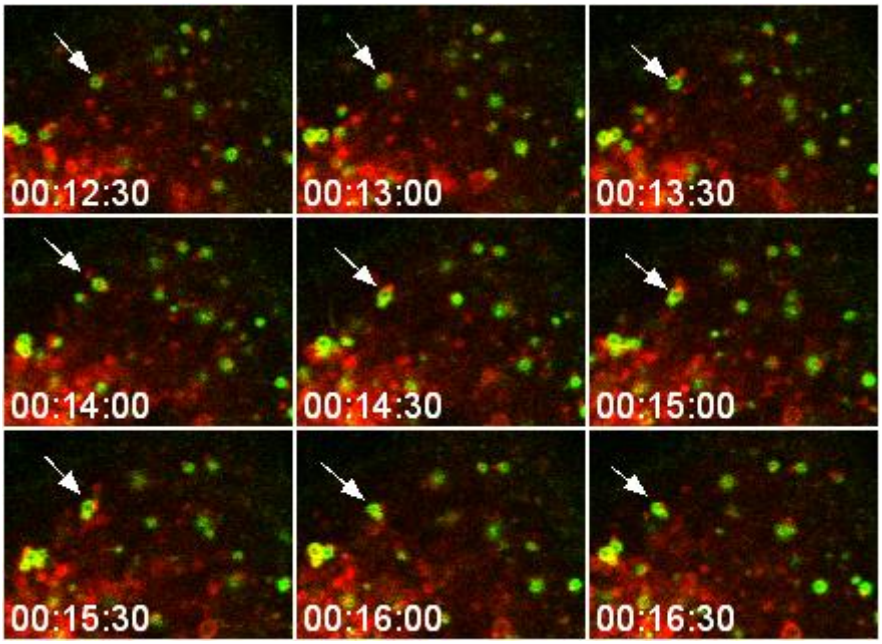

Figure 34 HeLa cell transiently transfected with Y3-EGFR and Rab7-mApple. Arrows follow an EGFR positive endosome, as Rab7-mApple formes a domain on the membrane, later detaching. The endosome fails to become completely Rab7-positive, indicating an altered endosomal progression and receptor sorting.

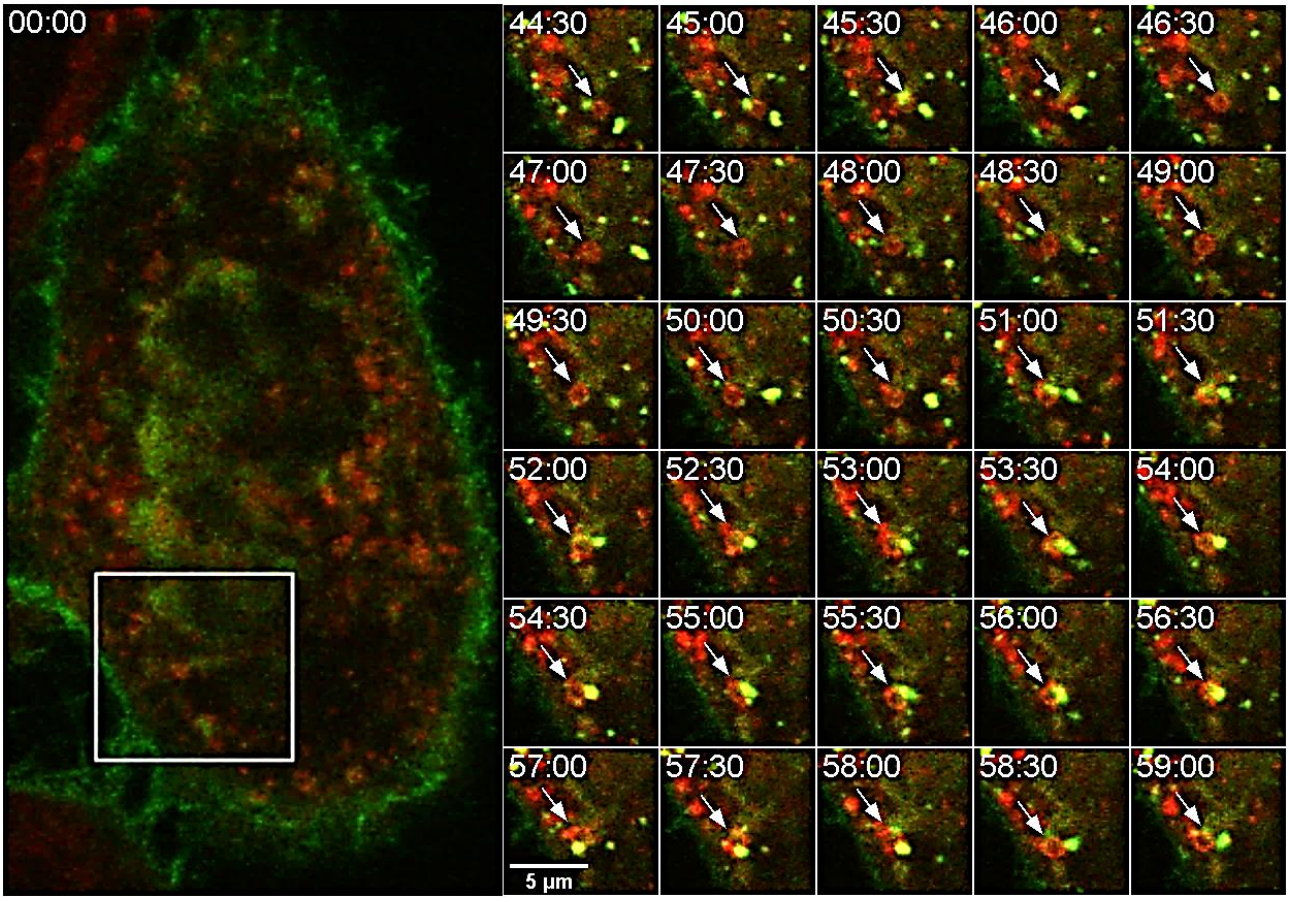

Figure 35 Co-transfected HeLa cell, Y3- EGFR & Rab7mApple. As indicated by the arrows Y3 positive endosome undergoes several failed attempts to fuse with an enlarged Rab7+ endosome.

4.3.3 EGFR Phosphorylation Affects Trafficking Towards Late Endosomes

As shown in Figure 32 the Wt-receptors are sorted into the lumen of Rab7-mApple positive endosomes. This leaves a Rab7-mCherry positive endosomal membrane with a Wt-EGFR positive lumen. The two fluorescent signals do not overlap but are localized to the same endosome. Therefore the colocalization data needs to be analyzed differently. In the Rab5-mCherry study there was clear colocalization, yet because of the enlarged endosomes the percent pixel overlap method is insufficient to describe the receptor progression. The Colocalization plugin was instead used to measure the initial colocalization. The method was used to compare the temporal difference between Wt- and Y3-EGFR for first Rab7-mApple attachments.

Figure 36 shows a delay in the colocalization pattern for Y3 compared to Wt-EGFR, lasting approximately 10 minutes. This is similar to the delay presented in the Y3/Rab5-mCherry colocalization data (Figure 23).

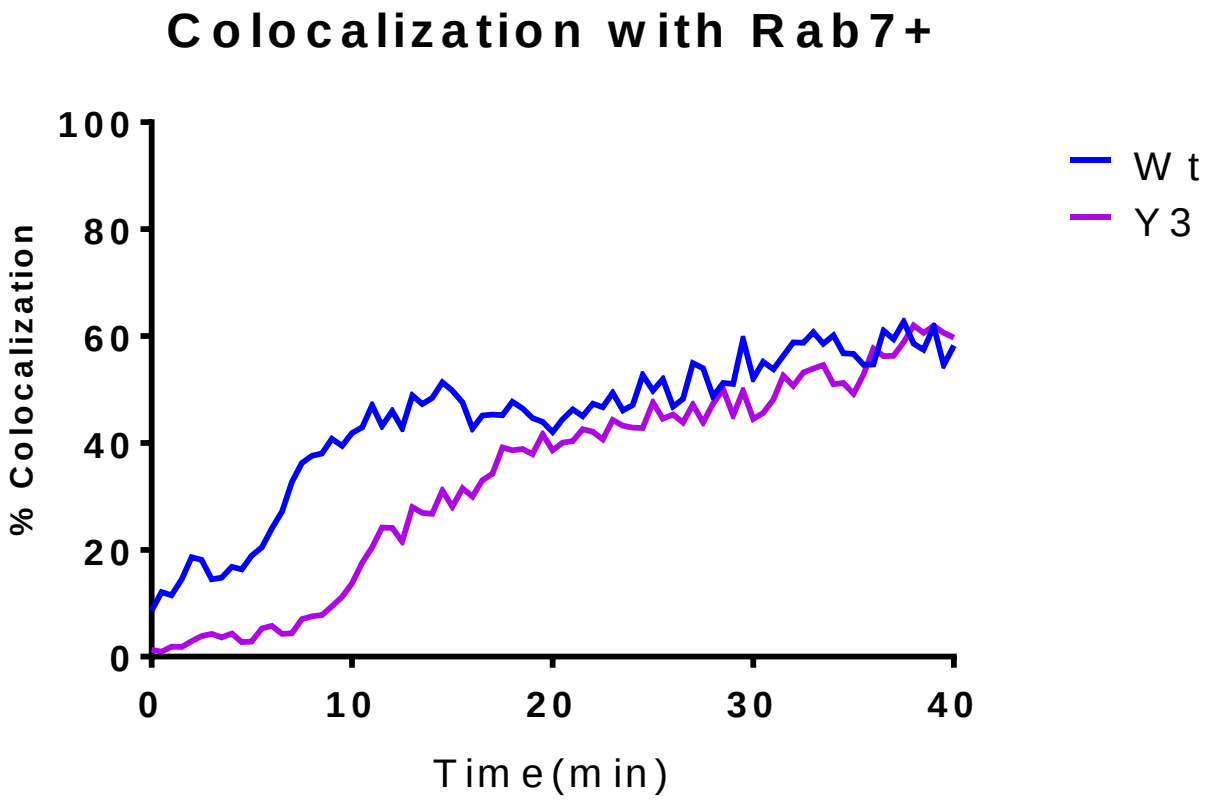

Figure 36 Wt-EGFR, and Y3 –EGFR colocalized with Rab7-mApple. HeLa cells were induced with 100ng/ml EGF alexa 647. Cells were imaged every 30 seconds for 120 minutes. Wt: $Cell_n$ =9, Y3: $Cell_n$ =9

Closer examination of selected points at the beginning of the time course showed a significant difference between Wt-EGFR and Y3- EGFR colocalization with Rab7-mApple (Figure 37). The Y3-EGFR cells displayed a significantly lower colocalization of EGFR with Rab7-mApple at 10, 20 and 30 minutes after EGF stimulation. The delay further confirms a different trafficking due to an altered phosphorylation pattern of the receptor. These results indicate that the triple mutant may be able to escape degradation (Figure 35). This was further examined by looking at colocalization of Wt and Y3 with Lysotracker, a stain used to identify lysosomes.

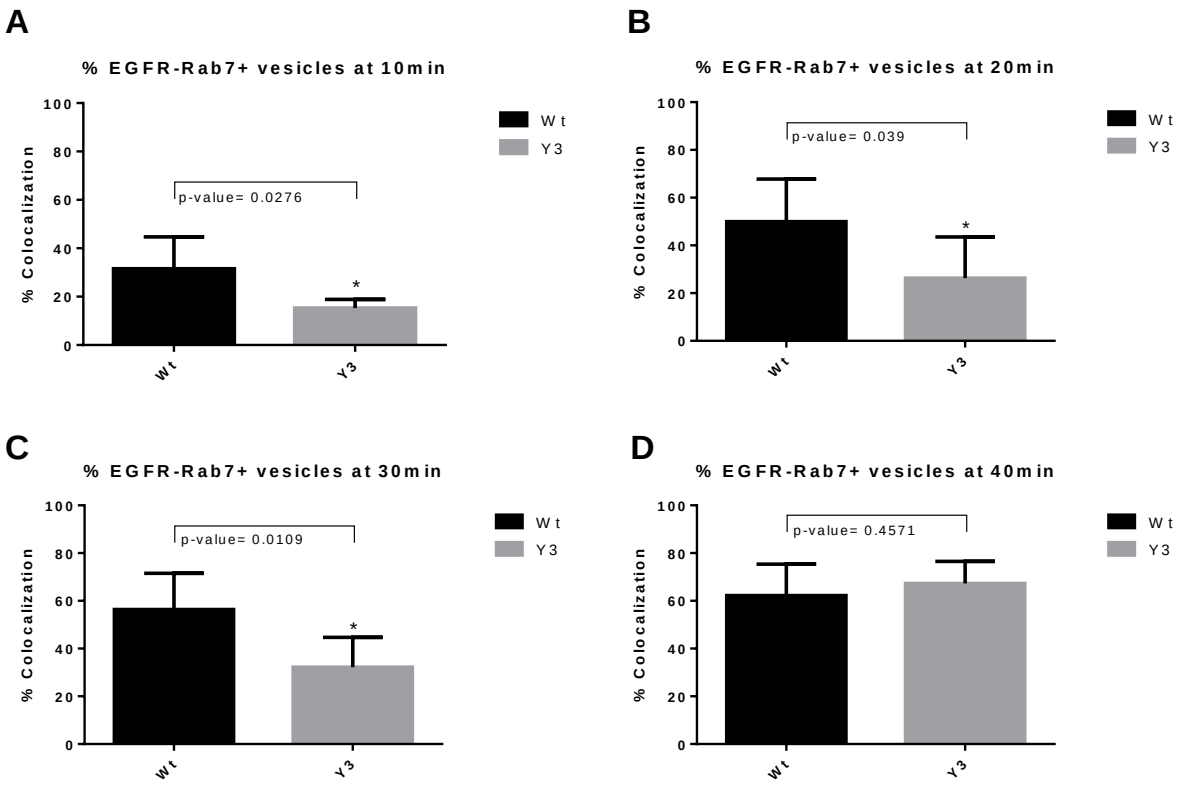

Figure 37 Colocalization with Rab7-mApple at selected time points, analyzed with Prism6. Two tailed t-test yielded statistical significance, comparing Wt-EGFR to Y3-EGFR. Values were plotted by mean with SD. p-values are presented in the graph. Percent amount of vesicles that colocalized at A: 10min, B: 20min, C: 30min, D: 40min.

4.4 Y3-EGFR Showed Impaired Sorting to Lysosomes

To better understand the difference in sorting for degradation between the Wt and the Y3 receptor we wanted to analyze the colocalization between the two individual receptors and LysotrackerRed. Lysotracker Red DND-99 is a dye that stains endosomal compartments with a pH lower than 5.5, therefore staining both maturing late endosomes and lysosomes.

Hela cells were transfected over-night, either with the Wt-EGFR or the mutant receptor, for imaging the following day. Prior to the experiment the cells were labeled with LysotrackerRed.

Originally we planned to image the cells for two hours and perform a similar colocalization analysis of the timelapse data. However, the LysotrackerRed bleached considerably during the experiment, enough to lose the fluorescent signal required for colocalization measurements. To further avoid the LysotrackerRed bleaching problem, we decided to EGF activate the LysotrackerRed labeled transfected cells for two hours in the incubator. After two hours we imaged the EGF stimulated cells at five random positions per experiment. Figure 38 shows an example cell expressing A: Wt-EGFR, and B: Y3-EGFR. After two hours there was substantial colocalization of the Wt-EGFR with LysotrackerRed. However, there was hardly any pixel overlap of Y3-EGFR and LysotrackerRed positive endosomes.

Performing an object-based colocalization (Materials and Methods, section 3.4) revealed a significant difference between the mutant receptor and the Wt (Figure 39). The measured colocalization of the Wt after 2 hours EGF stimulation was 44%, whereas the Y3 mutant was at 20%. This signified that the altered phosphorylation pattern for the triple mutant impaired maturation of the Y3-EGFR-containing-endosomes to lysosomes, as shown by reduced colocalization with Rab7-mApple (Figure 33) and LysotrackerRed (Figure 39).

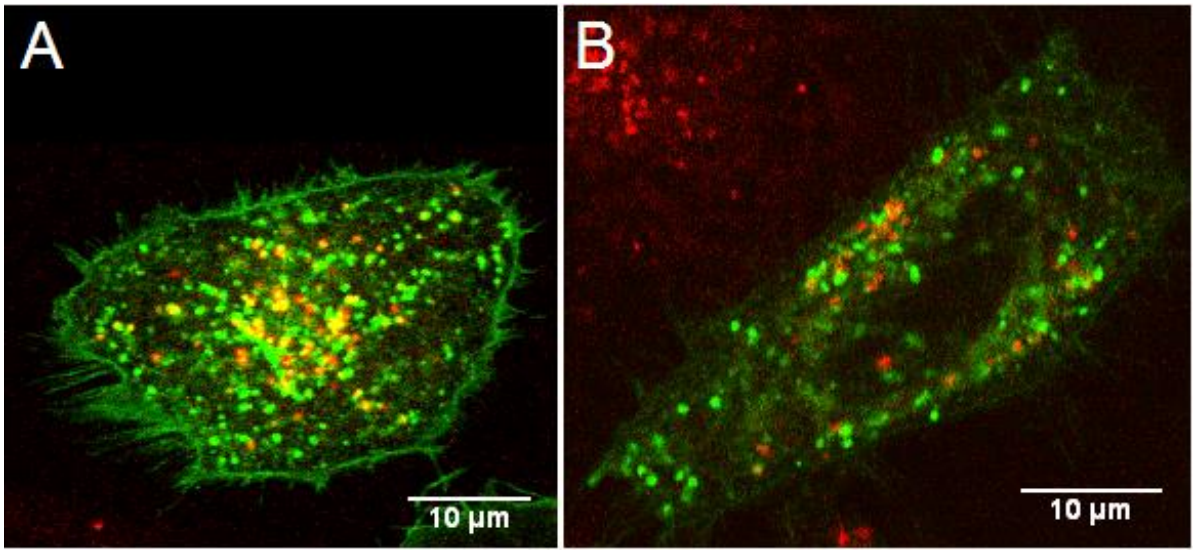

Figure 38 HeLa cells transiently transfected with Wt (A) or Y3 (B) receptor and stained with LysotrackerRed imaged after 120 minutes EGF stimulation. Pixel overlap is represented as yellow, indicating colocalization for Wt-EGFR. Little to no colocalization was observed in Y3-expressing cells, as indicated by the example cell.

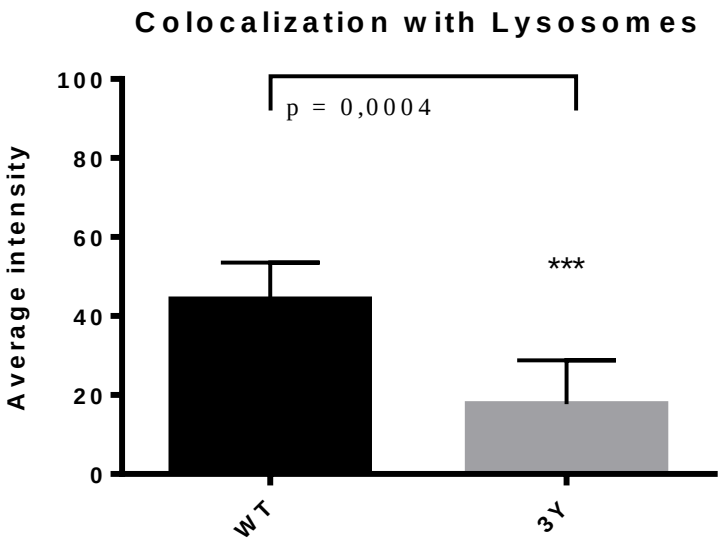

Figure 39 Endosomal colocalization between Wt- or Y3- EGFR and LysotrackerRed after 120minutes EGF stimulation. Data points were analyzed with Prism6 software. Two tailed t-test yielded statistical significance. Values were plotted by mean with SD. p-values are presented in the graph. $Cell_{Wt}$ =5 $Cell_{Y3}$ =5

4.5 EGFR Degradation

The LysotrackerRed experiment showed a 50% decreased colocalization of Y3-EGFR, a significant decrease in colocalization of Y3 with lysosomes. Additionally, the Rab7-mApple colocalization study showed that Y3-EGFR failed to fuse with late endosomes. This could indicate that the mutant receptor avoids degradation as well. In order to examine this we performed a degradation assay.

PAE cells stably transfected with either Wt or mutant EGFR were stimulated with 20ng/ml EGF for 0, 2, 4, and 6 hours, and then lysed and subjected to Western blotting (for more information see: Material and Methods section 3.6 Western Blotting & Transfer). Tubulin was used as the loading control for this experiment. The Western blot shows that the mutant receptors are less degraded than the Wt (Figure 40). The intensities were quantified and presented in a Western blot Densitometry (Figure 41). The Wt has a steady degradation the first 4 hours, after which the EGFR didn't seem to degrade any further. This could be the base level required for normal cell function or inactive receptor. There appeared to be more receptor present for the mutants. Y1-EGFR had a similar degradation as seen for Wt. The main differences occur for the double and triple mutant receptors. Y2 and Y3 had little to none degradation. The degradation assay is in agreement with the LysotrackerRed colocalization study, indicating that the mutant receptors avoid degradation.

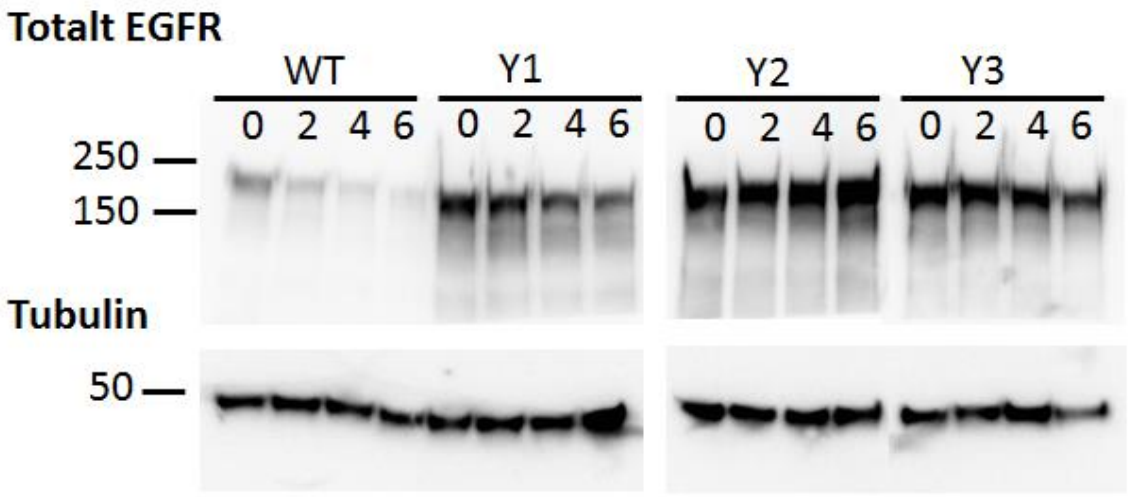

Figure 40 Western blot. PAE cells stably transfected with either Wt or mutant EGFR were stimulated with 20ng/ml EGF for 0, 2, 4, and 6 hours, and then lysed and subjected to Western blotting. The blot shows EGFR (~170kDa) degradation over time, and Tubulin (~50kDa), as the loading control.

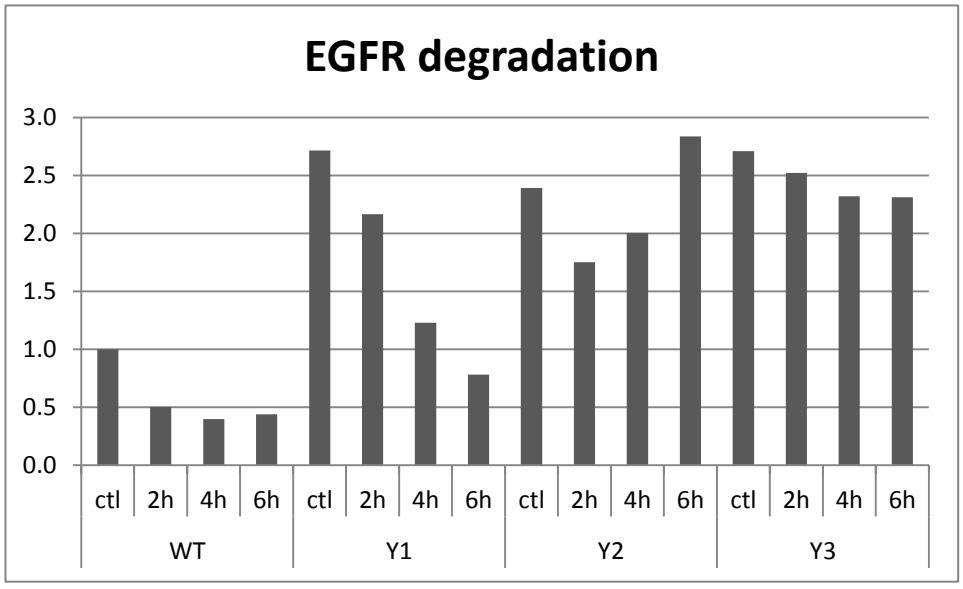

Figure 41 Western Blot Densitometry. The band intensities were to the normalized to reciprocal t=0. The Western blot analysis was quanitfied using ImageJ.

4.6 Inhibition of Clathrin-Mediated Endocytosis by Pharmacologic Inhibitor, Pitstop2

In addition to clathrin-mediated endocytosis, EGFR has been reported to be internalized via clathrin-independent endocytosis. Sigismund et al. showed that at high ligand concentrations the receptor was internalized exclusively via clathrin-independent endocytosis [172]. The results from our Rab5-mCherry colocalization revealed a delay in the trafficking of the EGFR mutants towards degradation. The delay was further found to be due to both the internalization and the early stage of trafficking. A possible explanation for this could be that the receptor undergoes an alternative internalization for example clathrin-independent endocytosis, which is generally slower. In order to analyze the endocytic characteristics for the different mutants we utilized the properties of a known clathrin-mediated inhibitor Pitstop2 [173].

Pitstop2 inhibits clathrin-mediated endocytosis, by obstructing the interaction between the clathrin terminal domain, and the B/C domain of amphiphysin. Amphiphysin binds both clathrin and AP-2 at its B/C domain, amino acids: 250-588 [174]. A previous study had tested the compound at various concentrations [173], showing that the concentration 20μM did not inhibit endocytosis completely; however there was a substantial decrease observed. Based on their results we decided to use Pitstop2 at a final concentration of 25μM. To avoid non-specific binding of the compound the manufacturer recommended the experiment not exceeded 30 minutes in total.

Our previous results showed that the Y3 had the most difference in trafficking, and sorting. Therefor in the experiment we compared the internalization of Wt-EGFR and Y3-EGFR. For simplicity the control used for the Pitstop2 experiment was the same data obtained in the Rab5-mCherry colocalization experiment. 12ng/ml EGF Alexa 647 was used to stimulate the cells as this was found to be the lowest concentration that still produced a measurable fluorescence signal. The concentration was decided based on a previous study showing that ligand concentration below 20 ng would induce clathrin-mediated endocytosis, anything above would result in both clathrin-mediated and clathrin- independent endocytosis[78].

HeLa cells were transiently transfected with either Wt- or Y3- EGFR. Prior to imaging the cells were incubated with Pitstop2 for 10 minutes. To catch the internalization and early trafficking event we acquired images every 15 seconds for 20 minutes. After 10 minutes

treatment with Pitstop2 the cells appeared to have more cell ruffling than normal. Additionally the Pitstop2 treatment seemed to induce a frozen state in certain cells, we chose to exclude these from the study. The control and Pitstop2 inhibited cells were analyzed by measuring percent pixel overlap between EGFR and EGF 6 minutes into the timelapse (Figure 42). The imaging intervals were different for both control and Pitstop2 treated cells, this was taken into consideration when analyzing the timeseries.

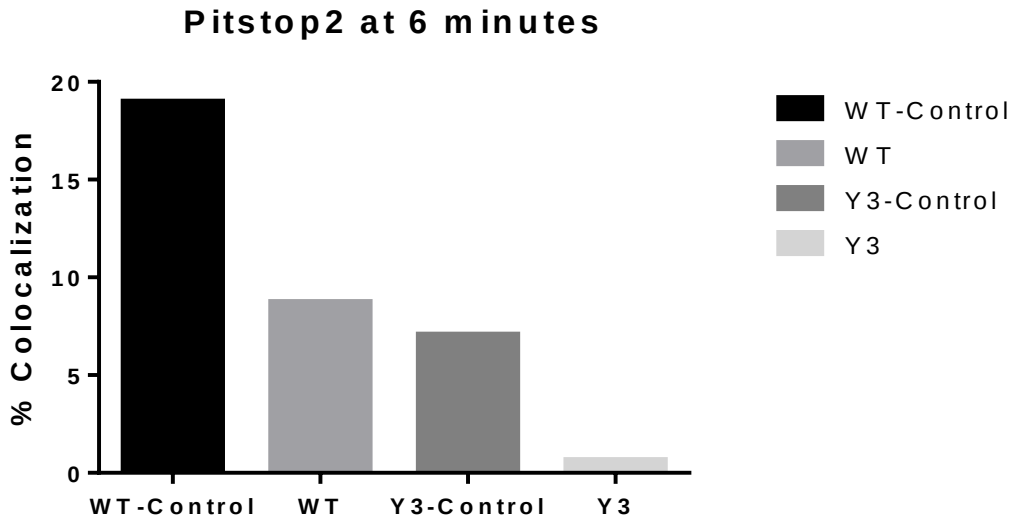

Figure 42 The control cell data, non-treated with Pitstop2, was extracted from the Rab5-mCherry colocalization study, as mentioned above. HeLa cells were transfected with Wt- or Y3- EGFRand treated with Pitstop2 onstage for 10 minutes before image acquisition was initiated. Analysis was performed by percent pixel overlap, using the data points after 6 minutes.

The receptors were expected to either be internalized, or not at all. Instead Figure 42 shows a decreased colocalization for both the Wt, and Y3-EGFR expressing cells treated with Pitstop2, compared to the control. This potentially indicates that the inhibitor has partially inhibited clathrin-mediated endocytosis, and both Wt and Y3 are internalized by this pathway. The control, Rab5-mCherry colocalization experiment, was stimulated with a higher ligand concentration 100ng/ml, the cell treated with Pitstop2 were stimulated with 12ng/ml. It is therefore a possibility that the control receptor cell show higher values due to both CME and CIE internalizing the receptor-ligand complex.

In order to control if the inhibitor actually worked the experiment was repeated with non-transfected HeLa cell. The cells were treated with Pitstop2 for 10 minutes before stimulation with EGF-Alexa 647. The control experiment showed a major reduction in endocytosis for endogenous EGFR. Although most of the EGF was stuck on the membrane, forming punctuate structures, a fraction of EGF was internalized. Some cells were found to have more internalization of EGF than others (Figure 43). EGF-stimulated cell, without Pitstop2, resulted in observable internalization. From this it is possible to conclude that Pitstop2 does not completely inhibit endocytosis, yet indicates that Wt-EGFR and Y3-EGFR are internalized by the same pathway, CME. The difference as observed in Figure 42 could be due to the small sample size and natural variation between cells. It is also possible that the difference is due to the initial lag as observed for the Y3 mutant. These results are therefore considered inconclusive and require further testing.

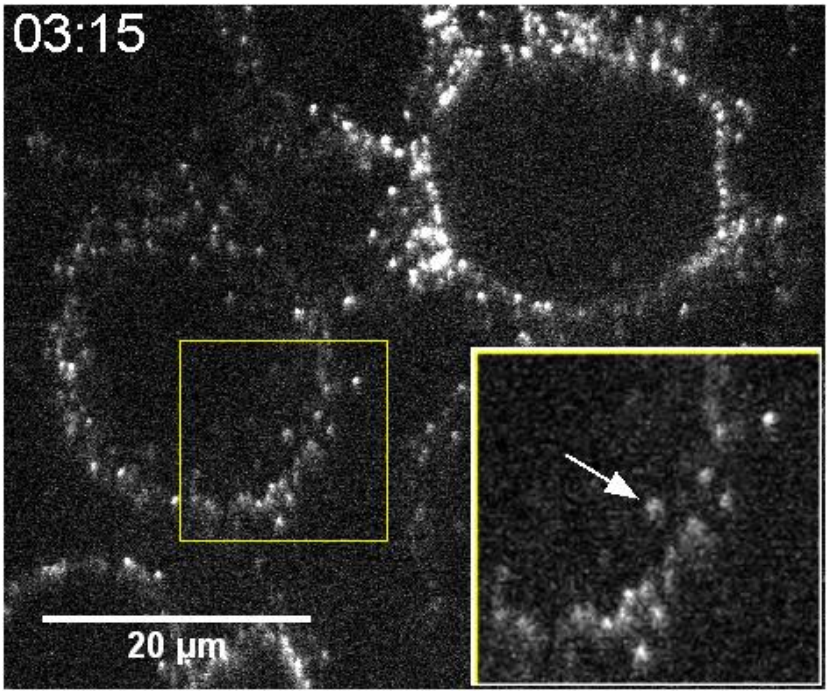

Figure 43 Control experiment. Non-transfected HeLa cells stimulated with EGF-Alexa 647[12ng/ml], after 10 minutes incubation with Pitstop2 [25mM].

5 Discussion

Pathways and mechanisms important for EGFR have been under scrutiny ever since its first discovery, in an attempt to comprehend the regulation of the receptor. A major focus has been receptor trafficking and how this regulates the signaling cascades, linking the receptor tyrosine kinases to cancer development. In this study we investigated how EGFR phosphorylation triggers the recruitment of various binding partners that affect endosomal sorting. Fluorescently tagged EGFRs carrying mutations at specific C-terminal phosphotyrosines (Y1045, Y1068, and Y1086) have been tracked through time and compared with the Wt-EGFR. We have established a live cell imaging analysis method to enable temporal characterization of receptor trafficking, from the plasma membrane through the endocytic pathway to the lysosomes. Our results show that mutation of these specific phosphotyrosines prompt changes in the internalization, endosomal maturation/ progression, late endosomal intraluminal sorting, and degradation.

5.1 Phosphorylation Pattern Determines Receptor Trafficking

From our analysis of the Wt-receptor we could observe a constant increase of colocalization towards maximum colocalization after 23 minutes (Figure 14). Following the maximum colocalization there was a decrease in the colocalization between Wt-receptor and Rab5-mCherry. This loss of colocalization was caused by a decrease in the intensity of Rab5-mCherry, characteristic of Rab5-mCherry detachment during endosomal maturation [168]. Wt-EGFR expressing cells were observed to form stable Rab7-mApple positive endosomes, internalizing the receptor to intraluminal vesicles, indicating endosome maturation (Figure 32). The object-based colocalization analysis study with LysotrackerRed showed that after 2hours 50% of the receptor was localized within lysosomes indicating lysosomal degradation (Figure 39). This was further substantiated by the degradation assay showing that after 2hours ~50% of the receptor had undergone degradation (Figure 41). The Wt was used as a standard for comparison of the aberrant trafficking of the mutants.

The Y1-EGFR contained a mutation of pY1045, the preferred binding site for Cbl. In our live cell imaging studies examining the Y(1045)F receptor's colocalization pattern with Rab5+ endosomes, we observed a slower trafficking into early endosomes. Later in the timecourse

the amount of colocalization reached a plateau and the receptor appeared to be retained in early endosomes (Figure 17). Y1-EGFR was internalized at a similar rate to the Wt (Figure 28), yet a delay was present at initial colocalization (Figure 29). This delay seemed to be propagated towards degradation as the receptor was found to take 4 hours before reaching 50% degradation (Figure 41).

The Y2-EGFR contained mutations at pY1068 and pY1086, important Grb2 receptor binding sites. The double mutant showed a slow internalization rate (Figure 28), including a slow initial colocalization at 6 minutes (Figure 29). However, at 10 mintues the colocalization had surpassed the single mutant (Figure 26). During the early phase of the timecourse, the Y2-EGFR showed similar behavior to the Wt-EGFR, having a similar time to maximum colocalization (Figure 27). However, unlike the Wt-EGFR the Y2 mutant was retained in early endosomes, as shown by the plateau in colocalization which demonstrates a lack of Rab5-mCherry detachment. This lack of endosomal progression correlated with the inhibited degradation of the Y2 EGFR as seen in the Western blot Densitometry (Figure 41).

Y3-EGFR contains mutations in all three phosphorylation sites, thereby abrogating the binding sites for both Cbl and Grb2. The Y(1045/1068/1086)F mutant had significantly different trafficking from the Wt-EGFR. Y3- positive endosomes were observed to move freely in the cytoplasm, maintaining a peripheral localization for a longer period of time (Figure 22), and demonstrated delayed colocalization with Rab5-mCherry (Figure 23). This was supported by a low internalization rate (Figure 28), and a decreased initial colocalization compared to the Wt (Figure 29). Y3-EGFR colocalization with Rab7-mApple positive endosomes showed a similar delay (Figure 36). The receptor failed to form Rab7+ endosomes with intraluminal receptor (Figure 34, Figure 35), indicating failure to progress to late endosomes. The Y3-positive regions also showed significantly less colocalization with lysosomes, compared to Wt-EGFR (Figure 39). This indicated a prominently decreased degradation, as supported by the degradation assay. The degradation assay (Figure 41) further substantiated that the receptor avoided degradation.

5.2 Phosphorylation Pattern: Cbl & Grb2 Functions

Receptor phosphorylation is important for signal transduction and formation of docking sites for phosphotyrosine-binding adaptors proteins, such as Grb2 and Cbl. Grb2 is a key adaptor for signal transduction, and the main adaptor for the Ras signaling pathway, which regulate

proliferation, differentiation, and migration to name a few. Cbl is involved in transferring ubiquitin to EGFR. Ubiquitin is required for recognition by the ESCRT complex. DUBs deubiquitinate the receptor as ESCRT ushers the receptor into ILVs, thereby promoting its degradation (Figure 44). Tyrosine phosphatases dephosphorylate the receptor as it is internalized in MVBs, terminating the signal [129]. The mutated receptors contain substitutions in the preferred Cbl and Grb2 binding sites. Despite there being some redundancy for the binding of these proteins, in that they can each form direct and indirect interactions with the receptor, the study showed significantly altered trafficking for the mutant receptors. The analysis of the data could potentially suggest a control mechanism for the endocytic pathway involving the ubiquitination pattern of the receptor.

5.2.1 Grb2 Mediates Internalization

Grb2 has recently been found to be involved in recruiting EGFR into clathrin coated pits [84]. In the same study depletion of Grb2 was shown to diminish receptor clathrin mediated internalization of the receptor. Their results implicated Ras as a regulator for the early stages of EGFR clathrin- dependent internalization further showing that c-Cbl was inefficiently recruited to EGFR resulting in a lack of polyubiquitin [84]. Our results showed that the mutant receptors were internalized, albeit slower than the Wt. The main difference between our study and this paper is they used RNA silencing of Grb2, while we removed specific sites on EGFR known to bind Grb2. Our study focuses more on the main interaction between receptor and Grb2, while theirs is an overall depletion of Grb2. RNA silencing has been found to have non-specific effects and could affect more than the gene of interest [175]. Taken together, these two studies indicated that Grb2 can possibly bind elsewhere on the receptor, so to mediate recruitment to clathrin coated pits. This could be an additional explanation for the delayed internalization of the phosphorylation mutants. From the internalization assay (Figure 28) the delay is more prominent for Y2 and Y3, the two receptors that lack the Grb2 binding sites. The single mutant had a similar internalization to the Wt-EGFR, further emphasizing Grb2's involvement in the receptors' internalization rate.

5.2.2 Cbl is Involved in Receptor Trafficking

Our study showed that the double mutant overcomes its delayed colocalization toward the point of saturation (Figure 27). Previous work done by the lab showed that Y1 and Y2 had a different ubiquitination pattern compared to Wt, while Y3-EGFR was not ubiquitinated, after

1 hour EGF stimulation [100ng/ml], on ice (manuscript in progress [162]). This suggests that Cbl, when bound to pY1045, may generate a different ubiquitination pattern that is more important for trafficking, than the ubiquitin signature generated when Cbl interacts indirectly with EGFR via Grb2. Additionally, ubiquitin has been found to be necessary for Rabex-5 recruitment, a Rab5 effector [176]. The Y1045 mutation was observed to affect the sorting into early endosomes and/ or early endosomal maturation pattern (Figure 17). During our colocalization experiments with Y1, Rab5-mCherry appeared to be recruited to a lesser extent. This could indicate a correlation between the different ubiquitination patterns and the recruitment of Rabex-5. Together with Rabaptin-5, Rabex-5 is an important regulator of fusion with early endosomes [121, 177]. This could be a possible explanation for the observed delay (Figure 27, Figure 29).

5.2.3 Induced Instability in Endosome Maturation

The later stages of the colocalization pattern for Y1 and Y2 reach a plateau (Figure 25). The fact that the mutant receptors are retained, further suggests that an unknown mechanism is disrupted. Given that Grb2 is involved in the internalization of EGFR, this could account for the quicker internalization of the single mutant. In comparison the slower trafficking of Y1 could be due to Cbl at its indirect position in conjunction with Grb2, producing a different ubiquitination pattern and/ or requiring more time to ubiquitinate the receptor. The fact that the receptor also maintained a peripheral localization indicates that the phosphorylation pattern introduces a new variable to the system. This could potentially be due to an inhibited Rab5 to Rab7 conversion [168], suggesting that instability had been introduced in the normally stable trafficking system. In Y3 expressing cells Rab5-mCherry was observed to be recruited to the receptor positive endosome, only to detach soon after. The Rab7-mApple colocalization data further substantiated the difference in Rab protein binding dynamic (Wt: Figure 32. Y3: Figure 34 and Figure 35).

5.2.4 Ubiquitin-Threshold-Dependent Trafficking

A possible explanation for the altered trafficking could be that fusion events between newly internalized vesicles and early endosomes are ubiquitin-threshold-dependent, further indicating that the initial colocalization is the rate limiting step for receptor trafficking. The Y3-EGFR receptor positive endosomes appeared incapable of moving away from the periphery of the cell, until reaching an “enlarged” state. The aggregated receptors then

collaborated by increasing the amount of local ubiquitin (Figure 45). The different ubiquitination pattern could potentially be why the mutants are retained, as the early endosomes fail to form MVBs. The receptors could be immobilized until the local concentration of ubiquitin is corrected, enabling stable interactions with ubiquitin- interacting motif, UIM, -containing proteins, such as Hrs. The endosomal size has not been quantified, yet the mutants, especially Y3 visibly created larger endosomes. However, this needs to be closer examined.

5.3 Inhibition of CME by Pitstop2

During our study we examined Wt- and Y3-EGFR internalization by use of a pharmacologic inhibitor, Pitstop2. We observed that the inhibitor was unsuccessful in fully inhibiting CME (Figure 43). However, there was still observed an inhibitory effect from the drug (Figure 42). It can therefore indicate that the receptors were being internalized by CME. This would corroborate a publication saying that the Y(1045)F mutation was found to be internalized via CME, regardless of ligand concentration [172]. The results from these experiments were inconclusive and further investigations are ongoing.

Due to the multiplicity of endocytic mechanisms, it is difficult to create a flawless clathrin-mediated endocytic inhibitor. There have been publications addressing the non-specificity of the inhibitor, concluding that the compound should not be used to examine specific clathrin interactions. It has further been reported that the compound can inhibit endocytosis of proteins that usually enter through clathrin- independent pathways [173]. However, in the study they exceeded the recommended time for that incubation with Pitstop2.The protocol states that after 30 minutes there could be non-specific binding.

5.4 Conclusion

In the study we have analyzed EGFR trafficking by colocalization with Rab5, Rab7 and lysosomes. Our results demonstrated that the receptor's phosphorylation pattern codes for its proper internalization and trafficking, ultimately deciding its fate. The phosphotyrosine mutations translated into a "Rab protein-instability" and as a consequence the normal maturation from early to late endosomes was disrupted. The study further indicated that receptor trafficking is ubiquitin-threshold-dependent.

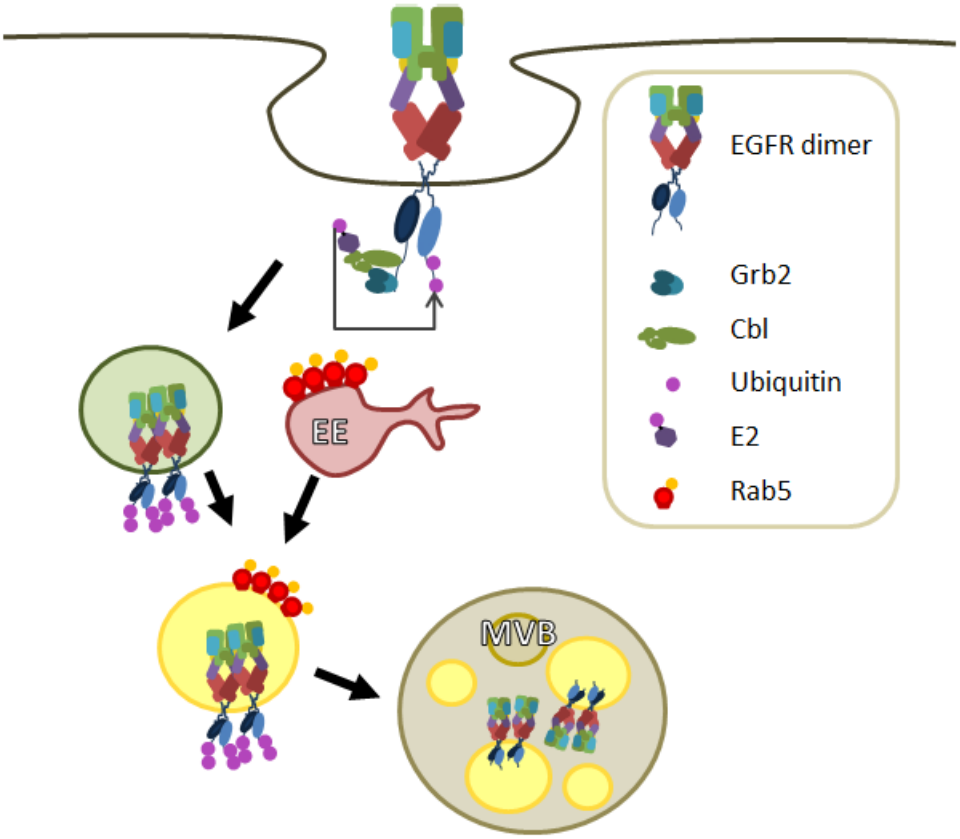

Figure 44 Schematic diagram of the Wt trafficking. Activated EGFR is autophosphorylated and Cbl and Grb2 are recruited to the phosphortyrosines. Grb2 recruits EGFR into clathrin coated pits in and initiates signal transduction, while Cbl ubiquitinates that receptors. UIM-containing proteins are recruited and mediate fusion between newly internalized vesicles and early endosomes. Receptors destined for degradation are internalized into ILVs and the early endosomes matures. ILVs accumulate and the endosomes forms a MVB. Eventually the receptor is degraded inside lysosomes.

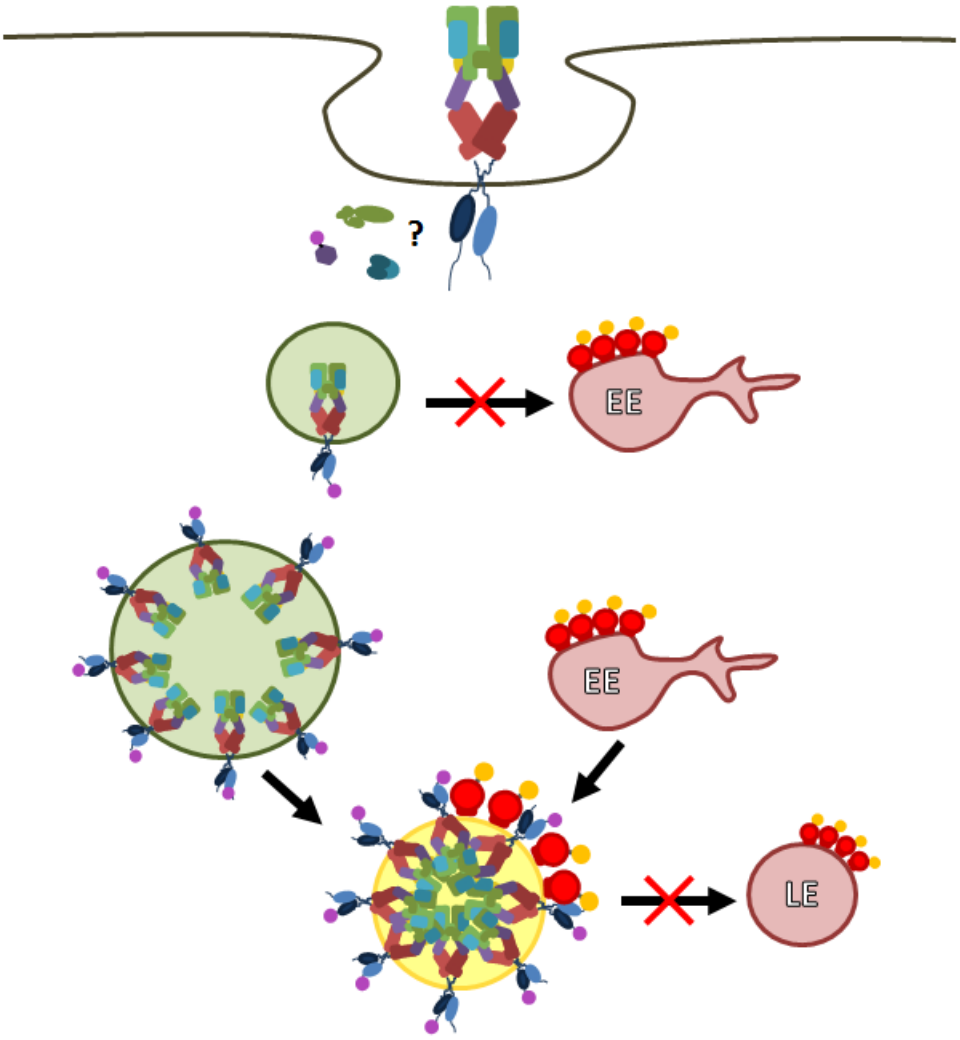

Figure 45 Schematic of proposed mechanism for the ubiquitin-threshold-dependent trafficking, based on observations and analysis that was revealed during our study. The internalized receptor positive endosomes, aggregate of fuse with each other, until the local concentration of ubiquitin reaches a certain threshold, allowing recruitment of ESCRT and fusion with early endosomes.

6 Future Perspectives

The live cell imaging study has shown that the EGFR phosphorylation pattern is important for the trafficking of the receptor, thereby controlling receptor fate. Abrogation of the binding sites for Cbl and Grb2 disrupted Rab protein binding dynamics, hindering the endosomal maturation. The internalization assay and the initial colocalization study suggested a two-part delay for receptor trafficking. The first stage of the delay was generated at internalization. The second stage of the delay appeared to be due to a lack of interactions between the receptor and endocytic machinery immediately after internalization. Closer examination of protein recruitment at the point of receptor activation and immediately after endocytosis would be of interest.

Supplementary experiments are required to characterize the reason for why the receptor is retained in early endosomes. Based on our results it is likely that MVB formation is hindered, due to a disrupted Rab conversion. Y1 and Y3 were observed to linger at the periphery of the cell during the first 15-20 minutes. It can therefore be speculated that ubiquitination is key to the early trafficking of the EGFR, and that the receptors may perhaps undergo several rounds of deubiquitination-reubiquitination cycles until the correct pattern is present.

Questions remain to be resolved concerning the induced instability of Rab protein binding dynamics in the presence of the Y3 EGFR. Such as does the receptor have a diminished ability to recruit Rab5, if so, is it due to a disrupted early homotypic fusion of the newly internalized endosomes. In addition the altered internalization pattern has been found to correlates with a different ubiquitination pattern (previous work done by the group). There could be a hierarchy of ubiquitination patterns which produce different endosomal sorting. The ubiquitination of the mutant receptors need to be further characterized, including determining the type of ubiquitination pattern, as a majority of branched ubiquitin could result in a different sorting compared to a linear ubiquitination.

As the mutants, especially Y3, linger at the periphery of the cell during the first 15-20 minutes it could be possible that the receptor is being recycled back the plasma membrane and possibly re-internalized. Another possibility could be that after sufficient time spent in the cell, past 2hours, the receptor-ligand complex is disposed of via exosomes. The methods used in this study constitute a novel colocalization analysis which is a valid method of study for a variety of other trafficking studies.

7 References

1. Dreyling, M.H., et al., *The t(10;11)(p13;q14) in the U937 cell line results in the fusion of the AF10 gene and CALM, encoding a new member of the AP-3 clathrin assembly protein family.* Proc Natl Acad Sci U S A, 1996. **93**(10): p. 4804-9.
2. Lutsenko, S. and M.J. Petris, *Function and regulation of the mammalian copper-transporting ATPases: insights from biochemical and cell biological approaches.* J Membr Biol, 2003. **191**(1): p. 1-12.
3. Harris, D.A., *Trafficking, turnover and membrane topology of PrP.* Br Med Bull, 2003. **66**: p. 71-85.
4. Segatto, O., S. Anastasi, and S. Alema, *Regulation of epidermal growth factor receptor signalling by inducible feedback inhibitors.* J Cell Sci, 2011. **124**(Pt 11): p. 1785-93.
5. Ushiro, H. and S. Cohen, *Identification of phosphotyrosine as a product of epidermal growth factor-activated protein kinase in A-431 cell membranes.* J Biol Chem, 1980. **255**(18): p. 8363-5.
6. Downward, J., et al., *Close similarity of epidermal growth factor receptor and v-erb-B oncogene protein sequences.* Nature, 1984. **307**(5951): p. 521-7.
7. Schwartz, A.L., *Receptor cell biology: receptor-mediated endocytosis.* Pediatr Res, 1995. **38**(6): p. 835-43.
8. von Zastrow, M. and A. Sorkin, *Signaling on the endocytic pathway.* Curr Opin Cell Biol, 2007. **19**(4): p. 436-45.
9. McCaffrey, M.W., et al., *Rab4 affects both recycling and degradative endosomal trafficking.* FEBS Lett, 2001. **495**(1-2): p. 21-30.
10. Alberts, B., *Molecular Biology of the Cell.* 2008: p. 742-743.
11. Aderem, A. and D.M. Underhill, *Mechanisms of phagocytosis in macrophages.* Annu Rev Immunol, 1999. **17**: p. 593-623.
12. Di Guglielmo, G.M., et al., *Distinct endocytic pathways regulate TGF-beta receptor signalling and turnover.* Nat Cell Biol, 2003. **5**(5): p. 410-21.
13. Pearse, B.M., *Clathrin: a unique protein associated with intracellular transfer of membrane by coated vesicles.* Proc Natl Acad Sci U S A, 1976. **73**(4): p. 1255-9.
14. Sorkin, A., et al., *Pool of ligand-bound platelet-derived growth factor beta-receptors remain activated and tyrosine phosphorylated after internalization.* J Cell Physiol, 1993. **156**(2): p. 373-82.
15. Sorkin, A. and M. Von Zastrow, *Signal transduction and endocytosis: close encounters of many kinds.* Nat Rev Mol Cell Biol, 2002. **3**(8): p. 600-14.
16. Sigismund, S., et al., *Endocytosis and signaling: cell logistics shape the eukaryotic cell plan.* Physiol Rev, 2012. **92**(1): p. 273-366.
17. Sorkin, A. and M. von Zastrow, *Endocytosis and signalling: intertwining molecular networks.* Nat Rev Mol Cell Biol, 2009. **10**(9): p. 609-22.
18. Teis, D., W. Wunderlich, and L.A. Huber, *Localization of the MP1-MAPK scaffold complex to endosomes is mediated by p14 and required for signal transduction.* Dev Cell, 2002. **3**(6): p. 803-14.
19. Di Guglielmo, G.M., et al., *Compartmentalization of SHC, GRB2 and mSOS, and hyperphosphorylation of Raf-1 by EGF but not insulin in liver parenchyma.* EMBO J, 1994. **13**(18): p. 4269-77.
20. Grimes, M.L., et al., *Endocytosis of activated TrkA: evidence that nerve growth factor induces formation of signaling endosomes.* J Neurosci, 1996. **16**(24): p. 7950-64.

21. Sorkin, A.D., L.V. Teslenko, and N.N. Nikolsky, *The endocytosis of epidermal growth factor in A431 cells: a pH of microenvironment and the dynamics of receptor complex dissociation.* Exp Cell Res, 1988. **175**(1): p. 192-205.
22. Gould, G.W. and J. Lippincott-Schwartz, *New roles for endosomes: from vesicular carriers to multi-purpose platforms.* Nat Rev Mol Cell Biol, 2009. **10**(4): p. 287-92.
23. Vieira, A.V., C. Lamaze, and S.L. Schmid, *Control of EGF receptor signaling by clathrin-mediated endocytosis.* Science, 1996. **274**(5295): p. 2086-9.
24. Kornilova, E.S., *Receptor-mediated endocytosis and cytoskeleton.* Biochemistry (Mosc), 2014. **79**(9): p. 865-78.
25. Harding, C., J. Heuser, and P. Stahl, *Receptor-mediated endocytosis of transferrin and recycling of the transferrin receptor in rat reticulocytes.* J Cell Biol, 1983. **97**(2): p. 329-39.
26. Lakadamyali, M., M.J. Rust, and X. Zhuang, *Endocytosis of influenza viruses.* Microbes Infect, 2004. **6**(10): p. 929-36.
27. Kirchhausen, T., S.C. Harrison, and J. Heuser, *Configuration of clathrin trimers: evidence from electron microscopy.* J Ultrastruct Mol Struct Res, 1986. **94**(3): p. 199-208.
28. Flannagan, R.S., V. Jaumouille, and S. Grinstein, *The cell biology of phagocytosis.* Annu Rev Pathol, 2012. **7**: p. 61-98.
29. Grimmer, S., B. van Deurs, and K. Sandvig, *Membrane ruffling and macropinocytosis in A431 cells require cholesterol.* J Cell Sci, 2002. **115**(Pt 14): p. 2953-62.
30. Duden, R., *ER-to-Golgi transport: COP I and COP II function (Review).* Mol Membr Biol, 2003. **20**(3): p. 197-207.
31. Russell, C. and S.M. Stagg, *New insights into the structural mechanisms of the COPII coat.* Traffic, 2010. **11**(3): p. 303-10.
32. Kirchhausen, T., *Adaptors for clathrin-mediated traffic.* Annu Rev Cell Dev Biol, 1999. **15**: p. 705-32.
33. Ungewickell, E. and D. Branton, *Assembly units of clathrin coats.* Nature, 1981. **289**(5796): p. 420-2.
34. ter Haar, E., et al., *Atomic structure of clathrin: a beta propeller terminal domain joins an alpha zigzag linker.* Cell, 1998. **95**(4): p. 563-73.
35. Brodsky, F.M., *Living with clathrin: its role in intracellular membrane traffic.* Science, 1988. **242**(4884): p. 1396-402.
36. Sigma-Aldrich Co. *Clathrin Structure*. [cited 2015 5 Feb]; Available from: http://www.sigmaaldrich.com/life-science/metabolomics/enzyme-explorer/learning-center/structural-proteins/clathrin.html#sthash.egxsxIkY.dpuf.
37. den Otter, W.K. and W.J. Briels, *The generation of curved clathrin coats from flat plaques.* Traffic, 2011. **12**(10): p. 1407-16.
38. Cocucci, E., et al., *The first five seconds in the life of a clathrin-coated pit.* Cell, 2012. **150**(3): p. 495-507.
39. Jackson, L.P., et al., *A large-scale conformational change couples membrane recruitment to cargo binding in the AP2 clathrin adaptor complex.* Cell, 2010. **141**(7): p. 1220-9.
40. Henne, W.M., et al., *FCHo proteins are nucleators of clathrin-mediated endocytosis.* Science, 2010. **328**(5983): p. 1281-4.
41. Henne, W.M., et al., *Structure and analysis of FCHo2 F-BAR domain: a dimerizing and membrane recruitment module that effects membrane curvature.* Structure, 2007. **15**(7): p. 839-52.

42. Itoh, T., et al., *Dynamin and the actin cytoskeleton cooperatively regulate plasma membrane invagination by BAR and F-BAR proteins.* Dev Cell, 2005. **9**(6): p. 791-804.
43. Kirchhausen, T., *Bending membranes.* Nat Cell Biol, 2012. **14**(9): p. 906-8.
44. Swan, L.E., *Initiation of clathrin-mediated endocytosis: all you need is two?* Bioessays, 2013. **35**(5): p. 425-9.
45. Tebar, F., et al., *Eps15 is a component of clathrin-coated pits and vesicles and is located at the rim of coated pits.* J Biol Chem, 1996. **271**(46): p. 28727-30.
46. Chen, H., et al., *Epsin is an EH-domain-binding protein implicated in clathrin-mediated endocytosis.* Nature, 1998. **394**(6695): p. 793-7.
47. Ford, M.G., et al., *Curvature of clathrin-coated pits driven by epsin.* Nature, 2002. **419**(6905): p. 361-6.
48. Takei, K., et al., *Functional partnership between amphiphysin and dynamin in clathrin-mediated endocytosis.* Nat Cell Biol, 1999. **1**(1): p. 33-9.
49. Masuda, M., et al., *Endophilin BAR domain drives membrane curvature by two newly identified structure-based mechanisms.* EMBO J, 2006. **25**(12): p. 2889-97.
50. Ringstad, N., Y. Nemoto, and P. De Camilli, *The SH3p4/Sh3p8/SH3p13 protein family: binding partners for synaptojanin and dynamin via a Grb2-like Src homology 3 domain.* Proc Natl Acad Sci U S A, 1997. **94**(16): p. 8569-74.
51. Slepnev, V.I. and P. De Camilli, *Accessory factors in clathrin-dependent synaptic vesicle endocytosis.* Nat Rev Neurosci, 2000. **1**(3): p. 161-72.
52. Takei, K., et al., *Tubular membrane invaginations coated by dynamin rings are induced by GTP-gamma S in nerve terminals.* Nature, 1995. **374**(6518): p. 186-90.
53. Eisenberg, E. and L.E. Greene, *Multiple roles of auxilin and hsc70 in clathrin-mediated endocytosis.* Traffic, 2007. **8**(6): p. 640-6.
54. Lund, K.A., et al., *Quantitative analysis of the endocytic system involved in hormone-induced receptor internalization.* J Biol Chem, 1990. **265**(26): p. 15713-23.
55. Wiley, H.S., *Anomalous binding of epidermal growth factor to A431 cells is due to the effect of high receptor densities and a saturable endocytic system.* J Cell Biol, 1988. **107**(2): p. 801-10.
56. Mayor, S., R.G. Parton, and J.G. Donaldson, *Clathrin-independent pathways of endocytosis.* Cold Spring Harb Perspect Biol, 2014. **6**(6).
57. Prenzel, N., et al., *The epidermal growth factor receptor family as a central element for cellular signal transduction and diversification.* Endocr Relat Cancer, 2001. **8**(1): p. 11-31.
58. Bazley, L.A. and W.J. Gullick, *The epidermal growth factor receptor family.* Endocr Relat Cancer, 2005. **12 Suppl 1**: p. S17-27.
59. Ritter, C.A. and C.L. Arteaga, *The epidermal growth factor receptor-tyrosine kinase: a promising therapeutic target in solid tumors.* Semin Oncol, 2003. **30**(1 Suppl 1): p. 3-11.
60. Salomon, D.S., et al., *Epidermal growth factor-related peptides and their receptors in human malignancies.* Crit Rev Oncol Hematol, 1995. **19**(3): p. 183-232.
61. Herbst, R.S., *Review of epidermal growth factor receptor biology.* Int J Radiat Oncol Biol Phys, 2004. **59**(2 Suppl): p. 21-6.
62. Yewale, C., et al., *Epidermal growth factor receptor targeting in cancer: a review of trends and strategies.* Biomaterials, 2013. **34**(34): p. 8690-707.
63. Giltaire, S., S. Lambert, and Y. Poumay, *HB-EGF synthesis and release induced by cholesterol depletion of human epidermal keratinocytes is controlled by extracellular ATP and involves both p38 and ERK1/2 signaling pathways.* J Cell Physiol, 2011. **226**(6): p. 1651-9.

64. Schneider, M.R. and E. Wolf, *The epidermal growth factor receptor ligands at a glance.* J Cell Physiol, 2009. **218**(3): p. 460-6.
65. Decker, S.J., *Epidermal growth factor and transforming growth factor-alpha induce differential processing of the epidermal growth factor receptor.* Biochem Biophys Res Commun, 1990. **166**(2): p. 615-21.
66. Ebner, R. and R. Derynck, *Epidermal growth factor and transforming growth factor-alpha: differential intracellular routing and processing of ligand-receptor complexes.* Cell Regul, 1991. **2**(8): p. 599-612.
67. Yarden, Y., *The EGFR family and its ligands in human cancer. signalling mechanisms and therapeutic opportunities.* Eur J Cancer, 2001. **37 Suppl 4**: p. S3-8.
68. Klapper, L.N., et al., *The ErbB-2/HER2 oncoprotein of human carcinomas may function solely as a shared coreceptor for multiple stroma-derived growth factors.* Proc Natl Acad Sci U S A, 1999. **96**(9): p. 4995-5000.
69. Yarden, Y. and M.X. Sliwkowski, *Untangling the ErbB signalling network.* Nat Rev Mol Cell Biol, 2001. **2**(2): p. 127-37.
70. Schlessinger, J., *Ligand-induced, receptor-mediated dimerization and activation of EGF receptor.* Cell, 2002. **110**(6): p. 669-72.
71. Lemmon, M.A., J. Schlessinger, and K.M. Ferguson, *The EGFR family: not so prototypical receptor tyrosine kinases.* Cold Spring Harb Perspect Biol, 2014. **6**(4): p. a020768.
72. Wood, E.R., et al., *A unique structure for epidermal growth factor receptor bound to GW572016 (Lapatinib): relationships among protein conformation, inhibitor off-rate, and receptor activity in tumor cells.* Cancer Res, 2004. **64**(18): p. 6652-9.
73. Ullrich, A., et al., *Human epidermal growth factor receptor cDNA sequence and aberrant expression of the amplified gene in A431 epidermoid carcinoma cells.* Nature, 1984. **309**(5967): p. 418-25.
74. Cummings, R.D., A.M. Soderquist, and G. Carpenter, *The oligosaccharide moieties of the epidermal growth factor receptor in A-431 cells. Presence of complex-type N-linked chains that contain terminal N-acetylgalactosamine residues.* J Biol Chem, 1985. **260**(22): p. 11944-52.
75. Moriki, T., H. Maruyama, and I.N. Maruyama, *Activation of preformed EGF receptor dimers by ligand-induced rotation of the transmembrane domain.* J Mol Biol, 2001. **311**(5): p. 1011-26.
76. Jura, N., et al., *Mechanism for activation of the EGF receptor catalytic domain by the juxtamembrane segment.* Cell, 2009. **137**(7): p. 1293-307.
77. Emlet, D.R., et al., *Subsets of epidermal growth factor receptors during activation and endocytosis.* J Biol Chem, 1997. **272**(7): p. 4079-86.
78. Sigismund, S., et al., *Threshold-controlled ubiquitination of the EGFR directs receptor fate*. Vol. 32. 2013. 2140-2157.
79. Ferguson, K.M., *Active and inactive conformations of the epidermal growth factor receptor.* Biochem Soc Trans, 2004. **32**(Pt 5): p. 742-5.
80. Odaka, M., et al., *Ligand-binding enhances the affinity of dimerization of the extracellular domain of the epidermal growth factor receptor.* J Biochem, 1997. **122**(1): p. 116-21.
81. Shan, Y., et al., *Oncogenic mutations counteract intrinsic disorder in the EGFR kinase and promote receptor dimerization.* Cell, 2012. **149**(4): p. 860-70.
82. Luschnig, S., et al., *The Drosophila SHC adaptor protein is required for signaling by a subset of receptor tyrosine kinases.* Mol Cell, 2000. **5**(2): p. 231-41.
83. Giubellino, A., T.R. Burke, Jr., and D.P. Bottaro, *Grb2 signaling in cell motility and cancer.* Expert Opin Ther Targets, 2008. **12**(8): p. 1021-33.

84. Jiang, X., et al., *Grb2 regulates internalization of EGF receptors through clathrin-coated pits.* Mol Biol Cell, 2003. **14**(3): p. 858-70.
85. Batzer, A.G., et al., *Hierarchy of binding sites for Grb2 and Shc on the epidermal growth factor receptor.* Mol Cell Biol, 1994. **14**(8): p. 5192-201.
86. Sakaguchi, K., et al., *Shc phosphotyrosine-binding domain dominantly interacts with epidermal growth factor receptors and mediates Ras activation in intact cells.* Mol Endocrinol, 1998. **12**(4): p. 536-43.
87. Okabayashi, Y., et al., *Tyrosines 1148 and 1173 of activated human epidermal growth factor receptors are binding sites of Shc in intact cells.* J Biol Chem, 1994. **269**(28): p. 18674-8.
88. Schmidt, M.H. and I. Dikic, *The Cbl interactome and its functions.* Nat Rev Mol Cell Biol, 2005. **6**(12): p. 907-18.
89. Tomas, A., C.E. Futter, and E.R. Eden, *EGF receptor trafficking: consequences for signaling and cancer.* Trends Cell Biol, 2014. **24**(1): p. 26-34.
90. Yamazaki, T., et al., *Role of Grb2 in EGF-stimulated EGFR internalization.* J Cell Sci, 2002. **115**(Pt 9): p. 1791-802.
91. Fukazawa, T., et al., *Tyrosine phosphorylation of Cbl upon epidermal growth factor (EGF) stimulation and its association with EGF receptor and downstream signaling proteins.* J Biol Chem, 1996. **271**(24): p. 14554-9.
92. Huang, F., et al., *Differential regulation of EGF receptor internalization and degradation by multiubiquitination within the kinase domain.* Mol Cell, 2006. **21**(6): p. 737-48.
93. Thien, C.B. and W.Y. Langdon, *c-Cbl and Cbl-b ubiquitin ligases: substrate diversity and the negative regulation of signalling responses.* Biochem J, 2005. **391**(Pt 2): p. 153-66.
94. Seabra, M.C., *Membrane association and targeting of prenylated Ras-like GTPases.* Cell Signal, 1998. **10**(3): p. 167-72.
95. Jorissen, R.N., et al., *Epidermal growth factor receptor: mechanisms of activation and signalling.* Exp Cell Res, 2003. **284**(1): p. 31-53.
96. Hallberg, B., S.I. Rayter, and J. Downward, *Interaction of Ras and Raf in intact mammalian cells upon extracellular stimulation.* J Biol Chem, 1994. **269**(6): p. 3913-6.
97. Johnson, G.L. and R.R. Vaillancourt, *Sequential protein kinase reactions controlling cell growth and differentiation.* Curr Opin Cell Biol, 1994. **6**(2): p. 230-8.
98. Impey, S., et al., *Cross talk between ERK and PKA is required for Ca2+ stimulation of CREB-dependent transcription and ERK nuclear translocation.* Neuron, 1998. **21**(4): p. 869-83.
99. Chi, S., et al., *Recycling of the epidermal growth factor receptor is mediated by a novel form of the clathrin adaptor protein Eps15.* J Biol Chem, 2011. **286**(40): p. 35196-208.
100. Klann, M., H. Koeppl, and M. Reuss, *Spatial modeling of vesicle transport and the cytoskeleton: the challenge of hitting the right road.* PLoS One, 2012. **7**(1): p. e29645.
101. Hirokawa, N., *Kinesin and dynein superfamily proteins and the mechanism of organelle transport.* Science, 1998. **279**(5350): p. 519-26.
102. Fuchs, E. and I. Karakesisoglou, *Bridging cytoskeletal intersections.* Genes Dev, 2001. **15**(1): p. 1-14.
103. Yildiz, A., et al., *Myosin V walks hand-over-hand: single fluorophore imaging with 1.5-nm localization.* Science, 2003. **300**(5628): p. 2061-5.
104. Yildiz, A., et al., *Kinesin walks hand-over-hand.* Science, 2004. **303**(5658): p. 676-8.

105. Yildiz, A., et al., *Myosin VI steps via a hand-over-hand mechanism with its lever arm undergoing fluctuations when attached to actin.* J Biol Chem, 2004. **279**(36): p. 37223-6.
106. Zerial, M. and H. McBride, *Rab proteins as membrane organizers.* Nat Rev Mol Cell Biol, 2001. **2**(2): p. 107-17.
107. Stoorvogel, W., et al., *Late endosomes derive from early endosomes by maturation.* Cell, 1991. **65**(3): p. 417-27.
108. Storrie, B. and M. Desjardins, *The biogenesis of lysosomes: is it a kiss and run, continuous fusion and fission process?* Bioessays, 1996. **18**(11): p. 895-903.
109. Solinger, J.A. and A. Spang, *Tethering complexes in the endocytic pathway: CORVET and HOPS.* FEBS J, 2013. **280**(12): p. 2743-57.
110. Sollner, T., et al., *A protein assembly-disassembly pathway in vitro that may correspond to sequential steps of synaptic vesicle docking, activation, and fusion.* Cell, 1993. **75**(3): p. 409-18.
111. Huotari, J. and A. Helenius, *Endosome maturation.* EMBO J, 2011. **30**(17): p. 3481-500.
112. Pfeffer, S. and D. Aivazian, *Targeting Rab GTPases to distinct membrane compartments.* Nat Rev Mol Cell Biol, 2004. **5**(11): p. 886-96.
113. Dumas, J.J., et al., *Structural basis of activation and GTP hydrolysis in Rab proteins.* Structure, 1999. **7**(4): p. 413-23.
114. Nielsen, E., et al., *Rab5 regulates motility of early endosomes on microtubules.* Nat Cell Biol, 1999. **1**(6): p. 376-82.
115. Hoepfner, S., et al., *Modulation of receptor recycling and degradation by the endosomal kinesin KIF16B.* Cell, 2005. **121**(3): p. 437-50.
116. Jordens, I., et al., *The Rab7 effector protein RILP controls lysosomal transport by inducing the recruitment of dynein-dynactin motors.* Curr Biol, 2001. **11**(21): p. 1680-5.
117. Bucci, C., et al., *Rab7: a key to lysosome biogenesis.* Mol Biol Cell, 2000. **11**(2): p. 467-80.
118. Hurtley, S. and G. Warren, *Reconstitution of an endocytic fusion event in a cell-free system: some characteristics of fusion in vitro.* Prog Clin Biol Res, 1988. **270**: p. 355-60.
119. Backer, J.M., *Phosphoinositide 3-kinases and the regulation of vesicular trafficking.* Mol Cell Biol Res Commun, 2000. **3**(4): p. 193-204.
120. McBride, H.M., et al., *Oligomeric complexes link Rab5 effectors with NSF and drive membrane fusion via interactions between EEA1 and syntaxin 13.* Cell, 1999. **98**(3): p. 377-86.
121. Stenmark, H., et al., *Rabaptin-5 is a direct effector of the small GTPase Rab5 in endocytic membrane fusion.* Cell, 1995. **83**(3): p. 423-32.
122. Nielsen, E., et al., *Rabenosyn-5, a novel Rab5 effector, is complexed with hVPS45 and recruited to endosomes through a FYVE finger domain.* J Cell Biol, 2000. **151**(3): p. 601-12.
123. van Weering, J.R. and P.J. Cullen, *Membrane-associated cargo recycling by tubule-based endosomal sorting.* Semin Cell Dev Biol, 2014. **31**: p. 40-7.
124. Cullen, P.J., *Endosomal sorting and signalling: an emerging role for sorting nexins.* Nat Rev Mol Cell Biol, 2008. **9**(7): p. 574-82.
125. Grant, B.D. and J.G. Donaldson, *Pathways and mechanisms of endocytic recycling.* Nat Rev Mol Cell Biol, 2009. **10**(9): p. 597-608.
126. Sachse, M., et al., *Bilayered clathrin coats on endosomal vacuoles are involved in protein sorting toward lysosomes.* Mol Biol Cell, 2002. **13**(4): p. 1313-28.

127. Raiborg, C., et al., *Hrs sorts ubiquitinated proteins into clathrin-coated microdomains of early endosomes.* Nat Cell Biol, 2002. **4**(5): p. 394-8.
128. Goh, L.K. and A. Sorkin, *Endocytosis of receptor tyrosine kinases.* Cold Spring Harb Perspect Biol, 2013. **5**(5): p. a017459.
129. Eden, E.R., et al., *Membrane contacts between endosomes and ER provide sites for PTP1B-epidermal growth factor receptor interaction.* Nat Cell Biol, 2010. **12**(3): p. 267-72.
130. Piper, R.C. and D.J. Katzmann, *Biogenesis and function of multivesicular bodies.* Annu Rev Cell Dev Biol, 2007. **23**: p. 519-47.
131. Katzmann, D.J., G. Odorizzi, and S.D. Emr, *Receptor downregulation and multivesicular-body sorting.* Nat Rev Mol Cell Biol, 2002. **3**(12): p. 893-905.
132. Pickart, C.M., *Ubiquitin in chains.* Trends Biochem Sci, 2000. **25**(11): p. 544-8.
133. Passmore, L.A. and D. Barford, *Getting into position: the catalytic mechanisms of protein ubiquitylation.* Biochem J, 2004. **379**(Pt 3): p. 513-25.
134. Sadowski, M. and B. Sarcevic, *Mechanisms of mono- and poly-ubiquitination: Ubiquitination specificity depends on compatibility between the E2 catalytic core and amino acid residues proximal to the lysine.* Cell Div, 2010. **5**: p. 19.
135. Pennock, S. and Z. Wang, *A tale of two Cbls: interplay of c-Cbl and Cbl-b in epidermal growth factor receptor downregulation.* Mol Cell Biol, 2008. **28**(9): p. 3020-37.
136. Lee, S.K., et al., *Vacuolar (H+)-ATPases in Caenorhabditis elegans: what can we learn about giant H+ pumps from tiny worms?* Biochim Biophys Acta, 2010. **1797**(10): p. 1687-95.
137. Dove, S.K., et al., *Phosphatidylinositol 3,5-bisphosphate and Fab1p/PIKfyve underPPIn endo-lysosome function.* Biochem J, 2009. **419**(1): p. 1-13.
138. Poteryaev, D., et al., *Identification of the switch in early-to-late endosome transition.* Cell, 2010. **141**(3): p. 497-508.
139. Poteryaev, D., et al., *Caenorhabditis elegans SAND-1 is essential for RAB-7 function in endosomal traffic.* EMBO J, 2007. **26**(2): p. 301-12.
140. Balderhaar, H.J. and C. Ungermann, *CORVET and HOPS tethering complexes - coordinators of endosome and lysosome fusion.* J Cell Sci, 2013. **126**(Pt 6): p. 1307-16.
141. Eskelinen, E.L., *Roles of LAMP-1 and LAMP-2 in lysosome biogenesis and autophagy.* Mol Aspects Med, 2006. **27**(5-6): p. 495-502.
142. Reczek, D., et al., *LIMP-2 is a receptor for lysosomal mannose-6-phosphate-independent targeting of beta-glucocerebrosidase.* Cell, 2007. **131**(4): p. 770-83.
143. Carrasco-Marin, E., et al., *LIMP-2 links late phagosomal trafficking with the onset of the innate immune response to Listeria monocytogenes: a role in macrophage activation.* J Biol Chem, 2011. **286**(5): p. 3332-41.
144. Forgac, M., *Vacuolar ATPases: rotary proton pumps in physiology and pathophysiology.* Nat Rev Mol Cell Biol, 2007. **8**(11): p. 917-29.
145. Raposo, G. and W. Stoorvogel, *Extracellular vesicles: exosomes, microvesicles, and friends.* J Cell Biol, 2013. **200**(4): p. 373-83.
146. Beaufay, H. and C. De Duve, *[The hexosephosphatase system. VI. Attempted fractionation of microsomes containing glucose-6-phosphatase]*. Bull Soc Chim Biol (Paris), 1954. **36**(11-12): p. 1551-68.
147. Wells, A., *EGF receptor.* Int J Biochem Cell Biol, 1999. **31**(6): p. 637-43.
148. Holbro, T., G. Civenni, and N.E. Hynes, *The ErbB receptors and their role in cancer progression.* Exp Cell Res, 2003. **284**(1): p. 99-110.

149. Voldborg, B.R., et al., *Epidermal growth factor receptor (EGFR) and EGFR mutations, function and possible role in clinical trials.* Ann Oncol, 1997. **8**(12): p. 1197-206.
150. Irby, R.B. and T.J. Yeatman, *Role of Src expression and activation in human cancer.* Oncogene, 2000. **19**(49): p. 5636-42.
151. Reardon, D.B., et al., *Dominant negative EGFR-CD533 and inhibition of MAPK modify JNK1 activation and enhance radiation toxicity of human mammary carcinoma cells.* Oncogene, 1999. **18**(33): p. 4756-66.
152. Qiao, L., et al., *Deoxycholic acid (DCA) causes ligand-independent activation of epidermal growth factor receptor (EGFR) and FAS receptor in primary hepatocytes: inhibition of EGFR/mitogen-activated protein kinase-signaling module enhances DCA-induced apoptosis.* Mol Biol Cell, 2001. **12**(9): p. 2629-45.
153. Sibilia, M., et al., *The epidermal growth factor receptor: from development to tumorigenesis.* Differentiation, 2007. **75**(9): p. 770-87.
154. Skjeldal, F.M., et al., *The fusion of early endosomes induces molecular-motor-driven tubule formation and fission.* J Cell Sci, 2012. **125**(Pt 8): p. 1910-9.
155. Dunn, K.W., M.M. Kamocka, and J.H. McDonald, *A practical guide to evaluating colocalization in biological microscopy.* Am J Physiol Cell Physiol, 2011. **300**(4): p. C723-42.
156. ImageJ. *Colocalization plugin*. 2003 [cited 2015 4 Jun]; Available from: http://imagej.nih.gov/ij/plugins/colocalization.html.
157. Vermeer, P.D., et al., *Segregation of receptor and ligand regulates activation of epithelial growth factor receptor.* Nature, 2003. **422**(6929): p. 322-6.
158. Khazaie, K., V. Schirrmacher, and R.B. Lichtner, *EGF receptor in neoplasia and metastasis.* Cancer Metastasis Rev, 1993. **12**(3-4): p. 255-74.
159. Wiley, H.S., et al., *The role of tyrosine kinase activity in endocytosis, compartmentation, and down-regulation of the epidermal growth factor receptor.* J Biol Chem, 1991. **266**(17): p. 11083-94.
160. Sorkin, A., *Internalization of the epidermal growth factor receptor: role in signalling.* Biochem Soc Trans, 2001. **29**(Pt 4): p. 480-4.
161. Carter, R.E. and A. Sorkin, *Endocytosis of functional epidermal growth factor receptor-green fluorescent protein chimera.* J Biol Chem, 1998. **273**(52): p. 35000-7.
162. Skjeldal, F.M., et al., *Differential binding of Cbl and Grb2 to EGFR controls receptor fate.*
163. Grovdal, L.M., et al., *Direct interaction of Cbl with pTyr 1045 of the EGF receptor (EGFR) is required to sort the EGFR to lysosomes for degradation.* Exp Cell Res, 2004. **300**(2): p. 388-95.
164. Levkowitz, G., et al., *Ubiquitin ligase activity and tyrosine phosphorylation underlie suppression of growth factor signaling by c-Cbl/Sli-1.* Mol Cell, 1999. **4**(6): p. 1029-40.
165. Waterman, H., et al., *A mutant EGF-receptor defective in ubiquitylation and endocytosis unveils a role for Grb2 in negative signaling.* EMBO J, 2002. **21**(3): p. 303-13.
166. Visser Smit, G.D., et al., *Cbl controls EGFR fate by regulating early endosome fusion.* Sci Signal, 2009. **2**(102): p. ra86.
167. Bucci, C., et al., *The small GTPase rab5 functions as a regulatory factor in the early endocytic pathway.* Cell, 1992. **70**(5): p. 715-28.
168. Rink, J., et al., *Rab conversion as a mechanism of progression from early to late endosomes.* Cell, 2005. **122**(5): p. 735-49.

169. Katayama, H., et al., *GFP-like proteins stably accumulate in lysosomes.* Cell Struct Funct, 2008. **33**(1): p. 1-12.
170. Shaner, N.C., et al., *Improving the photostability of bright monomeric orange and red fluorescent proteins.* Nat Methods, 2008. **5**(6): p. 545-51.
171. Kremers, G.J., et al., *Fluorescent proteins at a glance.* J Cell Sci, 2011. **124**(Pt 2): p. 157-60.
172. Sigismund, S., et al., *Clathrin-independent endocytosis of ubiquitinated cargos.* Proc Natl Acad Sci U S A, 2005. **102**(8): p. 2760-5.
173. Dutta, D., et al., *Pitstop 2 is a potent inhibitor of clathrin-independent endocytosis.* PLoS One, 2012. **7**(9): p. e45799.
174. von Kleist, L., et al., *Role of the clathrin terminal domain in regulating coated pit dynamics revealed by small molecule inhibition.* Cell, 2011. **146**(3): p. 471-84.
175. Persengiev, S.P., X. Zhu, and M.R. Green, *Nonspecific, concentration-dependent stimulation and repression of mammalian gene expression by small interfering RNAs (siRNAs).* RNA, 2004. **10**(1): p. 12-8.
176. Mattera, R. and J.S. Bonifacino, *Ubiquitin binding and conjugation regulate the recruitment of Rabex-5 to early endosomes.* EMBO J, 2008. **27**(19): p. 2484-94.
177. Horiuchi, H., et al., *A novel Rab5 GDP/GTP exchange factor complexed to Rabaptin-5 links nucleotide exchange to effector recruitment and function.* Cell, 1997. **90**(6): p. 1149-59.

8 Appendix

8.1 List of Materials

Material	Company	Country
10mm^2 cover slides	Agar Scientific	Stansted, USA
12-well cell culture plate nonpyrogenic, polysurene	Corning	NY, USA
25cm^2 tissue culture flask, vented	VWR chemicals	PA, USA
35mm Glassbottom uncoated dish	MatTek Corp.	MA,USA
6-well cell culture plate nonpyrogenic, polysurene	Corning	NY, USA
75cm^2 tissue culture flask, vented	VWR chemicals	PA, USA
AgeI	BioLab New England	MA, USA
Ampicillin	Sigma-Aldrich	MO, USA
BbvCI	BioLab New England	Ma, USA
Bradford protein reagent	Bio-Rad	CA, USA
Cryoprotective Ampules	Sarstedt AG & Co.	Nümbrecht, Germany
Cutsmart buffer	BioLab New England	Ma, USA
Cuvette		
Cyclohexamide	Sigma-Aldrich	MO, USA
DMSO	Sigma-Aldrich	MO, USA
DTT	Sigma-Aldrich	MO, USA
Dulbecco's Modified Eagle Medium	Biowhittaker	Walkerville, USA
EDTA	VWR chemicals	PA, USA
EGF alexa647	Life Technologies	CA, USA
Ethidium bromide	MERCK	Darmstadt, Germany
Fetal Calf Serum	Biological industries	Kibbutz Beit Haemek, Israel
GeneRuler 1 kb	Thermo Fisher Scientific	MA, USA
Geneticin G418 Sulphate	Gibco by Life technology a Thermo Fisher Scientific Brand	MA, USA
Glycerol	VWR chemicals	PA, USA
Imaging medium	Gibco by Life technology a Thermo Fisher Scientific Brand	MA, USA
Kanamycin	Sigma-Aldrich	MO, USA
Klenow DNA polymerase	BioLab New England	MA, USA

LB Broth	BD	NJ, USA
L-glutamine	Biowhittaker	Walkerville, USA
Lipofectamine 2000	Invitrogen / Life Technologies	CA, USA
LysoTracker® Red DND-99	Life Technologies	CA, USA
Mowiol	Sigma-Aldrich	MO, USA
NH_4Cl	KEBO Lab	Darmstadt, Germany
Opti-MEM	Gibco by Life technology a Thermo Fisher Scientific Brand	MA, USA
Penicillin/streptomycin	PAA the Cell Culture Company	Cölbe, Germany
Pitstop2	Abcam Biochemicals	Cambridge, UK
Puromycin Dihydrochloride	Life Technologies	CA, USA
Precise™ 8-16% Tris-Glycine Gels, 6.8 cm x 8 cm x 1 mm, 10-well	Thermo Fisher Scientific	MA, USA
PVDF membrane	Millipore Corp.	MA, USA
Recombinant EGF human	Bachem	Budendorf, Switzerland
Saponin	Sigma-Aldrich	MO, USA
T4 DNA Ligase	BioLab New England	Ma, USA
TopVision LE GQ agarose	Fermentas Inc.	Burlington, Canada
Trypsin	Biological industries	Kibbutz Beit Haemek, Israel

8.2 Buffers and Solutions

Lysis buffer:

Ingredients	Concentration
· Hepes	· 25mM
· K-acetate	· 125mM
· Mg-acetate	· 2.5mM
· EGTA	· 5mM
· dH_2O	· Adjusted to desired volume

Adjust pH to 7.2

Before use add:

· DTT	· 1mM
· NP-40	· 0.5%
· Protease inhibitor	· 1:100

Running buffer:

Ingredients	Concentration
· Tris-Base	10mM
· Hepes	35mM
· SDS	3mM
· dH_2O	Adjusted to desired volume

Transfer buffer:

Ingredients	Concentration
· Glycine	380mM
· Tris (base) hydromethylaminomethane	50mM
· dH_2O	Adjusted to desired volume

Before use add:

· Methanol	20%

2% Skim Milk

Ingredients	Concentration
· Blotting Grade Blocker (BioRad)	2%
· 1x PBS	Adjusted to desired volume

6xDNA sample Buffer

Ingredients	Concentration
· Tris-HCl	10mM
· SDS	0.5%
· Glycerol	70%
· dH_2O	Adjusted to desired volume
· Bromphenol blue	Added for color

TAE buffer

Ingredients	Concentration
· Tris-Base	40mM
· EDTA	1mM
· Acetic Acid	20mM
· dH_2O	Adjusted to desired volume

10xPBS pH6.8

Ingredients	Concentration
. NaH_2PO_4	16mM
· Na_2HPO_4	84mM
· NaCl	1.5mM
· dH_2O	Adjusted to desired volume

10xPBS was diluted to make 1xPBS ph7.4 used for experiments.

3%PFA pH 7.4

Ingredients	Concentration
· Paraformaldehyde	3%
. NaH_2PO_4	1.6mM
· Na_2HPO_4	8.4mM
· NaCl	150mM
· dH_2O	Adjusted to desired volume

Laemmli Loading dye

Ingredients	Concentration
· TrisHCL pH 6.8	100mM
. Glycerol	20%
· SDS	4%
· Bromphenol Blue	0.2%
· dH_2O	Adjusted to desired volume

Before use 200mM DTT was added to the loading dye

8.3 Protocols

Wizard® Plus Midipreps DNAPurification System, Promega.

1. Pellet 10–100ml of cells by centrifugation at 10,000 × *g* for 10 minutes at 4°C. Pour off the supernatant and blot the tube upside down on a paper towel to remove excess liquid.
2. **Completely** resuspend the cell pellet in 3ml of Cell Resuspension Solution. (To aid resuspension, manually disrupt the pellet with a 12-inch applicator stick or by pipetting until no clumps are visible. Complete resuspension is **critical** for optimal yields.)
3. Add 3ml of Cell Lysis Solution and mix by inverting the tube four times. Do not vortex. The cell suspension should clear immediately.

Note: Some bacterial cells are more resistant to lysis and may require incubation for 3–5 minutes for efficient lysis. Additionally, culture volumes >50ml will take an extra 3–5 minutes to clear. The lysate may not appear completely clear, but do not extend lysis time beyond 3–5 minutes as this may result in the formation of single-stranded DNA in the preparation.

4. Add 3ml of Neutralization Solution and mix by inverting the tube 4 times. **Alternatively**, if using an EndA+ strain, add 6ml of Neutralization Solution, mix by inverting the tube 4 times, and incubate the lysate at room temperature for 10 minutes. Proceed.
5. Centrifuge at 14,000 × *g* for 15 minutes at 4°C. If a tight pellet has not formed by the end of the centrifugation, centrifuge for another 15 minutes.
6. Carefully decant the supernatant to a new centrifuge tube, avoiding the white precipitate. Alternatively, transfer the cleared supernatant by filtering it through Miracloth™ (Calbiochem Corp. Cat.# 475855), filter paper (Whatman® #1, GFA or GFC) or an autoclaved coffee filter into the new centrifuge tube. Proceed immediately to Section 4.

Plasmid DNA Purification

Thoroughly mix the Wizard® Midipreps DNA Purification Resin before removing an aliquot.

1. Add 10ml of resuspended Wizard® Midipreps DNA Purification Resin to the DNA solution from Section 3. Swirl to mix.

Note: Extended incubation of the resin and lysate is not necessary. Do not allow the resin to remain in contact with the lysate for longer than it takes to load the Midicolumns.

2. For each Midiprep, use one Midicolumn. Insert the Midicolumn tip into the vacuum manifold port.
3. Transfer the resin/DNA mixture into the Midicolumn. Apply a vacuum of at least 15 inches of Hg to pull the resin/DNA mix into the Midicolumn. When all of the sample has passed through the column, break the vacuum at the source.
4. Add 15ml of Column Wash Solution to the Midicolumn and apply a vacuum to draw the solution through the Midicolumn.
5. Break the vacuum at the source and add another 15ml of Column Wash Solution to the Midicolumn. Reapply a vacuum to draw the solution through the Midicolumn.

Note: The Column Wash procedure may take up to 30 minutes.

6. Dry the resin by continuing to draw a vacuum for 30 seconds after the solution has been pulled through the column. **Do not dry the resin for more than 30 seconds.** Remove the Midicolumn from the vacuum source. Separate the Reservoir from the Midicolumn by breaking or cutting with sharp scissors as shown in Figure 1. Transfer the Midicolumn to a 1.5ml microcentrifuge tube. Centrifuge the Midicolumn at 10,000 × *g* in a microcentrifuge for 2 minutes to remove any residual Column Wash Solution. Transfer the Midicolumn to a new microcentrifuge tube.
7. Add 300µl of preheated (65–70°C) Nuclease-Free Water to the Midicolumn and wait 1 minute. Elute the DNA by centrifuging the Midicolumn at 10,000 × *g* for 20 seconds in a microcentrifuge. Remove and discard the Midicolumn. For elution of large plasmids (≥20kb), the use of water preheated to 80°C may increase yields.

8. A white pellet of resin fines may be present in the final eluate. Whether visible or not, it is important to separate the fines from the DNA. Centrifuge the sample at 10,000 × *g* in a microcentrifuge for 5 minutes to pellet the fines. Carefully transfer the DNA-containing supernatant to a clean microcentrifuge tube.

9. The plasmid DNA may be stored in the microcentrifuge tube using these storage recommendations: DNA is stable in water without addition of buffer if stored at –20°C or below. DNA is stable at 4°C in TE buffer. To store the DNA in TE buffer, add 30µl of 10X TE buffer to the 300µl of eluted DNA.

QIAquick Gel Extraction Kit Protocol, using a microcentrifuge

This protocol is designed to extract and purify DNA of 70 bp to 10 kb from standard or low-melt agarose gels in TAE or TBE buffer. Up to 400 mg agarose can be processed per spin column. This kit can also be used for DNA cleanup from enzymatic reactions (see page 8).

For DNA cleanup from enzymatic reactions using this protocol, add 3 volumes of Buffer QG and 1 volume of isopropanol to the reaction, mix, and proceed with step 6 of the protocol. Alternatively, use the MinElute Reaction Cleanup Kit.

Important points before starting

- The yellow color of Buffer QG indicates a pH ≤7.5.
- Add ethanol (96–100%) to Buffer PE before use (see bottle label for volume).
- All centrifugation steps are carried out at 17,900 x g (13,000 rpm) in a conventional table-top microcentrifuge at room temperature.

Procedure

1. Excise the DNA fragment from the agarose gel with a clean, sharp scalpel.

Minimize the size of the gel slice by removing extra agarose.

2. Weigh the gel slice in a colorless tube. Add 3 volumes of Buffer QG to 1 volume of gel (100 mg ~ 100 µl).

For example, add 300 µl of Buffer QG to each 100 mg of gel. For >2% agarose gels, add 6 volumes of Buffer QG. The maximum amount of gel slice per QIAquick column is 400 mg; for gel slices >400 mg use more than one QIAquick column.

3. Incubate at 50°C for 10 min (or until the gel slice has completely dissolved). To help dissolve gel, mix by vortexing the tube every 2–3 min during the incubation.

IMPORTANT: Solubilize agarose completely. For >2% gels, increase incubation time.

4. After the gel slice has dissolved completely, check that the color of the mixture is yellow (similar to Buffer QG without dissolved agarose).

If the color of the mixture is orange or violet, add 10 µl of 3 M sodium acetate, pH 5.0, and mix. The color of the mixture will turn to yellow.

The adsorption of DNA to the QIAquick membrane is efficient only at pH ≤7.5. Buffer QG contains a pH indicator which is yellow at pH ≤7.5 and orange or violet at higher pH, allowing easy determination of the optimal pH for DNA binding.

5. Add 1 gel volume of isopropanol to the sample and mix.

For example, if the agarose gel slice is 100 mg, add 100 µl isopropanol. This step increases the yield of DNA fragments <500 bp and >4 kb. For DNA fragments between 500 bp and 4 kb, addition of isopropanol has no effect on yield.

Do not centrifuge the sample at this stage.

6. Place a QIAquick spin column in a provided 2 ml collection tube.

7. To bind DNA, apply the sample to the QIAquick column, and centrifuge for 1 min.

The maximum volume of the column reservoir is 800 µl. For sample volumes of more

than 800 µl, simply load and spin again.

8. Discard flow-through and place QIAquick column back in the same collection tube.

Collection tubes are reused to reduce plastic waste.

9. Recommended: Add 0.5 ml of Buffer QG to QIAquick column and centrifuge for 1 min.

This step will remove all traces of agarose. It is only required when the DNA will subsequently be used for direct sequencing, in vitro transcription, or microinjection.

10. To wash, add 0.75 ml of Buffer PE to QIAquick column and centrifuge for 1 min.

Note: If the DNA will be used for salt-sensitive applications, such as blunt-end ligation and direct sequencing, let the column stand 2–5 min after addition of Buffer PE, before centrifuging.

11. Discard the flow-through and centrifuge the QIAquick column for an additional 1 min at 17,900 x g (13,000 rpm).

IMPORTANT: Residual ethanol from Buffer PE will not be completely removed unless the flow-through is discarded before this additional centrifugation.

12. Place QIAquick column into a clean 1.5 ml microcentrifuge tube.

13. To elute DNA, add 50 µl of Buffer EB (10 mM Tris·Cl, pH 8.5) or water (pH 7.0–8.5) to the center of the QIAquick membrane and centrifuge the column for 1 min. Alternatively, for increased DNA concentration, add 30 µl elution buffer to the center of the QIAquick membrane, let the column stand for 1 min, and then centrifuge for 1 min.

IMPORTANT: Ensure that the elution buffer is dispensed directly onto the QIAquick membrane for complete elution of bound DNA. The average eluate volume is 48 µl from 50 µl elution buffer volume, and 28 µl from 30 µl.

Elution efficiency is dependent on pH. The maximum elution efficiency is achieved between pH 7.0 and 8.5. When using water, make sure that the pH value is within this range, and store DNA at –20°C as DNA may degrade in the absence of a buffering agent. The purified DNA can also be eluted in TE (10 mM Tris·Cl, 1 mM EDTA, pH 8.0), but the EDTA may inhibit subsequent enzymatic reactions.

14. If the purified DNA is to be analyzed on a gel, add 1 volume of Loading Dye to 5 volumes of purified DNA. Mix the solution by pipetting up and down before loading the gel.

Loading dye contains 3 marker dyes (bromophenol blue, xylene cyanol, and orange G) that facilitate estimation of DNA migration distance and optimization of agarose gel run time. Refer to Table 2 (page 15) to identify the dyes according to migration distance and agarose gel percentage and type.